LOW WORK FUNCTION CATHODE DEVELOPMENT

CONTRACT NO: NAS 3-7114

by

W. KNAUER AND H. GALLAGHER

prepared for

NATIONAL AERONAUTICS
AND
SPACE ADMINISTRATION

HUGHES

HUGHES AIRCRAFT COMPANY

RESEARCH LABORATORIES

MALIBU, CALIFORNIA
90265

NOTICE

This report was prepared as an account of Government sponsored work. Neither the United States, nor the National Aeronautics and Space Administration (NASA), nor any person acting on behalf of NASA:

A.) Makes any warranty or representation, expressed or implied, with respect to the accuracy, completeness, or usefulness of the information contained in this report, or that the use of any information, apparatus, method, or process disclosed in this report may not infringe privately owned rights; or

B.) Assumes any liabilities with respect to the use of, or for damages resulting from the use of any information, apparatus, method or process disclosed in this report.

As used above, "person acting on behalf of NASA" includes any employee or contractor of NASA, or employee of such contractor, to the extent that such employee or contractor of NASA, or employee of such contractor prepares, disseminates, or provides access to, any information pursuant to his employment or contract with NASA, or his employment with such contractor.

Requests for copies of this report should be referred to

National Aeronautics and Space Administration
Office of Scientific and Technical Information
Attention: AFSS-A
Washington, D.C. 20546

167

NASA CR-54682

SUMMARY REPORT

LOW WORK FUNCTION CATHODE DEVELOPMENT

by

W. Knauer and H. Gallagher

prepared for

NATIONAL AERONAUTICS AND SPACE ADMINISTRATION

October 1966

CONTRACT NAS 3-7114

Technical Management
NASA Lewis Research Center
Spacecraft Technology Division
(R. R. Nicholls)
Cleveland, Ohio

HUGHES RESEARCH LABORATORIES
a Division of Hughes Aircraft Company
Malibu, California

TABLE OF CONTENTS

LIST OF ILLUSTRATIONS

I. INTRODUCTION AND SUMMARY

It is generally acknowledged that the most problematical component in a Kaufman ion thruster is the electron emitter. Refractory metal cathodes are prohibitive in their power consumption; ordinary oxide cathodes, which require less power, have proven to be very short lived. Oxide and dispenser cathodes fail since ion bombardment rapidly removes their emissive coating.

The specific power consumption of cathodes varies widely for different types of emitters. Since the ion thruster cathodes must consume less than 40 W/A, it is important to know which of the different emitter types can fulfill this requirement. The Richardson-Dushman emission equation

$$J = AT^2 e^{-\frac{\phi}{\epsilon T}}$$

and the Stefan-Boltzmann radiation law

$$P = \sigma \epsilon T^4$$

can be combined to give an expression for the specific power consumption under ideal conditions

$$\frac{P}{J} = \frac{\sigma \epsilon}{A} T^2 e^{\frac{\phi}{kT}}$$

where

J ≡ current density

P ≡ radiated power

σ ≡ Stefan-Boltzmann constant

ε ≡ emissivity

ϕ ≡ work function

T ≡ temperature.

Figure I-1 shows the resulting power per ampere requirements for various thermionic emitter types. Since operating temperature is an important design consideration, the data are presented as a function of temperature. According to Fig. I-1, the 40 W/A requirement can be met by practically all commonly used emitters. However, the values given are quite optimistic since they are obtained under the assumption that (1) all heat is lost by radiation, and (2) all radiating surfaces emit. Furthermore, the emissivities of Cade[1] and the work functions taken from Lemmens[2] and Beck[3] may

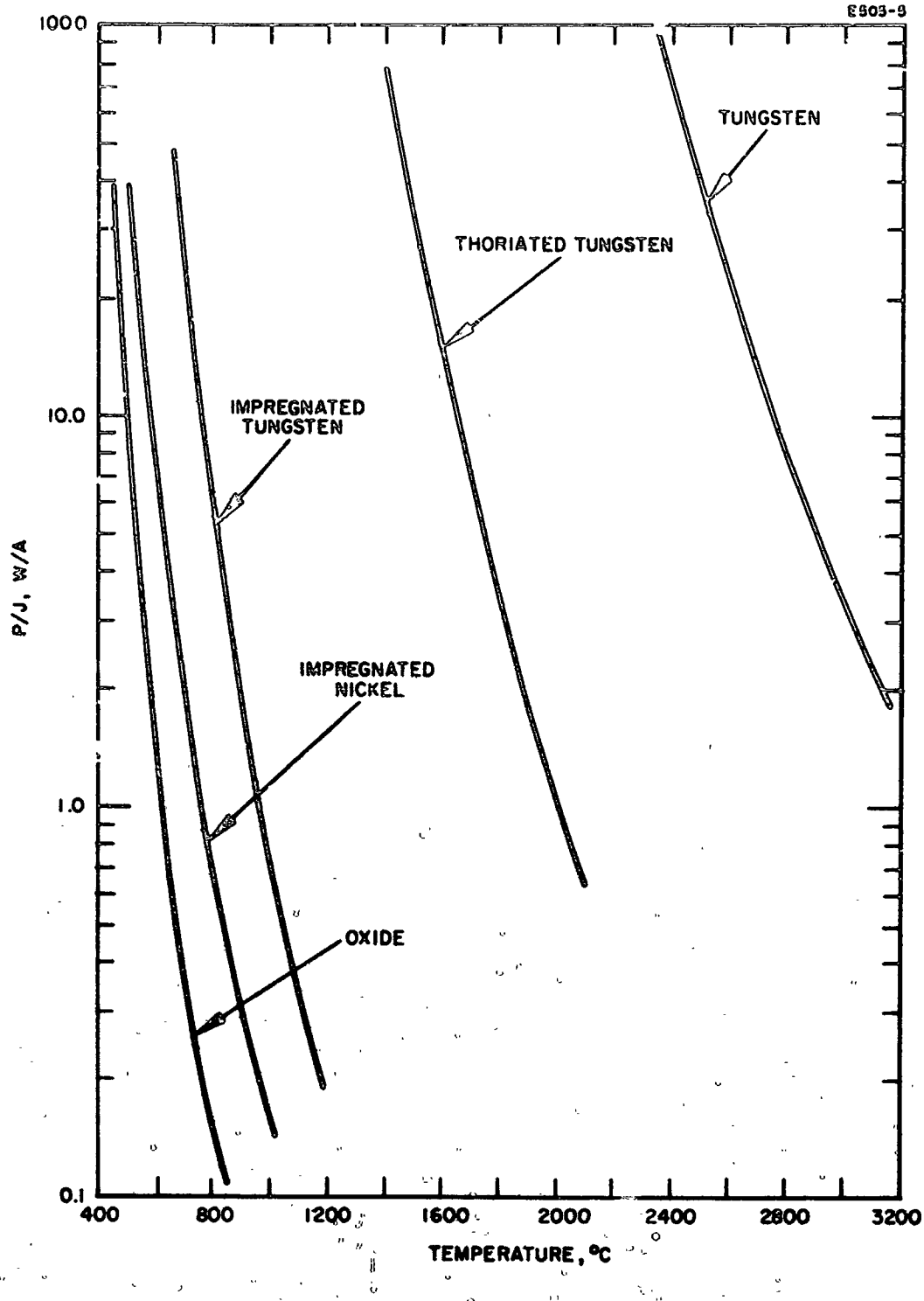

Fig. I-1. Required heater power per emitted ampere as a function of electrode temperature.

be optimistic. Nevertheless, Fig. I-1 serves to place the various emitters in a relative order with respect to temperature. Accordingly, oxide cathodes should be the most desirable type of emitters and dispenser cathodes would rate second.

During the contract period covered by this report, emphasis was placed upon the development of low work function cathodes which not only endure the intensive ion bombardment but also remain in an equilibrium state of activation over long time periods while subjected to a discharge environment. At the outset, a survey was taken of the various environmental factors which can affect the performance of a cathode in a discharge. It was found that, in addition to ion bombardment, the presence of a plasma sheath adjacent to the cathode is of major importance. Indeed, the fields of the sheath are of such magnitude that up to current densities of many A/cm^2, emission from the cathode remains temperature limited. If the emissive layer is too thick, resistive heating of the layer by the emission currents becomes important. The associated increase in temperature raises the electron emission which, in turn, leads to still more heating. This thermal runaway is well known, and ultimately causes the destruction of the emissive layer.

In Section III the emission density or arc current (for a given cathode design) is found to be a function of other parameters, in addition to the cathode heating power. Three of these parameters are resistive heating in the emissive layer, mercury flow rate, and arc power. Since a portion of the arc power is dissipated in the cathode, the cathode temperature is determined partially by the arc power level. The mercury flow determines the plasma density, and hence the sheath width. As a result, the arc current is a function of the cathode heating power, resistive heating, arc power, and mercury flow.

In the course of this contract, cathodes of several different designs were evaluated. Common to all designs was an optimization of the thickness of the emissive layer, such that runaway could not become a problem, while sufficient emissive material was available to avoid depletion by sputtering in less than 10,000 hours. The designs differed with respect to the method by which a large store of emissive material was kept and was made available under ion bombardment, while avoiding the excessive electrical and thermal resistance responsible for runaway and arcing in conventional thick coatings. The essential features of these designs, as well as their merits and faults, are summarized here.

Initially, an approach was considered in which a specially tailored porous matrix was to be utilized. As in dispenser cathodes, the emissive material was to be embedded in the pores of the matrix and made available at the surface by diffusion and migration. A semi-quantitative analysis of the mechanisms involved made it clear that the required high rate of dispensation could not be achieved with the coarse structures of ordinary cathode matrices. In fact, even matrices composed of the finest known tungsten powders seemed marginal. This was considered too uncertain to warrant further pursuit of the dispenser cathode concept.

At a later time during the contract, NASA LeRC supplied several conventional dispenser cathodes for tests in a Kaufman ion thrustor. Aside from unexpected periodic emission bursts in the initial phases of their life cycle, these cathodes behaved just as would have been expected. In order to emit, they had to be maintained considerably above the recommended operating temperature. Considering the large pore separation in conventional matrices, only a small fraction of the surface should have been covered with emissive material. Thus, the high operating temperature was required for (1) sufficient total emission from this small fraction of covered surface and (2) diffusion of sufficient emitting material to the surface to overcome the losses. All dispenser cathodes tested consumed large quantities of heater power and failed prematurely due to heater failures.

The concept used in a second configuration was to take advantage of a geometrical shielding effect against the impacting ions. A ribbon shaped oxide cathode was folded into a compact volume and was exposed to the discharge plasma only at one edge. This led to a reduction in the ion impact rate by about one order of magnitude and it permitted the use of coatings sufficiently thin to exclude runaway heating. In the course of this contract, four versions of this cathode type, called "Flower Cathode," were designed and about 19 sample cathodes were tested. The results obtained were very favorable and the flower cathode is presently considered the most promising cathode type developed under this contract. The latest version, utilizing an oxide coating of nickel encapsulated barium oxide particles for increased coating conductivity, has passed a 1000 hour test in actual thrustor operation. It showed no signs of deterioration in emission in spite of exposure to air after 800 hours because of a feed system failure.

While the suitability of the flower cathodes for use in Kaufman engines has thus been demonstrated, several further improvements seem advisable. At present, flower cathodes consume on the order of 35 W/A of emitted current, which is high. The average emission density has been maintained at about 0.25 A/cm^2 which is a proven value for oxide cathodes in vacuum tubes. Any significant increase above this level would benefit the power efficiency substantially. Tests of limited duration at increased emission rates have indicated that flower cathodes coated with nickel encapsulated barium oxide may well be able to operate at substantially increased current densities without damage to the oxide by resistive overheating. Future work toward higher emission density operation should include a study of the effects of varying the thickness of the nickel encapsulating the barium oxide particles. The emission density, without destructive overheating, will be a function of this nickel encapsulant thickness.

Another area of potential improvements is the choice of ribbon material. So far, mesh composed of cathode nickel has been used exclusively. One of the early flower cathodes failed after 850 hours of operation due to breakage of the mesh. This caused some concern about the reliability of the mesh. Since then, a four times heavier mesh made of a nickel alloy with superior strength has been used. A more recent, additional failure involving mesh burn out should not be attributed to the mesh. It occurred while the system pressure had risen to about 1 Torr. At this high pressure the cathode must have become inactivated and the arc can be assumed to have focused upon a small region of the mesh which then overheated and burned out. Another shortcoming of nickel mesh is its tendency to sag in long term operation. Al-

together, it would seem an appropriate precaution, therefore, to consider other, higher melting mesh materials, for example, tungsten.

The concept underlying the third approach was to use a thick slab of emissive material, rendered more conductive through interspaced threads of conductive material. The emission currents were expected to follow the conductive paths up to the emitter surface where they would branch out into barium oxide gains and be emitted. Under ion bombardment, the entire slab was to wear down gradually, together with the conductive inclusions.

This concept has led to the development of the so-called "Disk Cathode." As the label implies, this cathode type utilizes disks as the conductive medium. A thick slab is manufactured by stacking up a large number of disks, each coated with barium oxide. The disks must be extremely thin in order to wear down uniformly with the oxide. This requirement turns out to be rather critical. While the electrical conductivity of even the thinnest disks is quite sufficient, the heat flow along these disks encounters a considerable impedance. This results in a large temperature gradient across the slab which, in turn, leads to inefficient heater power utilization. In several tests, disk cathodes performed well as electron emitters; however, their power consumption was undesirably high because of the heat flow problem.

Undoubtedly, improvement of the disk cathode concept is possible. On all earlier built disk cathodes, the heater has been mounted in the rear of the oxide slab. If the heater were to be buried inside the disk stack, the heater power would be utilized considerably more efficiently and a more useful cathode would result.

The last approach, under this contract was a preliminary attempt to utilize nickel encapsulated barium oxide in a thick emitter slab configuration. This cathode type was developed after the heat conductance problem with disk cathodes arose. Therefore, a cup shaped configuration with the heater on the inside was adopted. The outside of a nickel cup was coated with a heavy layer of nickel encapsulated barium oxide. Initially, this "Cup Cathode" functioned satisfactorily. However, after some life testing the heater power had to be raised substantially to maintain the emission current. This eventually resulted in a heater failure. Post mortem inspection revealed that the coating had flaked off the nickel support. This led to the conclusion that the nickel encapsulant, surrounding the barium oxide grains was not sufficiently thick to prevent flaking. It should be added that the emissive layer used here was about 10 times as thick as that of the latest type of flower cathode. Obviously, the cup cathode will require further development effort in order to determine the optimum nickel encapsulant thickness for these thick oxide emissive layers.

The results obtained during the contract may be summarized as follows: The basic problems, from which cathodes in a discharge environment suffer, have been elucidated. Several workable concepts for economical and durable cathodes have been evolved. Many test cathodes were built and operated. The test results suggest that at least one cathode type, the flower cathode with nickel encapsulated barium oxide, has reached an advanced status, and that prototype cathode can now be put to use confidently in Kaufman ion thrustors.

II. PHYSICAL CONCEPTS

When thermionic cathodes are operated in a discharge plasma, they are subjected to intense ion bombardment. Such bombardment causes rapid removal of the cathode coating and thereby leads to premature loss of emission. Observations by Kerslake,[4] for example, have shown that the surface of oxide cathodes which were operated in a mercury plasma became eroded at the rate of one monolayer every 4 sec. With a plasma density of the order of 10^{12} particles/cm^3, an ion temperature equivalent to 1V and a discharge potential of 40V, this corresponded to a sputtering rate of 5×10^{-3} atoms/ion for 40V mercury ions. In contrast, typical metals sputter at the rate of 10^{-4} to 10^{-5} atoms/ion under 40V mercury ion bombardment.

This significant difference between metals and BaO cannot be explained on the basis of the familiar laws for low energy sputtering. According to Wehner,[5] the sputtering rates should vary inversely with the heat of sublimation. For typical metals, the latter quantity possesses values between 2 and 8 eV. With a heat of sublimation of 3.8 eV,[6] the sputtering rate of BaO should be comparable to that of metals.

A possible explanation for the anomalously high sputtering rates of BaO may be advanced along the lines considered by Yoshida, et al.,[7] for the evolution of barium from BaO under electron impact. According to these authors, most of the kinetic energy of the impacting electrons is expended in the production of hole-electron pairs. Holes and electrons diffuse about the BaO crystal and eventually recombine. Some annihilate at the surface and their energy becomes available for the ejection of barium and oxygen atoms. In BaO the valence band is approximately 3.8V below the conduction band,[8] so that each hole-electron pair carries an energy of 3.8 eV. The heat of sublimation of the reaction

$$BaO\,(s) \rightarrow 1/2\ O_2(g) + Ba(g)$$

is approximately 4.5 eV.[9] Hence, hole-electron recombination at the surface can almost completely supply the energy of disassociation. The small 0.7 eV deficiency can be made up thermally.

Presumably, a similar process takes place under ion bombardment. It is well known that most of the kinetic energy of impacting low energy ions is used up in the generation of hole-electron pairs. Since ions penetrate much less deeply into the crystal than electrons of comparable energies, the number of holes reaching the surface (and, hence, the number of barium atoms liberated) will be considerably larger in the case of ions. This is in general agreement with the experimental results. Yoshida has observed a production rate of approximately 10^{-6} barium atoms per impacting 40 eV electron. This compares with 5×10^{-3} atoms per 40 eV mercury ion.

In addition, the described free barium generation mechanism may explain the ease with which oxide cathodes in discharge plasmas can be activated. It has been observed, for example, that new cathodes can be activated simply by increasing the temperature to the operating level and initiating the arc plasma. Similarly, oxide cathodes using a passive nickel base have been found to activate readily, even though they lack the usual activators. (These activators have the task of generating free barium atoms which then diffuse into the BaO lattice and provide the donor states required to render the crystal semiconducting.) Both observations suggest that some of the free barium atoms generated by hole-electron pair annihilation diffuse into the BaO lattice and provide the required donor population.

The number of barium atoms diffusing into the lattice is small compared with that evaporating into vacuum. This is evident from a comparison of the evaporation rate[10] of 4 $\mu g/cm^2$ or 5.5×10^{12} barium atoms/cm^2 sec with the diffusion rate as given by

$$S = -D \frac{dc}{dx}$$

where

$D \equiv$ diffusion constant

and

$\frac{dc}{dx} \equiv$ barium concentration gradient.

For a monolayer at the surface of a 100μ thick coating $dc/dx \cong 4 \times 10^{16}$ barium atoms/cm^3, and $D = 2.5 \times 10^{-11}$ cm^2/sec,[11] the diffusion becomes $S = 10^6$ barium atoms/cm^2 sec, which is considerably less than the evaporation rate. Using the above mentioned loss rate of 0.25 monolayers/sec, the total loss of BaO during a lifetime of, e.g., 10,000 hours amounts to 0.5 g/cm^2. This constitutes an oxide layer 0.5 cm thick. Unfortunately, such a large layer thickness is not compatible with sound cathode construction practice. The difficulty arises from the fact that the semiconducting oxide layer possesses a finite electrical resistance. The emission current passing through this layer generates heat. The resulting rise in temperature causes the emission to increase, which in turn increases the current flow through the cathode. Thus, a runaway condition arises which leads to autocathode operation (also called "sparking"). Observations by Kerslake have shown that overheating usually occurs in spots, that these spots frequently change location, and that the overall activity of the cathode eventually begins to deteriorate.

To prevent this undesirable effect, the oxide layer must be kept sufficiently thin. The maximum tolerable thickness may be estimated as follows.[3] The heat balance in the oxide layer is given by the equation

$$P_H + J^2R = CT^4 + J\left(\phi + \frac{2kT}{e}\right)$$

where P_H is the heater input-power per square centimeter transmitted through the oxide coating, J^2R is the Joule heating by the emission current in the coating, CT^4 is the heat radiation from the coating surface and $J(\phi + 2k\,T/e)$ is the heat removed by the emitted electrons. The standard terminology is used here:

$J \equiv$ current density

$R \equiv$ resistance

$C \equiv$ radiation constants

$\phi \equiv$ work function

$k \equiv$ Boltzmann constant

$T \equiv$ temperature

$e \equiv$ electron charge

Since the emission current density J varies exponentially with T, the term CT^4 is relatively constant with constant heater power. Thus, the above equation is essentially balanced when

$$J \leq \frac{1}{R}\left(\phi + \frac{2kT}{e}\right) \cong \frac{\phi}{R} \quad .$$

If the coating impedance R is expressed in terms of the volume resistivity ρ and thickness t, the latter relation can be written as

$$t_{max} = \frac{\phi}{J\rho} \quad .$$

In vacuum devices, the current drawn between cathode and anode is limited due to the presence of space charge. The maximum current density then is determined by the Child-Langmuir law

$$J = C\,\frac{V^{3/2}}{d^2}$$

where V is the anode potential, d the separation between cathode and anode, and C a constant for planar geometry = 2.3×10^{-6} $A/V^{3/2}$. In a plasma, the situation is more complicated. Here, the potential is applied between cathode and plasma, and the potential rise takes place across the plasma sheath. The width of the sheath depends upon the plasma density and plasma temperature. The flow of electrons across this sheath is influenced by the counterflow of ions from

the plasma to the cathode. Both ions and electrons partially compensate the other's space charge, so that the current flow is somewhat larger than in the case of a vacuum diode of comparable gap width and voltage. According to Langmuir,[12] the limiting electron flow rate can be determined without knowing the sheath width and voltage; it is given by

$$J_e = J_i \left(\frac{m_i}{m_e}\right)^{1/2}$$

where J_i is the random ion current density at the plasma edge:

$$J_i = \frac{1}{4} N \cdot e \cdot v_{th} \quad .$$

Here, N is the plasma density and v_{th} the thermal ion velocity.

Introduction of the last two equations into the expression for t_{max} yields

$$t_{max} = 4 \left(\frac{m_e}{m_i}\right)^{1/2} \frac{\phi}{\rho N e v_{th}}$$

For a mercury plasma of 2×10^{12} particles/cm^3 with a thermal ion velocity of 10^5 cm/sec (equivalent to 1 eV thermal energy), for an oxide coating with a resistivity ρ of 100 Ω-cm, and for a work function ϕ of 1.5 eV, one obtains a maximum coating thickness t_m of approximately 5×10^{-3} cm.

This small coating thickness of less than 10^{-2} cm, required for safe cathode operation, obviously is in conflict with the large coating thickness of 0.5 cm required for BaO storage against sputter losses. The primary objective of this contract is to overcome this incompatibility. Two novel cathode configurations, the "Flower Cathode" and the "Disk Cathode," and a novel type of active material, the "Nickel Encapsulated Powder," have been evolved to combine safe operation and sufficient material storage for long cathode life. The principles of operation of these cathodes will now be discussed briefly. Test results will be presented in Section III.

A. Flower Cathode

The ion current density with which a cathode at the edge of a plasma is bombarded is given by

$$J_i = \frac{1}{4} N e v_{th}$$

where N is the plasma density and v_{th} is the thermal ion velocity. If the cathode surface is not flat, but contains folds (see Fig. II-1), the effective bombarding current density may be reduced by a factor equal to the ratio of the frontal to total cathode surface area. This reduction of ion bombardment density depends upon the distance from the cathode at which the average cathode-bound ion is born. This distance must be large compared with the separation between cathode folds. Ion production within that part of the plasma which extends into the cathode folds is then comparatively small. Ions generated in the bulk of the plasma bombard the cathode surface at a rate which depends upon the frontal to surface area ratio. A surface ratio of 1:10, which is quite practical, permits reduction of the oxide coating thickness from 0.5 cm (required for a lifetime of 10,000 hours) to 0.05 cm. This is still too large by a factor of 10. If the cathode is constructed of a folded wire mesh (see Fig. II-1), the coating thickness can be reduced still further by another factor of the order of 2 because of the additional increase in surface area. Finally, the plasma density decreases toward the back of the folds (because of the progressive loss of ions). Therefore, the maximum permissible t_m becomes larger. At the deep end of a fold which, for example, is ten times deeper than it is wide, the plasmas density should have decreased by an order of magnitude; therefore, the layer thickness could be as high as 0.05 cm. Therefore, if a layer of varying thickness is adopted, increasing from 0.005 cm thickness at the front of the fold to 0.05 cm at the rear (refer to Fig. III-9), sparking should not be a problem and a full 10,000 hour supply of BaO should be available.

In the dimensioning of the cathode folds it is of importance that the plasma be able to penetrate into the folds. Only then will the cathode be able to emit sufficient numbers of electrons into the plasma. The critical distance is thus the Langmuir sheath width, which is obtained from Child-Langmuir's law by solving for d_L and introducing the expression given earlier for the random current density J_i,

$$d_L = \left[4C \frac{V^{3/2}}{Ne\, v_{th}} \right]^{1/2}$$

In order that the plasma can penetrate into the folds, they must be at least two plasma sheath widths wide. With a plasma density N of 2×10^{11} particles/cm^3 at the deep end of the fold, a thermal ion velocity of 10^5 cm/sec, and a sheath potential of 30V, the sheath width becomes approximately 0.5 cm. Therefore, the folds of a flower cathode must be approximately 1 cm apart under these plasma conditions.

B. Disk Cathode

The dilemma between safe cathode operation without overheating and a 10,000 hour storage capability for BaO stems from the finite resis-

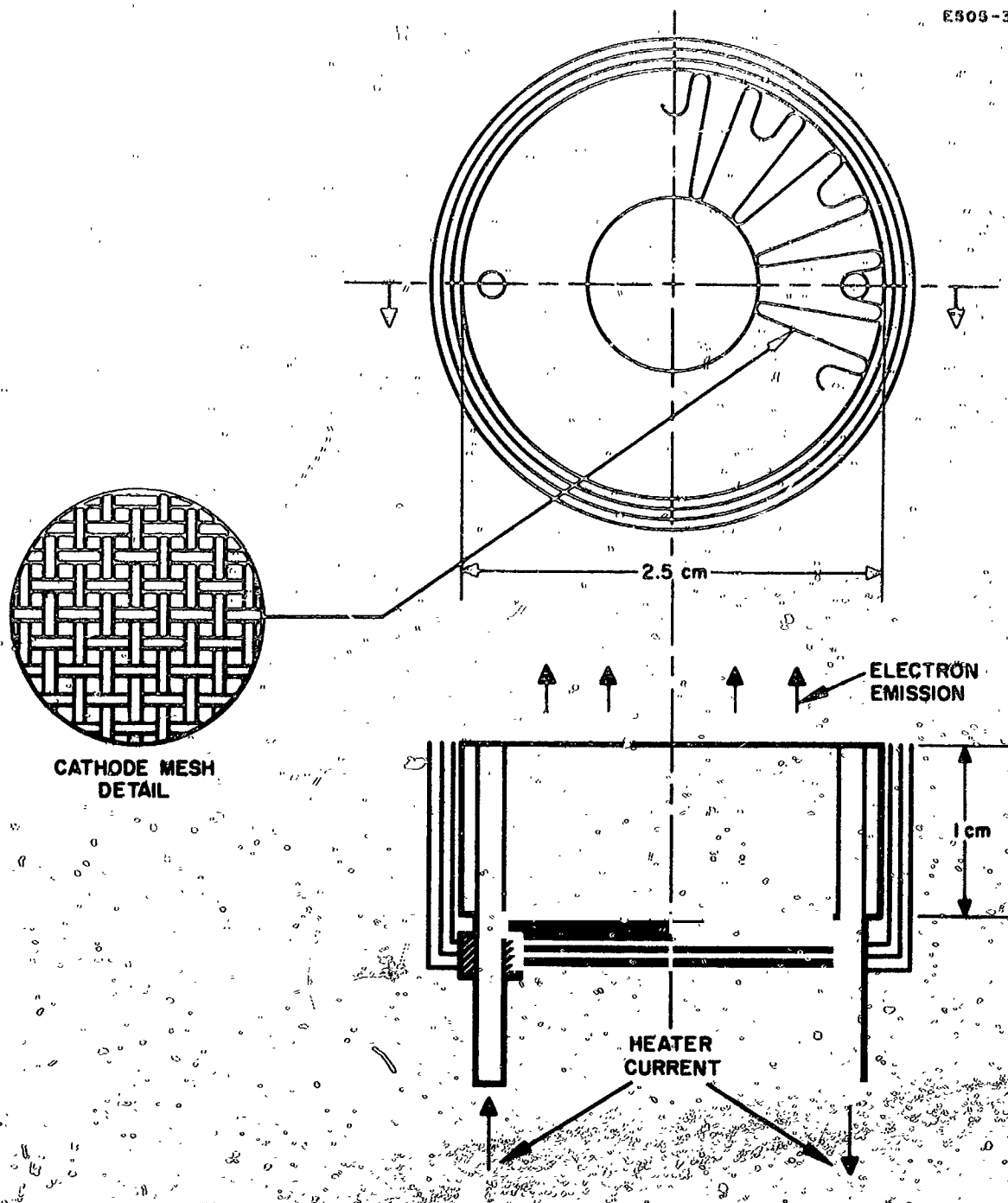

Fig. II-1. Flower cathode design 2.

tivity of the oxide coating. If it were possible to eliminate this resistance, the problem would be resolved. An approach in this direction is to interspace the coating with threads of conductive material. The emission currents then follow conducting paths up to near the coating surface, where they branch out into BaO grains and are emitted.

A basic requirement of this concept is that the conductor material must sputter as rapidly as the BaO. Because most metals which could serve as conductors sputter at least 10 times more slowly than the oxide, the fractional amount of the metal must be less than 10% (in weight) of the BaO. In terms of the volume fraction, this reduces to approximately 2%. This small quantity of conductive material must be interspaced between the BaO so that the distance between conductive threads nowhere is larger than about 10^{-2} cm.

Figure II-2 shows a possible embodiment of this concept. The cathode is composed of a large number of nickel disks approximately 10^{-3} cm thick, each coated with a layer of 10^{-2} cm BaO. Actually, the nickel disks should be less than 2×10^{-4} cm thick, but nickel sheet of such a small thickness is not commercially available. The larger than optimum thickness of the nickel will cause the nickel to stand out somewhat beyond the barium oxide (see insert, Fig. II-2). In order to ascertain that the described disk configuration fulfills its function, one must compute the potential drop under the flow of the emission currents. With a resistivity of 1.8×10^{-5} Ω-cm at 1000°K for nickel and an average emission density of 0.5 A/cm^2, the potential drop along disks of 1 cm length, 10^{-3} cm thickness, and 10^{-2} cm separation becomes approximately 10^{-1} V. Obviously, the potential drop is sufficiently low. The temperature drop across a nickel disk was calculated under the assumption that the power loss is given by the radiation equation, $P = \sigma \epsilon A T^4$, and that the power input is given by the conduction equation, $P_i = kA \frac{\Delta T}{\Delta r}$. After equating power input and power loss, and solving the resulting differential equation with a short computer program, the temperature drop was found to be approximately 4°C for 10^{-3} cm thick disks, and 20°C for 2×10^{-4} cm thick disks. The actual temperature of the disks will depend to a large extent on the thermal contact between disks and from disks to their support cylinder.

C. Impregnated Cathodes

Another class of electron sources utilize porous metal bodies as hosts for the active substances. Activation of these emitters is accomplished through continuous diffusion of the active materials to the surface. The composition of the activated surface is somewhat different from that of oxide cathodes and results generally in a higher work function. Accordingly, the operating temperature must also be higher (it ranges from 1250°K to 1450°K).

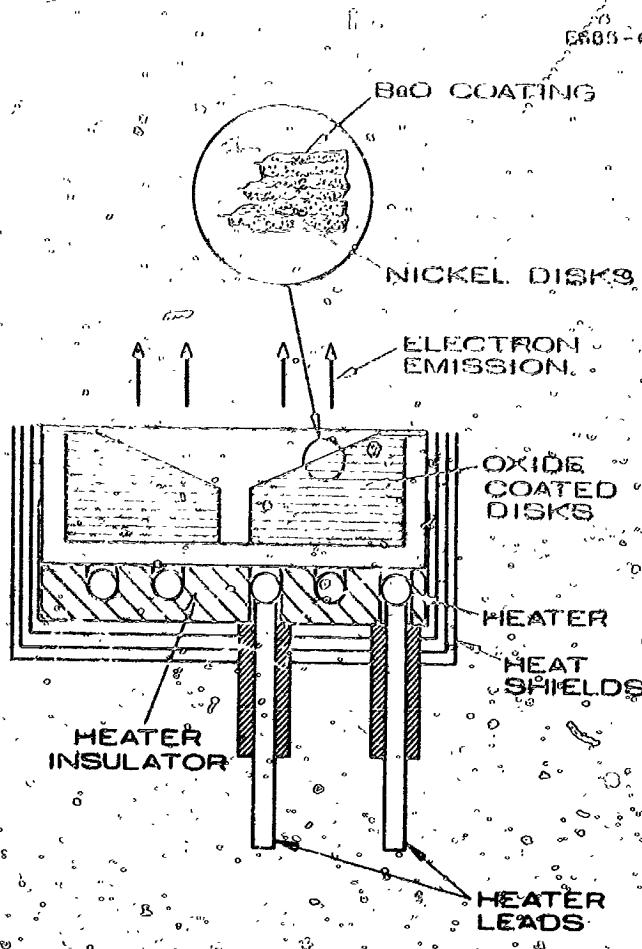

Fig. II-2. Disk cathode geometry.

While oxide cathodes wear down from the top under ion bombardment, the body of impregnated cathodes remains intact since the sputtering rates for metals are comparatively small. (Most metals are eroded at the rate of approximately 10^{-5} to 10^{-4} atoms/ion under bombardment of 30 to 50 eV mercury ions. In the course of a 10,000 hour bombardment with 5 mA/cm^2, therefore, depletion should not exceed 10^4 to 10^5 atom layers.) In contrast, the active material on the metal surface is sputtered quite rapidly (at rates of the order of 3×10^{-3} atoms/ion). Impregnated cathodes can therefore remain activated only if their surface layers are replenished with unusual speed. In the following sections, the physical mechanisms in impregnated cathodes are discussed.

There are two basic versions of dispenser cathodes. In the impregnated cathode, the active material is stored within the pores of the matrix; in the other (the so-called L-cathode), the active material is stored in a separate reservoir. Because of its greater simplicity, the former type currently is used most. The L-cathode, on the other hand, has the advantage of a large storage capacity for active material, and this is of considerable importance here. In fact, it will be seen that the total consumption of active material during a life span of 10,000 hours approaches the limit of what can be stored within a matrix.

The most common impregnated cathode utilizes tungsten as a matrix and contains fillings of calcium and barium aluminates.

The mechanism in impregnated cathodes is described utilizing a simplified but experimentally well supported model. Figure II-3 shows a reaction chamber representing the pores in a matrix. The chamber contains barium and calcium compounds which react with an "activator" to produce a temperature dependent barium vapor pressure. The reaction chamber is connected to the cathode surface by thin channels or pores through which barium is forced to the surface. The transport to the surface may take place as free molecular flow (Knudsen flow) and/or migration along the channel surfaces. The portion of barium which passes the channel via free molecular flow streams out into the surrounding vacuum and is lost to surface activation. The migrating part, however, spreads over the surface, thereby reducing the work function of the surface. The activated area extends in a circle around the channel opening. In equilibrium, the supply to the surface layer is balanced by evaporation and by sputtering losses.

To assess this model more quantitiatively, a shortened account of an analysis originally given by N. D. Morgulis, et al.,[13-17] is followed.

1. Barium Production

A common method of obtaining barium oxide is to decompose the carbonate $BaCO_3$ or aluminate BaO, CaO, Al_2O_3. The barium oxide reacts with various activators to supply to the free barium. The barium pressure can be varied significantly by the proper choice of acti-

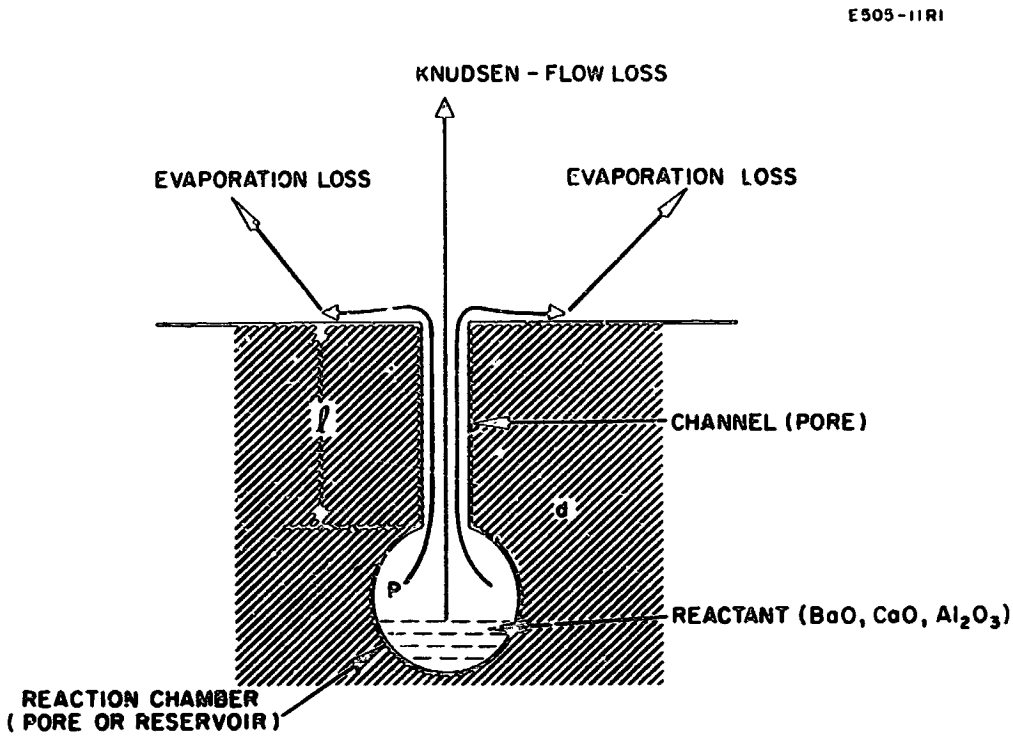

Fig. II-3. Schematic representation of surface activation of dispenser cathodes.

vators. With tungsten, for example, the following reaction occurs

$$6\ BaO + W = Ba_3WO_6 + 3\ Ba$$

with a vapor pressure of the order of 10^{-7} Torr at 1250°K.

The barium pressure in the reaction chamber can be adjusted over a wide range of pressures, from 10^{-10} to 10^{-3} Torr, depending upon the activator used. This is important since the barium flow rate to the surface depends directly upon the barium pressure.

2. Barium Transport to the Surface

With barium vapor pressures of generally less than 1 Torr and with pore diameters of the order of 1 to 10 μ, diffusion through the channel which connects reaction chamber and surface can be expected to be Knudsen flow. In this regime, barium atoms fly straight from wall to wall, are absorbed upon impact, and reevaporated after a finite lifetime τ_s. While adsorbed, the barium atoms travel a distance

$$s = \sqrt{D_s \tau_s}$$

where D_s is the surface migration coefficient. Since the travel distance in the evaporated state per free flight is of the order of the channel diameter d, it can be concluded that if s is comparable to d, surface migration becomes an important contributor to the total barium flow. In fact, since the Knudsen flow component disperses into vacuum at the open end of the channel and therefore constitutes a complete loss, the channels must have such dimensions that

$$d \leq \sqrt{D_s \tau_s}$$

so that barium can be utilized efficiently. The rate n_o at which barium is transported along the channel walls is determined by the surface diffusion equation

$$n_o = \pi d\ D_s \frac{d\sigma}{dx}$$

where σ is the surface coverage. The latter is related to the rate δ of evaporation from the surface by

$$\sigma = \tau_s \delta$$

Furthermore, the rate of evaporation is related to the vapor pressure p through

$$\delta = \frac{1}{4} N V_{th} = \frac{1}{4} \frac{p}{kT} V_{th}.$$

Here the thermal velocity V_{th} can be expressed as

$$V_{th} = \left(\frac{8}{\pi} \frac{kT}{m}\right)^{1/2}$$

If the above expressions are introduced into the equation for the flow rate, one obtains

$$n_o = \frac{\pi d D_s \tau_s}{(2\pi mkT)^{1/2}} \frac{dp}{dx} .$$

Finally, if n_o is assumed to be constant throughout the length ℓ of the channel and if the pressure at the open end is negligible, the flow rate can be expressed as

$$n_o = \frac{\pi d D_s \tau_s}{(2\pi mkT)^{1/2}} \frac{p}{\ell}$$

where p is the vapor pressure in the reaction chamber. The last equation thus yields the flow rate n_o of barium to the surface, once the barium pressure is known.

3. Dispersion of Barium Over the Surface

Upon reaching the open end of the channel, barium migrates radially outward and spreads over a circular area. The migration over the surface is governed by the same basic rules as that along the channel walls, except that at the surface barium gradually vanishes through various loss processes, the most important of which are evaporation and sputtering. The effective surface lifetime for these processes can be expressed as

$$\frac{1}{\tau} = \frac{1}{\tau_E} + \frac{1}{\tau_{sp}}$$

Using τ, the flow balance in steady state for barium in a circular surface element can be expressed as

$$2\pi r dr \frac{\sigma}{\tau} = - \left[2\pi r D_s \frac{d\sigma}{dr} - 2\pi (r + dr) D \left(\frac{d\sigma}{dr} + d \frac{d\sigma}{dr}\right)\right]$$

which leads to

$$\frac{d^2\sigma}{dr^2} + \frac{1}{r}\frac{d\sigma}{dr} - \frac{1}{D_s\tau}\sigma = 0$$

With the boundary conditions $n = n_o$ for $r_o = d/2$ and $n = 0$ for $r = \infty$, one obtains

$$n = n_o \frac{K_o\left(\frac{r}{\sqrt{D_s\tau}}\right)}{K_o\left(\frac{r_o}{\sqrt{D_s\tau}}\right)}$$

This relation determines the size of the surface area covered by barium. In order to insure that the surface is covered more or less uniformly, for uniform electron emission, neighboring pores must be spaced less than approximately

$$\Delta = \sqrt{D_s\tau} \quad .$$

This last condition is considered critically important to the design of impregnated type emitters with long life under ion bombardment. To determine the required inter-pore distance numerically, the surface migration constant D_s and the effective lifetime τ must be known. Both quantities have been measured under conditions which are more or less applicable to impregnated cathodes. The migration constant D_s is known for monolayer films of barium on clean tungsten surfaces.[15] (Actually, it is presumed that impregnated cathode surfaces are covered partially with oxygen.) According to these measurements, D_s can be represented by

$$D_s = D_\infty e^{-\frac{Q}{kT}}$$

with $D_\infty \cong 1\ cm^2/sec$ and $Q \cong 1.8\ eV$. Thus, at 1250^oK,

$$D \cong 10^{-8}\ cm^2/sec.$$

The lifetime τ_E (for evaporation alone) has been found to be a more complicated function of temperature. It depends substantially upon surface coverage. Furthermore, it differs by many orders of magnitude for monolayers and multilayers (bulk material). Table I gives lifetimes τ_E for various fractional coverages and for bulk material. Also presented is the lifetime under sputtering of a monolayer of barium by argon ions of 50 eV at a current density of 5 mA/cm^2 and the estimated lifetime under sputtering by argon and mercury ions of 40 eV at 5 mA/cm^2.

TABLE I

Lifetimes (sec) of Barium Atoms on Tungsten Surfaces at 1250°K

Evaporation			Sputtering, 5 mA/cm^2		
Fractional Monolayer		Bulk	Argon Ions		Hg^+
0.6	0.8		50 eV	40 eV extrapolated	
4×10^2	2×10^2	7×10^{-6}	10^{-1}	1	4

First, because of the extremely high rate of evaporation from a multilayer (bulk), the barium film must shrink to monolayer thickness within a very short distance from the pores. Hence, one can draw the important conclusion that an increased rate of barium supply to the surface helps to increase surface coverage only up to the point where a full monolayer spreads over the surface from each pore opening. If barium is supplied at rates which exceed the carrying capability of a monolayer, it will be wasted.

Furthermore, Table I shows that the relatively long lifetime τ_E for evaporation alone is shortened by several orders of magnitude under ion bombardment of an intensity which occurs in bombardment ion engines. Thus, the distance Δ must be extremely short. According to the above equation, the distance between pores should be not larger than Δ, which amounts to 2×10^{-4} cm at a temperature of 1250°K with tungsten as substrate. This distance obviously is close to the practical limit.

The stringent requirement for pore spacing could be relaxed somewhat by operation at a higher cathode temperature. It can be expected that an increase in T also increases the surface migration rate D_s. From past experience, it appears that the lifetime τ_{sp} under ion impact should not vary significantly. Hence, increased temperature should increase the distance Δ.

To complete the description of the cathode model, the following must be computed: (1) flow rate n_o per channel, (2) pressure in the reaction chamber required to produce this flow rate, and finally, from the total flow rate through all pores, (3) the amount of barium required during a lifetime of 10,000 hours.

For simplicity, let it be assumed that each pore supplies a square of area Δ^2 with barium. The rate n_s at which material is sputtered from this layer and must be replenished is

$$n_s = \frac{\Delta^2}{\tau_{sp}} N_o$$

where $N_o = 4 \times 10^{14}/cm^2$ is the number of barium atoms per unit area in a full monolayer. Using the numbers derived above for Δ and τ_{sp} ($\cong \tau$), one obtains $n_s \cong 4 \times 10^6$ particles/sec.

This amount of barium must be delivered under pressure p through a single pore of diameter d and length ℓ. Using an equation derived earlier, one obtains for p

$$p = \frac{(2\pi mkT)^{1/2}}{\pi d D_s \tau_s} \ell n \quad .$$

Under the assumption that $d \cong 5 \times 10^{-5}$ cm and $\ell = 1$ cm, the pressure becomes $p \cong 10^{-2}$ Torr. Thus, an activator that generates barium copiously is required.

Finally, the total amount of barium consumed per square centimeter during a lifetime of 10^4 hours can be determined from n_s Z t, where z is the number of pores/cm^2 ($z \cong 2.5 \times 10^7/cm^2$), and t the total time ($t = 3.6 \times 10^7$ sec). One obtains a total of 3.5×10^{21} atoms, or approximately 0.8 g of barium. Obviously, this is close to the limit which can be stored within a matrix. Therefore, it may be necessary to attach a reservoir to the cathode.

4. Summary

The impregnated cathode under ion bombardment must lose large quantities of barium from its surface (order of 1 g/cm^2 in 10,000 hours). Continuous full coverage of the surface with barium requires close spacing of the pores (on the order of 2×10^{-4} cm or a pore density on the order of $10^7/cm^2$) and a high flow rate through the individual pores (order of 4×10^6 particles/sec). This high flow rate requires a relatively high vapor pressure (order of 10^{-2} Torr) which can be provided only by high temperature and the most active barium sources. This analysis indicates that

the commercially available impregnated cathodes, with a pore density the order of $10^6/cm^2$, will not provide sufficient barium flow to the emitting surface. The fine grain (2.8×10^{-4} cm) spherical powder at the HRL with a pore density of $8 \times 10^6/cm^2$ will provide only a marginal barium coverage.

D. Encapsulated Powder Cathode

Another technique for obtaining adequate BaO storage with low oxide coating resistance is to encapsulate the individual particles of cathode powder with a thin layer of nickel and to apply a heavy coating of this material to a cathode base. The nickel encapsulate is to provide the low resistance paths for the emitted current. Also, fusion of the nickel encapsulate should minimize the oxide flaking problem that is present when emitting layer thickness approaches several millimeters. Figure II-4 illustrates schematically the difference between a standard oxide cathode and a nickel encapsulated oxide cathode. Each of the carbonate particles is to be encapsulated with a nickel layer.

This nickel encapsulated cathode powder can serve as the emitting layer for either the flower, disk, or cup cathodes. This cathode material was developed especially for the thick (2 mm) emitting layers to be used with the cup cathode. This cup cathode design, shown schematically in Fig. II-5, provides a means of using an indirectly heated cathode with a small emitting area, and adequate BaO storage without resistive overheating. This cup cathode is considered an extention of the disk cathode design, in that the current and heat conducting disks have been replaced by the nickel encapsulate on the cathode powder.

Using the cup cathode as an example, the advantage of the nickel encapsulated cathode powder is illustrated. With 100 Ω-cm[16] the resistivity of ordinary barium oxide and the cup cathode coating thickness of 2mm, an oxide coating resistance per unit area of 20 Ω-cm^2 would result. For maximum emission density on the order of 1 A/cm^2, the power generated would be 20 W/cm^2 and cathode overheating clearly would exist, since the cathode power density radiated is only about 4 W/cm^2. For a nickel encapsulate on the cathode powder of only 1% by weight, but providing continuous current paths, the cathode coating resistance would drop to below 0.1 Ω-cm^2. The resulting power density generated by 0.1 W/cm^2 is well below the power density radiated (4 W/cm^2); therefore, the cathode overheating problem is eliminated. The nickel coating thickness of 0.05 μ on each powder particle is sufficiently thin that the Ba can diffuse to the surface; therefore, this nickel coating does not interferre with the activation mechanism.

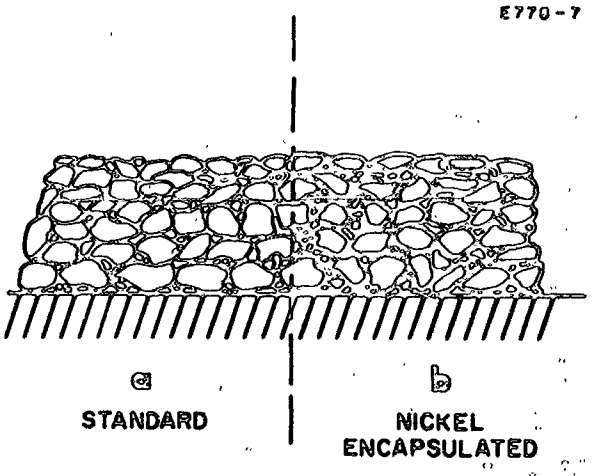

Fig. II-4. Standard oxide coating and nickel encapsulated oxide coating.

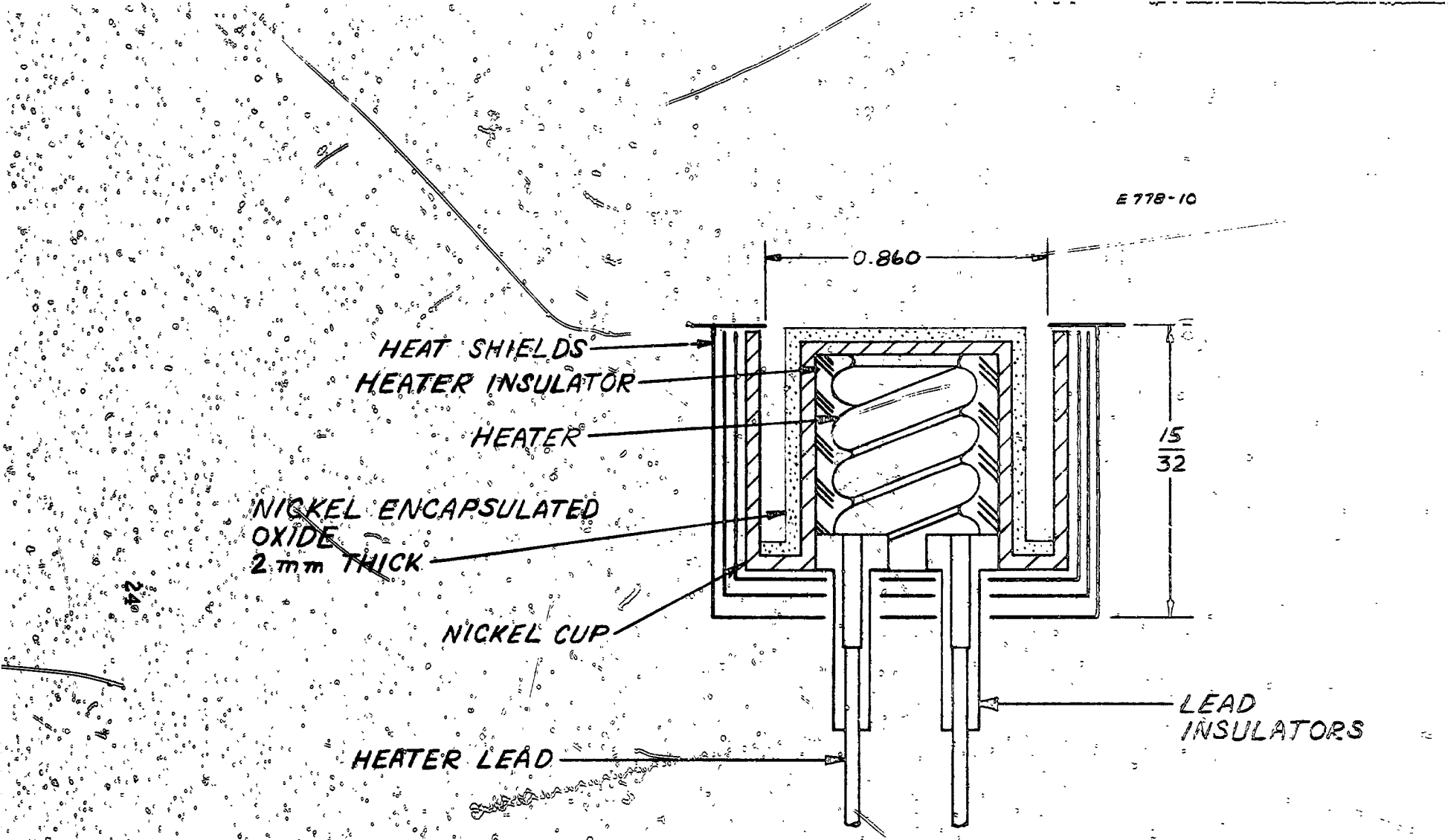

Fig. II-5. Cup cathode geometry.

III. EXPERIMENTAL RESULTS

A. Introduction

The cathode tests performed during the contract can be classified as evaluation tests, and 200, 500, and 1000 hour life tests. Some evaluation tests were for the purpose of determining voltage current and power temperature characteristics of the cathodes. Other evaluation tests determined the effects of cathode protecting grids and varied directions of mercury vapor flow. The 200 hour cathode life tests were performed in simulated thrustor operation, whereby no ions were extracted. These tests were carried out in either an ion sublimation vacuum chamber or a mercury diffusion vacuum station. Some of the 500 and 1000 hour life tests were performed in actual thrustor operation with ion extraction whereby either the 2 ft. or 9 ft. diameter cyrowall vacuum chambers were utilized.

Twenty-six flower cathodes of four different designs were fabricated, and 19 of these were tested. Three cathodes were delivered to NASA-Lewis Research Center for evaluation. The dimensions of the four flower cathodes designs are listed in Table II.

TABLE II

Dimensions of Flower Cathode Designs

Cathode			Emitting Mesh				
Design No.	Diameter, in.	Area, cm^2	Wires, N/in.	Width, in.	Length, in.	Diam. in.	Area cm^2
1	1-3/8	9.6	50 x 50	1/2	18	0.009	116
2	1-3/8	9.6	50 x 50	5/8	14	0.009	113
3	13/16	3.3	70 x 70	1/2	6	0.0045	39
4	1-1/4	8	50 x 50	5/8	5-1/2	0.009	44
4A	1-1/4	8	50 x 50	5/8	5	0.009	40
4B	1-1/4	8	50 x 50	3/8	5-1/2	0.009	27

Designs 1 and 2 were intended for use with 15 or 20 cm thrustors, design 3 for a smaller 10 cm thrustor, and design 4 for 15 cm thrustors. Design 1, which was used only for flower cathode No. 1, provided a relatively large number of folds. In design 2, which originally was adopted for all other large thrustor cathodes, the number of folds was reduced to prevent short circuits between neighboring surfaces and to provide sufficient space for the plasma to penetrate to the deep end of the folds. In the latter part of this

program, design 4 was adopted. Its purpose was to lower the emission current to about 4 A, since it was found that the highly efficient 15-cm thrustors developed at Hughes required only half of the original design current of 4 A. In these latest flower cathodes, the emission density is somewhat increased which does not appear to be detrimental to the cathodes. Design 4 cathodes were wound into a spiral shape (see Fig. III-12), as contrasted with the original flower folds (Fig. III-6).

In general, the flower cathodes were found to withstand the adverse environment of discharge-plasma remarkably well. All of the designs evaluated easily passed the required 200 hour test. The first few cathode models gave projected lifetimes of the order of several thousand hours, which fell short of the planned 10,000 hour life span. Apparently, the oxide coating in these cathodes was still too thick, and overheating may have caused excessive loss of BaO by flaking. Later cathode models incorporated a coating of varying thickness which was sufficiently thin at the top of the folds to prevent overheating. Three of these cathodes ran for approximately 1000 hours. The cathode used in the latest 1000 hour test performed exceptionally well, even though it was exposed to atmosphere during a repair of the mercury feed system.

Two of the flower cathodes failed due to rupture of the supporting nickel mesh. After the first failure, the nickel alloy was changed and the mesh wire diameter was doubled. Subsequent flower cathodes used a mesh made from a nickel-tungsten alloy with a tensile strength twice that of the previously used alloy. A second failure which occurred after these modifications were made can be attributed to a vacuum failure.

Four disk cathodes were fabricated, and of these, three were tested. These disk cathodes were of two different designs. Design No. 1 incorporated relatively thick (1.2×10^{-3} cm) disks. It was found that disks and oxide coatings were eroded unequally. Since the disks were eroded at a smaller rate than the coating, this disk eventually stood out above the coatings and obstructed electron emission. The second generation of disk cathodes (no. 3 and 4), therefore, utilized substantially thinner disks (5×10^{-4} cm). Unfortunately, this led to another complication. Heat conduction along the disks to the cathode surface was made so difficult that a large temperature gradient arose. As a result, the nickel cup, containing the disks, had to be maintained at a high temperature which led to excessive power consumption.

The three impregnated cathode tested were supplied by NASA Lewis Research Center. These impregnated cathodes were of two designs: cylindrical and hole. Test of these impregnated cathodes show that the problems remaining are those of (1) maintaining an active emitting surface, (2) lowering the heater power to emitted current ratio, and (3) eliminating heater failures.

The nickel encapsulated cathode powder was used for a coating on the flower and cup cathode designs. The encapsulated powder was used for most of the spiral wound flower cathodes (Design 4), and for Flower Cathode No. 18 (Design 2). Flower Cathode No. 22, coated with the encapsulated

powder to a thickness of approximately 0.2 and 0.4 mm, performed satisfactorily in an operating thrustor for a period in excess of 1000 hours. This coating thickness is calculated to provide sufficient emittering material to withstand the mercury ion bombardment for 10,000 hours. This cathode remained an active emitter during the 1000 hour test, even though it was exposed to air during the repair of the feed system. Although the somewhat unreliable weight measurements indicate a 30% loss of coating weight for the 1000 hour test, visual inspection after test shows negligible ion erosion of the encapsulated oxide coating.

As previously discussed, the cup cathode using a 2 mm thick coating of encapsulated cathode powder can be considered an extension of the disk cathode design. The nickel coating on the powder serves as the conducting medium for the emission current and radiated heat. This encapsulated powder-cup cathode remains as a possible candidate for a 10,000 hour cathode, although it failed in its first test as a result of a heater failure. A larger heater area in relation to the electron emitting area and additional nickel encapsulate on the cathode powder for oxide layers as thick as 2 MM would be required for additional tests of this cathode design.

A description and the performance of each cathode is summarized in Table III. A more detailed discussion of the test results for each cathode is contained in the paragraphs that follow. The cathode temperature-heater power relationship and the emission current obtainable at the operating temperature are basic performance characteristics. The normal operating and activation temperatures for the oxide coated cathodes are 850 and 1000°C Br., respectively. The normal operating and activation temperatures for the impregnated cathodes are 1050 and 1150°C Br. The deviations shown from the normal operation temperatures (see Table III) resulted from (1) difficulty in maintaining an active emitting surface, (2) change in temperature-power relationship by cathode darkening, and (3) measuring the cathode temperature by its reflection from a mirror (for example, see Flower Cathode No. 22). Normally, the cathodes were evaluated at a fuel utilization (mercury flow) of about 85%. In some cases, e.g., with the impregnated cathodes, an abnormally high mercury flow was required to maintain an arc current. Tests conducted with abnormally high flow or poor fuel utilization are noted in the text.

B. Methods of Estimating Cathode Life

Cathode life estimates reported here will be different from some of the estimates reported earlier in the Monthly Progress Letters. Therefore, the different methods of estimating cathode life should be explained. Initially, the cathode assembly weights, including shields, insulators, leads, etc., before and after test were used to calculate the cathode coating loss. Nickel sputtered from the shields, deposits on the insulators, and the large ratio of assembly to coating weight contributed to inaccurate life estimates. In addition, water absorption to form barium hydroxide and hydrate after exposure to air led to false life estimates. In the latter part of the program, the method of determining the coating loss, was as follows. A sample of the coated mesh, not subjected to ion bombardment, was processes to remove the binder and CO_2 and was allowed to absorb water. The weight change of this sample was com-

TABI

Summary of Cathode Des

Cathode			Test Objective	Thruster Diameter, cm	Chamber Pressure, Torr	Mercury Flow, mA	Initial		
Type	Design No	Serial No					Heating Power, W	Temperature, °C, Br	Heating Power, W
Flower	1	1	Measure temperature – power characteristics		5×10^{-6}		62	800	90
Flower	2	2	200 hour life test	10	5×10^{-7}	230	85	890	115
Flower	2	3							
Flower	2	4	200 hour life test	10	$\sim 10^{-6}$	~200	17		36
Flower	2	5	200 hour life test	10	$\sim 10^{-6}$	175	60		80
Flower	3	6	1000 hour life test	10	$\sim 10^{-6}$	~200	25	750	50
Flower	2	7 to 10 and 12	20 cm thruster evaluation and study of cathode protecting grids	20					
Flower	3	11							
Flower	3	13	1000 hour life test	10	$<10^{-6}$	150	35	840	55
Flower	2	14-16	Delivered to NASA-Lewis Research Center						
Flower	2	17							
Disk	1	1	200 hour life test	15	$10^{-6} - 10^{-5}$	370	50	790	52
Flower	2	18	200 hour life test of Ni coated $BaCO_3$	15	$10^{-7} - 0.1$	~200	70	800	70
Disk	1	1	Continuation of disk cathode life test	15	$10^{-7} - 10^{-8}$	600	70	800	180
Disk	1	2							
Impregnated Cyl		2	200 hour life test	15	$10^{-7} - 10^{-4}$	~200	100	1090	170
Impregnated Cyl		3	200 hour life test	15	10^{-7}	~200	130	1100	234
Impregnated Hole		1	200 hour life test		10^{-7}	~900	210	1130	250
Disk	2	3	200 hour life test	15	$10^{-6} - 10^{-5}$	~250	117	890	180
Disk	2	4	200 hour life test	15	$10^{-7} - 10^{-6}$	~250	80	~700	150
Flower	4	19	Measure cathode voltage-current and temperature-power characteristics						
Flower	4A	20 & 21	Measure thruster performance	15					
Flower	4A	24	500 hour life test	15	10^{-7}	300	72	820	112
Flower	4B	22	1000 - 3000 hour life test	15	10^{-7}	300	50	~740	58
Flower	4A	25	Backup for 500 life test						
Flower	4A	26	500 hour life test	15	10^{-7}	300	50	810	82
Cup	1	1	200 hour life test	15	10^{-7}	~200	39	890	75

Note 1. – The mesh of the Design 4 flower cathode was wound into a spiral shape (Fig. III-18).

Note 2 – Flower cathode Nos. 18, 22, 23, and 26; and cup cathode No. 1 were coated with the nickel encapsulated cathode powder.

...E III

...cription and Performance

Final	Initial			Final		Test Duration, Hours	Cause of End of Test	Projected Life, Hours
Temperature, °C, Br	Arc Voltage, V	Arc Current, A	Heating Power/Arc Current W/A	Arc Voltage, V	Arc Current, A			
600						113	Test completed	
850	30-40	2-3	28	30-40	2-3	192	Hg supply exhausted	2,500
							Not tested – damaged in final fabrication stage	
	20	6	3	40	6	92	To install improved ion collector	1,200
	40	2	30	40	2	200	Test completed	1,450
< 900	40	2	13	40	2	835	Cathode open circuit – improperly applied voltage	> 3,000
						< 10 for each cathode	Test complete	
							Not tested – coating thickness modified at this point (see text)	
<900	40	1.2	29	40	1.6	945	Cathode open circuit	10,000
							Not yet tested	
700	40	4	13	40	4	324		~10,000
800	50	3.8	18	50	3.8	317	Cathode open circuit – high chamber pressure	
~950	20-60	4-1		20-60	4-1	480	Lack of cathode activation	10,000
							Not tested (see text)	
1200	20-100	4-0.1				97	Heater open circuit – high chamber pressure	
~1240	45	0-8		40	1.8	500	Heater open circuit – test complete	
1235	50	0-2		50	0-2	70	Heater open circuit	
1000	40	1.75	67	40	1.5-0	260	Test complete – high chamber pressure	
870	40	1.6	50	40	1.6	190	Test complete – W/A requirement too high	
							Test complete	
						~ 10 each	Test complete	
960	36	2.3	31	36	2.3	230	To replace power supply transformer	~10,000
~770	40	1.7	34	40	2.0	4014	Test complete	> 3,000
							Not tested	
							Not tested	
910	36	2.3		36	2.3	270	Test complete	~10,000
1050	45	1.0	39	45	~1	67	Heater open circuit	

pared with the weight change of a coated sample subjected to ion bombardment. The difference in coating weight changes between the two samples represented the loss of useful oxide resulting from ion bombardment. The loss due to ion bombardment was used in estimating the oxide coating life.

The procedure for determining weights of binder, CO_2, and water absorbed is as follows. The binder is eliminated by baking in air at 250°C. Weight losses resulting from this bakeout, from a group of 4 samples, ranged from 6.7 to 12.2%, with an average loss of 7.4%. For another group of 3 samples, the loss ranged from 3.4 to 4.1%, with an average of 3.7%. McNair[18] measured a 5.1% binder loss for a triple carbonate sprayed to a density of 2 g/cm^2. The CO_2 was removed from the carbonates by heating in vacuum at 1000°C. The average loss of CO_2 measured 22.2% for the first group of samples and 24.1% for the second group. The deviation of the individual samples from the group average was less than 5% except for one sample. The calculated or theoretical weight loss for CO_2 is 25.3%. From these results, it appears that a reasonably accurate and consistent measure of the CO_2 loss was obtained. Water absorption was determined after CO_2 and binder removal by measuring the sample weight as a function of time after exposure to air. The first weight measurement was made as soon as possible after removal from the vacuum system, within 1 to 3 min. The second weight was taken a few minutes later, and the resulting weight difference served as the first calculated weight gain. Thus the weight gain during the time from exposure to the first weighing, was not included as water absorbed, but dis subtract from the CO_2 loss. This method of determining the weight gain due to water absorption, with the inaccuracy resulting from the lack of a weight measurement before exposure to air, was used to avoid the complexity of making weight measurements within the vacuum system. The weight gain or water absorbed as a function of time is shown in Fig. III-1 for the mesh from three flower cathodes, Nos. 6, 18, and 24. The coating for cathodes No. 6 and 24 was the triple carbonate sprayed at 10 and 20 mg/cm^2, respectively. The coating for cathode No. 18 was nickel coated barium carbonate sprayed at 20 mg/cm^2. Assuming water is absorbed until an alkaline earth hydroxide-hydrate (e.g., Ba $(OH)_2 \times H_2O$) was formed, the weight gain due to water absorption amounts to 21.5%. As shown in Fig. III-1, the measured weight gain due to water absorption ranged from about 12 to 35%. This large range of measured water absorption is not unexpected since Haas and Jensen[19] measured one to five water molecules absorbed per oxide molecule, depending upon humidity and temperature. The large range of values for binder loss and water absorptions contributes to inaccurate life estimates. In other words, the uncertain weight changes by the binder and water cannot be distinguished from the loss of oxide coating by mercury ion sputtering. Although the life estimates are not as accurate as desired, the last column of Table III lists the projected life, based on these weight measurements, for a number of cathodes tested.

C. Flower Cathodes (with standard coating)

Flower cathode No. 1, design 1, was used to measure voltage-current and temperature-power characteristics and to establish whether or not the methods of supporting the mesh, lead attachment, lead insulation shielding, etc., were satisfactory. The voltage-current and temperature-power relationships were measured and this cathode was maintained at operation temperature,

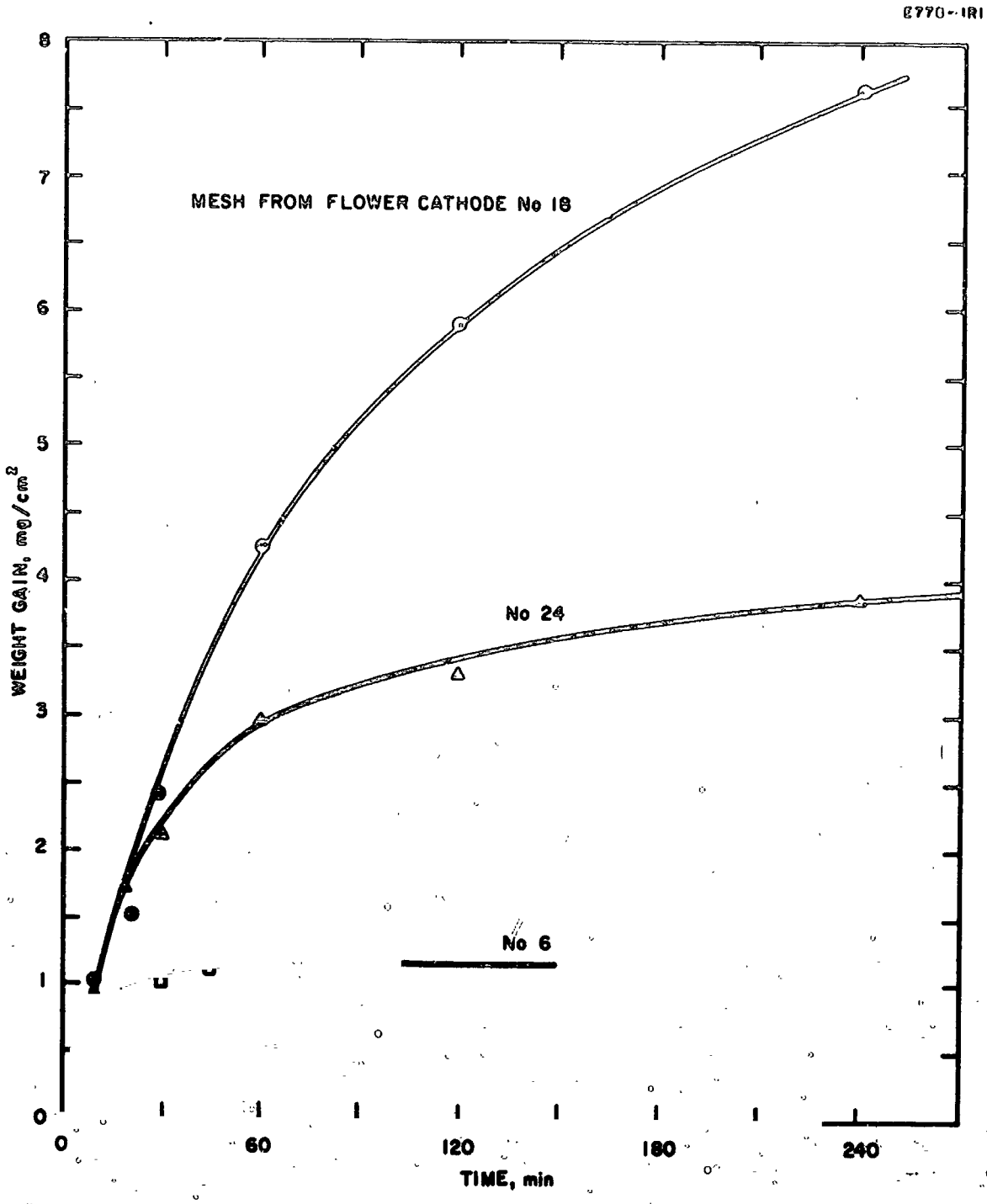

Fig. III-1. Weight gain or water absorption by a oxide coating as a function of time after removal from the vacuum system.

800°C Br or above, for 113 hours. A change in the temperature-power characteristic with time was measured. The hi[illegible]er power needed for a given temperature was assumed to hav[illegible] esulted from the darkening with time, which led to an increased radiation emissivity. This cathode was tested in a demountable oil diffusion vacuum system. The blackening was caused by a carbon deposit on the emitting surface. The emitting material was analyzed spectrographically after test and was found to contain 6.1% carbon, 33.5% barium, and 60% strontium. The performance of this cathode was considered satisfactory. The test was terminated after 113 hours to release the test set-up for other use.

Flower cathode No. 2, design 2, was fabricated for the first 200 hour test. The design change made increased the spacing between folds of the mesh to insure against short circuits. The standard triple carbonate (57% $BaCO_3$, 39% $SrCO_3$, and 4% $CaCO_3$) with a lucite binder was used. The coating thickness and weight were 0.012 in. and 27.9 mg/cm^2, respectively. The appearance of the coated mesh is shown by the photomicrograph of Fig. III-2. This cathode was installed in a 10 cm diameter thrustor and tested in a ft vacuum chamber. The voltage-current and temperature-power characteristics of the design 2 cathodes were only slightly different from those of design 1 (see Figs. III-3 and III-4). Cathode power, arc current, and arc voltage are shown as a function of time in Fig. III-5. A cathode power of 85 W was used initially; toward the end of test, it had to be raised to approximately 115 W. The initial and final heating power to emitted-current ratios were 28 and 58 W/A, respectively. The arc was maintained at approximately 2 to 3 A and 30 to 40 V. The test was terminated after 192 hours of arc time and 42 hours of mercury ion beam time when the mercury supply became exhausted (the mercury reservoir contained a change calculated for a 200 hour test.)

A photograph of the cathode after the test is shown in Fig. III-6. A large portion of the emitting coating on the top edge of the mesh has been sputtered away. Two small spheres of nickel are on the top edge of the mesh. These spheres were created by an arc concentration on a small area, which melted the nickel. This arc concentration, or concentration of emission within a small area, was thought to be caused by resistive heating in the oxide coating by the emitted current. (In order to solve this problem, the coating thickness of the following cathodes was reduced considerably.) In addition, the coating was blackened as can be seen from Fig. III-6. Spectroscopic analysis of the coating shows its major constituents to be 6% carbon, 36% barium, and 57% strontium. The presence of a significant amount of carbon stressed the need for an improved vacuum system. Accordingly, a new cryosystem was installed in the 2 ft chamber. A separate, ultraclean vacuum system was also developed which uses sublimation and ion pumps only. These vacuum facilities are discussed in Section IV.

The anticipated life of this cathode was estimated to be 2500 hours using the cathode weight measurements before and after the 192 hour test, as previously discussed.

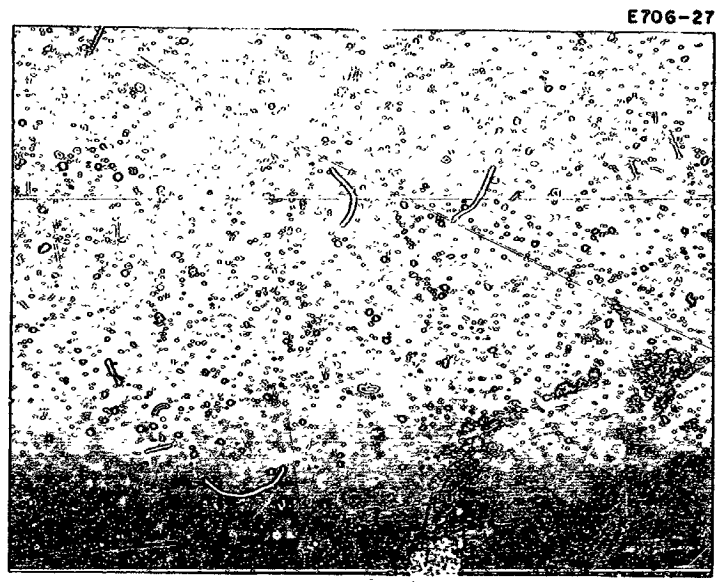

Fig. III-2. Triple carbonate coated ... sh of flower cathode No. 2, design 2.

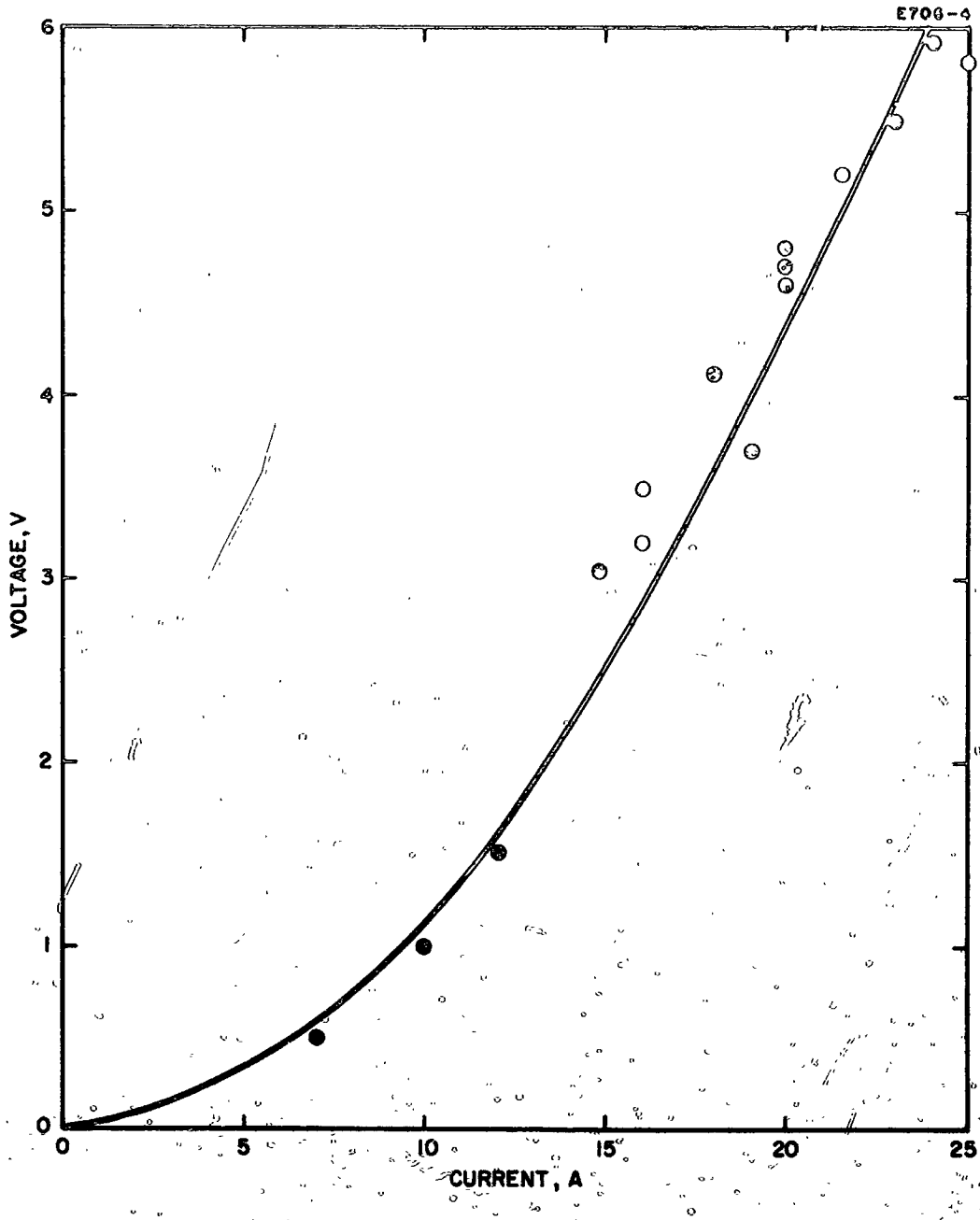

Fig. III-3. Voltage-current relationship for flower cathode No. 2, design 2.

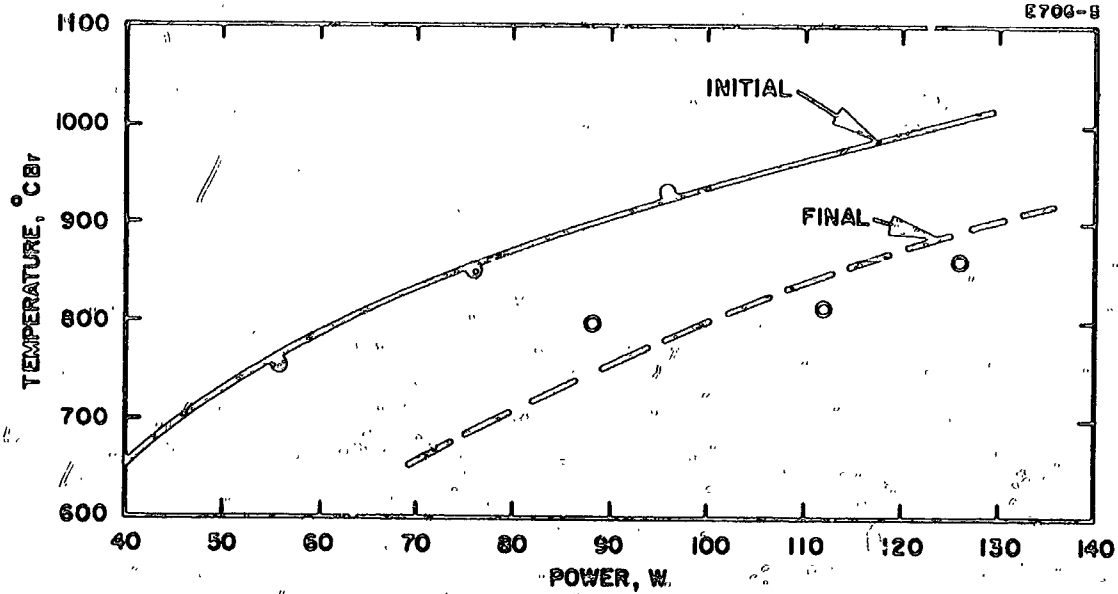

Fig. III-4. Temperature-power relationship for flower cathode No. 2, design 2.

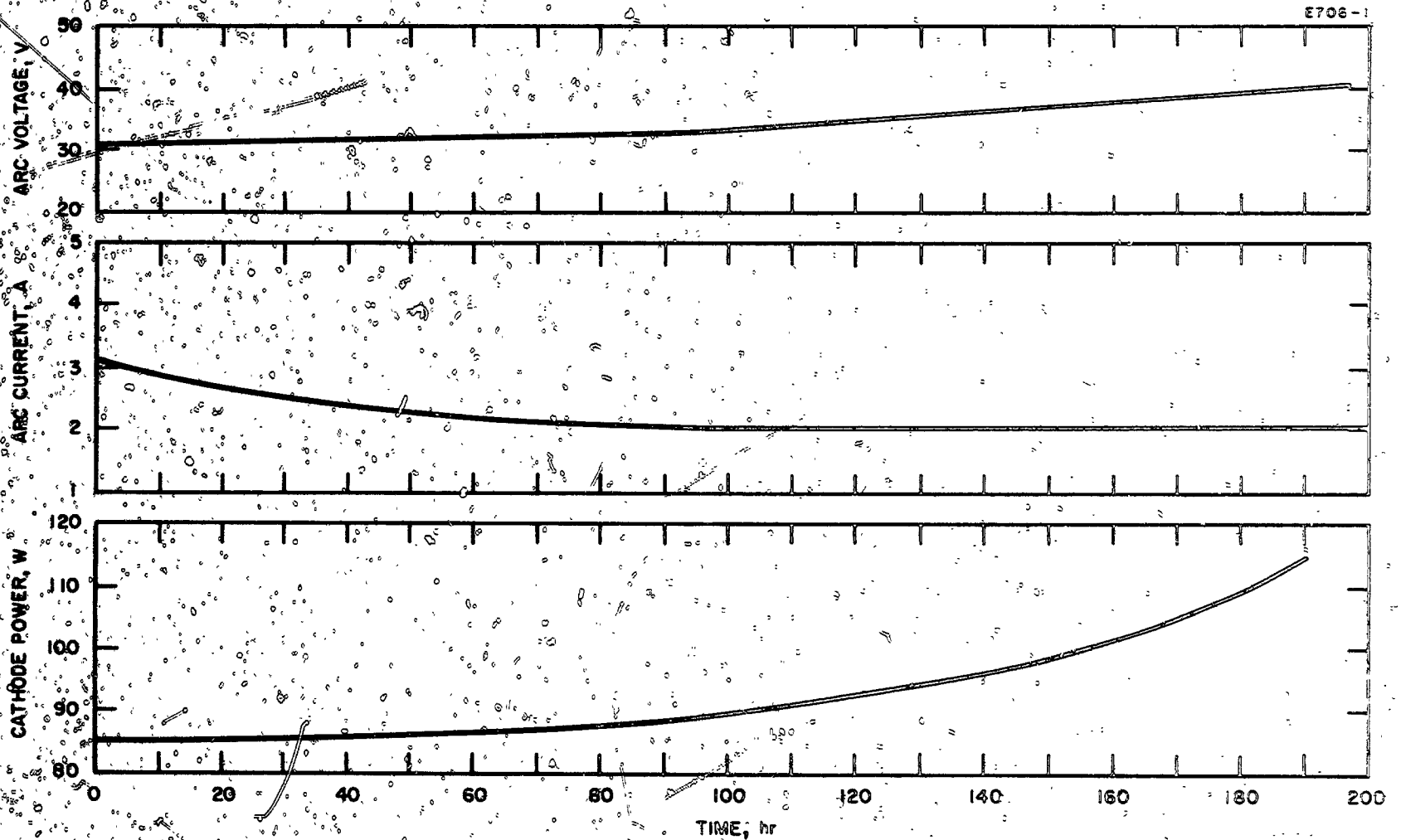

Fig. III-5. Cathode power, arc current, and arc voltage as a function of time for flower cathode No. 2, design 2.

M 3817

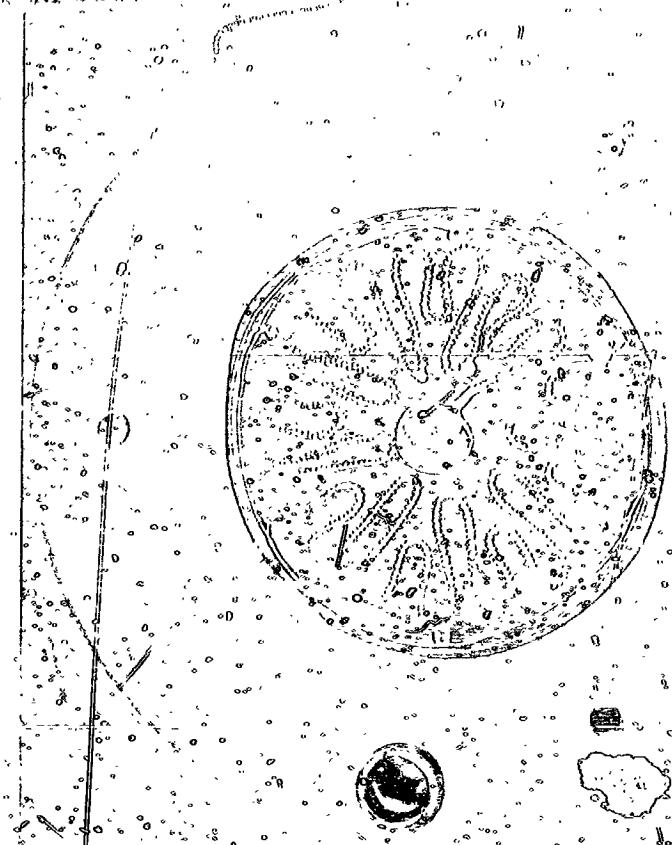

Fig. III-6. Flower cathode No. 2, design 2 after 192 hour life test.

In addition to the above discussed difficulties of obtaining accurate life estimates from weight measurements, some other difficulties in obtaining accurate coating weights involve (1) removing a portion of the mesh without losing any coating and (2) determining the amount of coating lost by flaking. Although some ion sputtering was noticeable at the top of the mesh, some cathode coating was lost by flaking and in removing the mesh from its supports.

Flower cathode No. 3 was lost in the final stages of fabrication and was discarded without testing.

Flower cathode No. 4, design 2, was assembled in a 10 cm thruster and tested in the 2 ft vacuum chamber. The initial coating weight was 28.7 mg/cm^2. Flower cathodes No. 4 and 5 were fabricated before the test results of cathode No. 2 were available, and their test evaluations were continued to substantiate the results obtained with cathode No. 2. The cathode was maintained at operating temperature for 92 hours. An arc current of 4 to 6 A was drawn for most of this period, and a mercury ion beam current of 150 mA was maintained for a small portion of this period. The test was terminated for the purpose of installing an improved ion collector in the 2 ft chamber. Using the initial coating weight of 28.7 mg/cm^2, the expected loss is 3.4 mg/cm^2. From weight measurements of the cathode assembly before and after test, the loss amounted to 1.9 mg/cm^2. The difference (1.5 mg/cm^2), or the loss as a result of life testing, was 7.5% of the initial net coating; therefore, from the 92 hour test a life projection of 1200 hours could be made. Visual inspection of this cathode shows that the coating loss resulted from flaking and no appearance of sputtering exists. For these relatively thick coatings, flaking appeared to be a severe problem.

Flower cathode No. 5, design 2, was also assembled into a 10 cm thruster and tested in the 2 ft vacuum chamber. The initial coating weight for this cathode mesh was .34 mg/cm^2. The duration of this life test period was 200 hours for cathode and arc, and approximately 70 hours for the ion beam. The cathode power used initially was approximately 60 W, and that used near the end of the 200 hour test was about 80 W. The arc voltage and current were varied considerably, but typical values were 40 V and 2 A. The ion beam current was approximately 125 mA. Again from cathode assembly weight measurements before and after test, the coating loss was 8.65 mg/cm^2. The loss from binder, CO_2, and water gain results in an expected loss of 5.4 mg/cm^2. The loss of useful coating of 3.25 mg/cm^2, or 37.8%, for the 200 hour test results in a calculated anticipated life of 1450 hours. Again from visual inspection, it is clear that the major loss of useful coating is a result of flaking instead of sputtering; therefore, the next flower cathode fabricated was coated with a thinner oxide layer.

Flower cathode No. 6 was a cathode using design 3, which was obtained by scaling down design 2. Design 2 was intended for a 15 cm thruster, but the thruster available initially was 10 cm in diameter and therefore required a smaller cathode for optimum performance. The earlier cathodes (No. 4 and 5) exhibited some autocathode effects in addition to the coating

flaking problem, which resulted in loss of control over the arc current. Therefore, cathode No. 6 was sprayed with a coating weight of only 10 mg/cm^2. This cathode was mounted in a 10 cm thrustor and life tested for 835 hours in the 2 ft. vacuum chamber. A mercury ion beam current of approximately 130 mA was drawn for over 100 hours. The initial cathode power was 25 W, increasing to 50 W near the end of the test. The voltage-current and power-temperature characteristics of this cathode design are shown in Figs. III-7 and III-8. The arc voltage and current were 40 V and 2 A throughout most of the 835 hours. This test exceeded the normal 200 hour test for the purpose of improving the accuracy of the anticipated life estimates. The test was terminated after 835 hours because of damage inflicted on the cathode during repair of a power supply. Line voltage became accidentally connected across the cathode, melting a portion of the mesh and shields. As a result, weight measurement of the total cathode assembly after test was meaningless. A portion of the undamaged mesh was removed from the cathode, and the coating weight remaining after test was compared with that of an unused portion of the same mesh. This unused coated mesh was an excess portion of the mesh used in the fabrication of cathode No. 6. The unused mesh was fired to remove binder and CO_2, and water was absorbed so the coating weights of the unused and tested mesh were comparable. The original coating weight of 10 mg/cm^2 was reduced to 8.55 mg/cm^2 after removal of binder and CO_2 and after water absorption. The coating weight after test was 6.25 mg/cm^2. A loss of 2.30 mg/cm^2 could be attributed to ion bombardment during this 835 hour life test, resulting in a projected life of over 3000 hours. However, some coating was lost as the tested mesh was removed from the cathode and, therefore, life considerably in excess of 3000 hours could be expected.

Cathodes No. 7 through 10 and No. 12 were all of design 2. These cathodes were installed in 20 cm diameter thrustors and tested in the 9 ft. vacuum chamber. These tests were conducted for the purpose of studying various aspects of 20 cm thrustor performance and they lasted for only several hours. One objective of these tests was to determine the utility of grids for shielding against ion bombardment. The grids were placed in front of the cathode and consisted of two types: (1) 1/8 in. diameter holes spaced so that 33% open area resulted in a 0.030 in. thick plate, and (2) a honeycomb 1/4 in. by 1/4 in. and 1/4 in. thick. The required arc current for reasonable arc voltages (less than 100 V) could not be obtained with either of these grids.

Cathode No. 11 was of design 3. This cathode was completed with a coating weighing 10 mg/cm^2. On the basis of the test results for cathode No. 6, obtained during construction of Cathode No. 11, it was concluded that additional coating was needed to obtain 10,000 hour lifetimes. It was thus decided to coat future cathodes with a stacked multithickness coating. Cathode No. 11 was set aside untested.

Cathode No. 13, of design 3, was coated on the top third of the mesh with 10 mg/cm^2; the middle third was coated 20 mg/cm^2 and the bottom third with 30 mg/cm^2. Figure III-9 is a photograph of this multithickness coated mesh. The cathode was installed in a 10 cm thrustor and tested in the 2 ft.

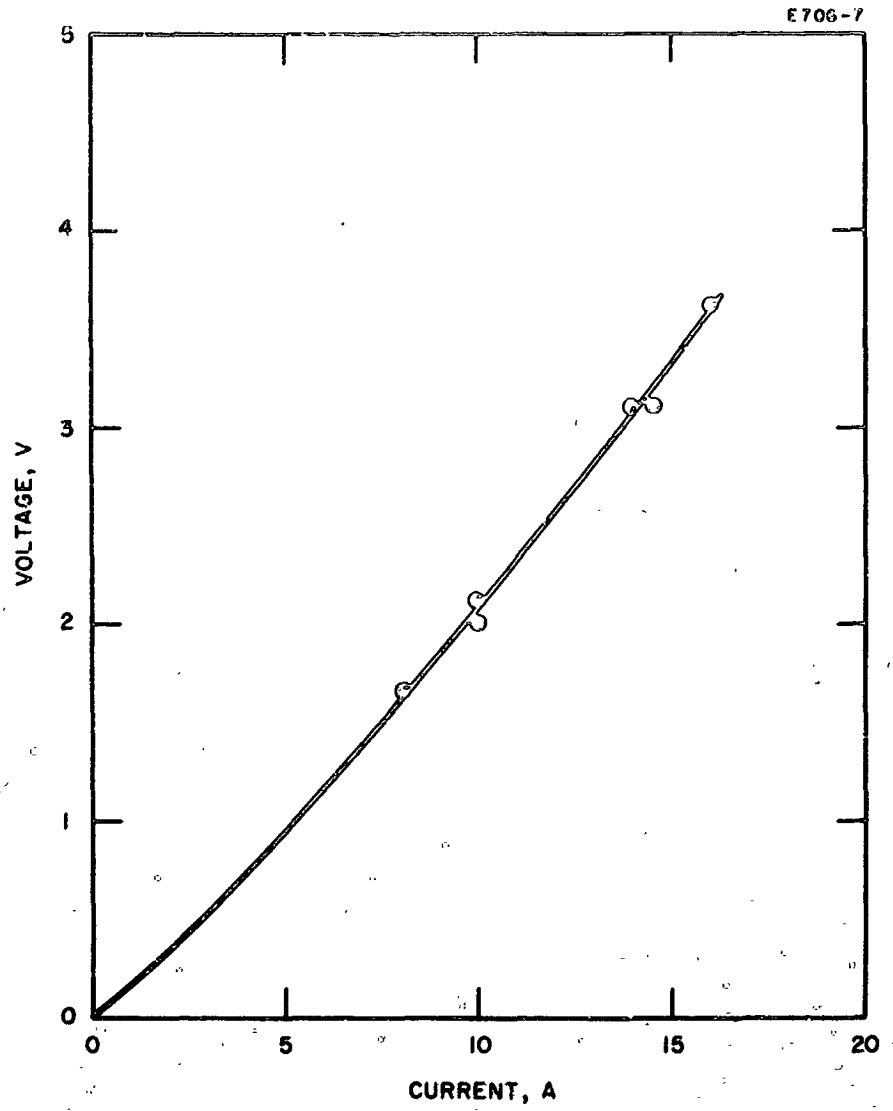

Fig. III-7. Voltage-current relationship for flower cathode No. 6, design 3.

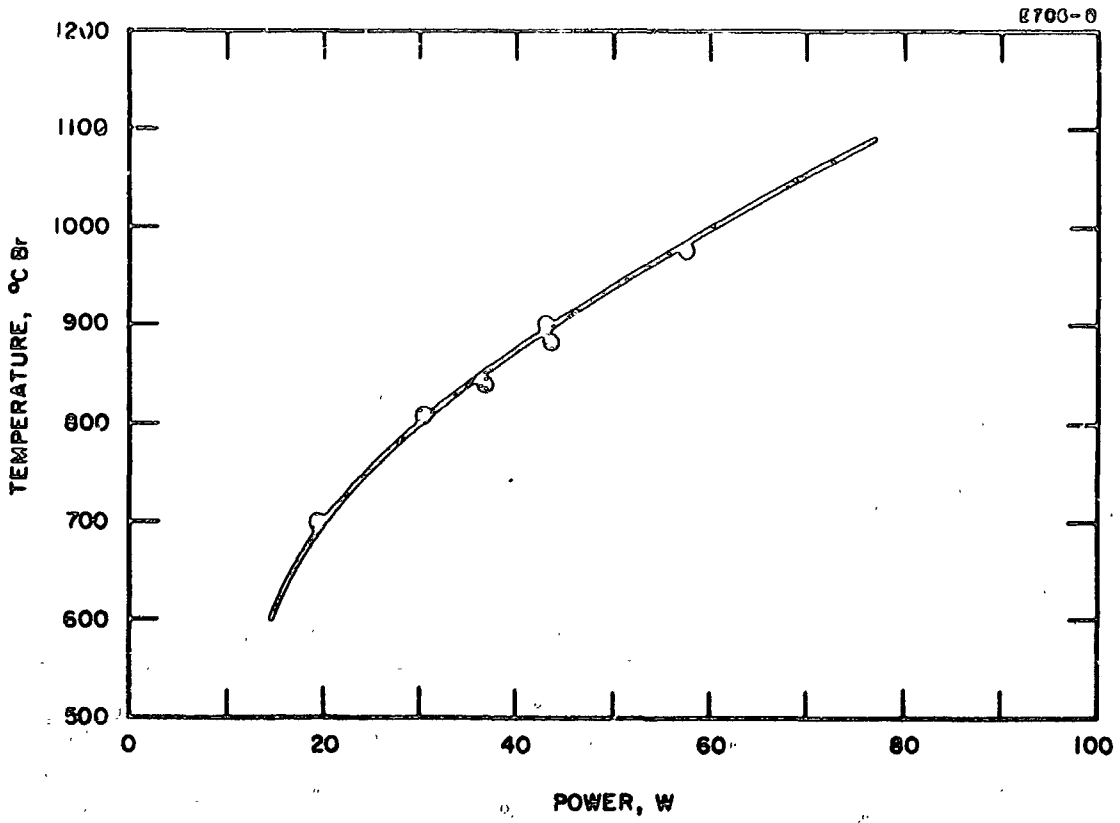

Fig. III-8. Temperature-power relationship for flower cathode No. 6, design 3.

E706-20

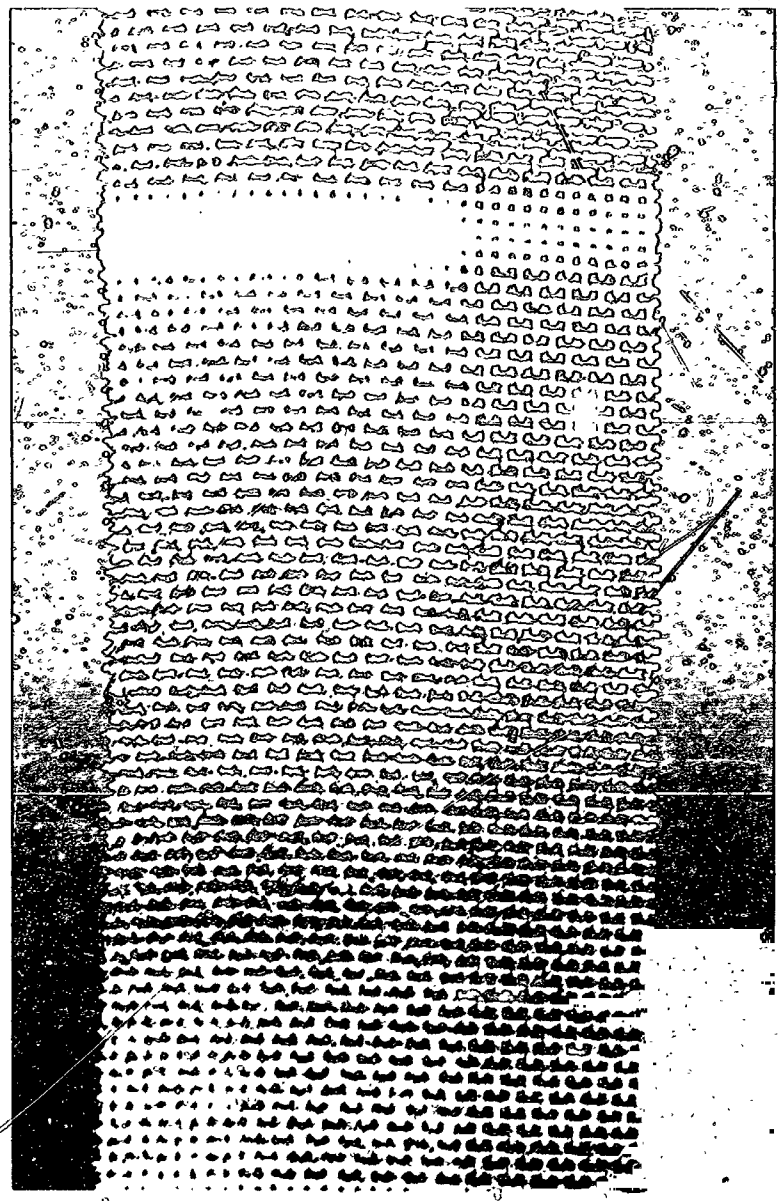

Fig. III-9. Multithickness coated mesh (10, 20, and 30 mg/cm^2) of flower cathode No. 13, design 3.

vacuum chamber. A mercury ion beam current of approximately 125 mA was maintained for 846 hours, and an arc current and voltage of about 1.2 A and 40 V were maintained for 915 hours. The cathode was at operating temperature for 945 hours. This test was scheduled for 1000 hours, but terminated short of this goal because of an open circuit in the cathode mesh. Figure III-10 shows this cathode assembly after test. The open circuit is shown in the upper left portion of the Fig. III-10. Figure III-11 shows the effect of the ion bombardment. Several of the nickel wires are eroded away at the top of the mesh; some of the coating missing at the bottom of the mesh was lost in removing and straightening the mesh. Figure III-12 is a photomicrograph showing a portion of the mesh. At the top, the nickel wires are eroded away. Farther down, the oxide coating is sputtered from the wires, still farther down the oxide coating is covered with a layer of nickel, and at the bottom the oxide coating is unaffected. Figure III-13 is a greatly enlarged view of the nickel wire which clearly shows the deposited nickel on the oxide coating.

The original calculation of coating lost from cathode No. 13 during test was 10.1%, as reported in the Monthly Progress Letter. However, the present coating weight measurements, taken by stripping a tested and untested portion of mesh, including the expected changes due to binder and CO_2 loss and water absorption, show a 1.3% gain in coating weight during test. These measurements include the nickel deposited on the oxide coating as useful oxide. This deposited nickel is stripped from the mesh along with the oxide coating. Neither the 10.1% loss nor the 1.3% gain accurately represents the change in amount of useful oxide coating during test. A precise method of determining the life on the basis of coating weight changes has not yet been developed. Even so, Figs. III-10, III-11, and III-12 show most of the coating remaining after this 945 hour test. On this basis, it is not unreasonable to expect a 10,000 hour life for the oxide coating.

While the effects of the mercury ion sputtering upon cathode No. 13 were essentially as expected, the open circuit or failure of the nickel wire is not completely understood. The ends of the nickel wire at the open circuit are shown in Fig. III-14, and the wires appear to be broken rather than melted. Figure III-15 compares the surface of the wires before and after test. After test, smoothness of the surface is lost. Figure III-16 shows the grain structure before and after test. The grain structure does not appear significantly altered. The nickel used in all cathodes to this point was International Nickel Co. Alloy 200. Subsequent cathodes, No. 14 to 26, were made using Superior Tube Co. Alloy A33. This alloy contains 2% tungsten and has a tensile strength twice that of Alloy 200 at operating temperature. In addition, all cathodes subsequent to No. 13 were fabricated with 0.009 in. diameter wire instead of 0.0045 in. diameter wire.

Cathodes No. 14 through 17 were fabricated using design 2 and sprayed with multithickness coatings of 10, 20, and 30 mg/cm^2. The first three of these cathodes were sent to NASA-Lewis Research Center as part of the contract commitment. Life testing of cathode No. 17 was deferred in order to evaluate other cathode designs.

M 4216

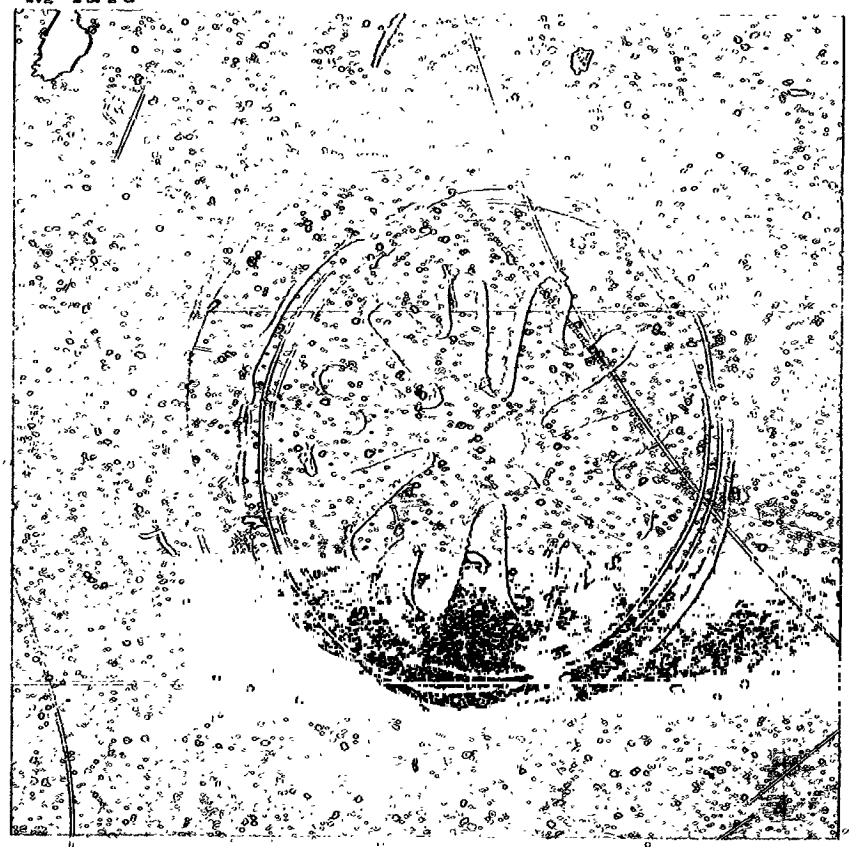

Fig. III-10. - Flower cathode No. 13, design 3 after 945 hour life test.

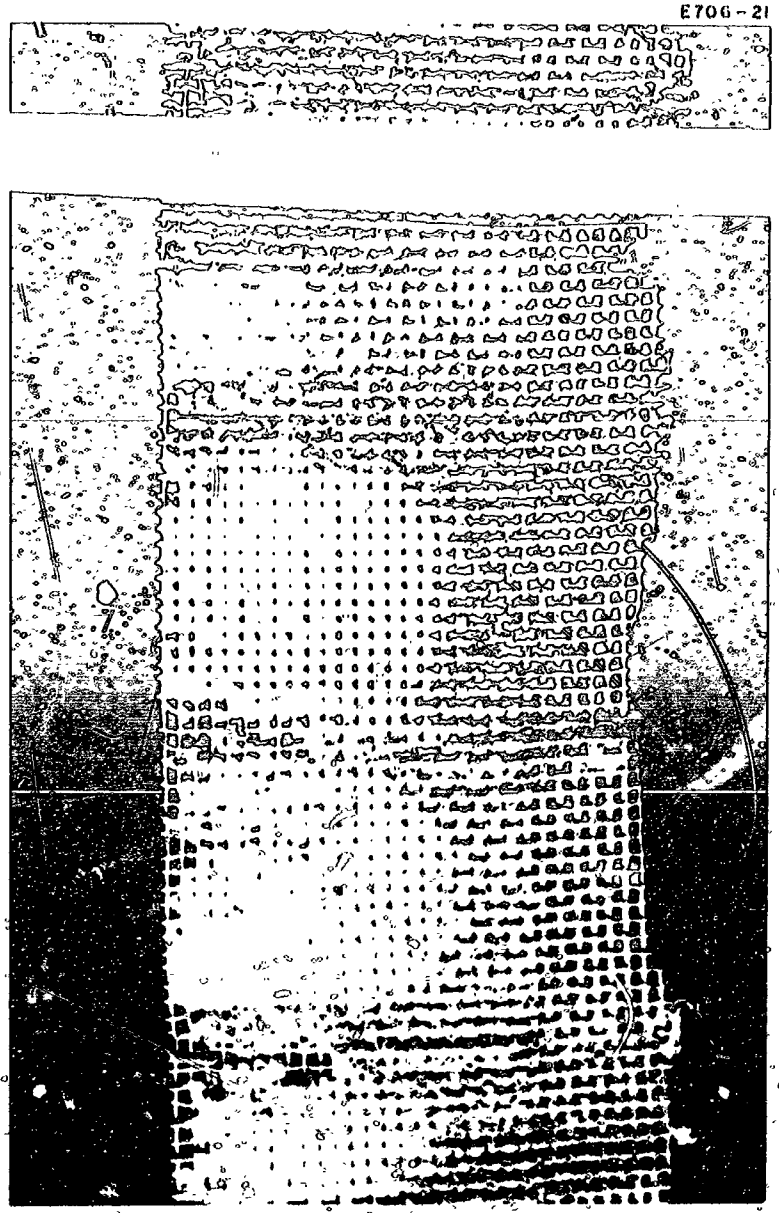

Fig. III-11. Detail of the coated mesh after test, showing the erosion by mercury ion bombardment. Flower cathode No. 13, design 3.

E706-26

Fig. III-12. Photomicrograph of flower cathode No. 13 mesh after life test showing erosion of nickel wires, nickel deposit on oxide coating and normal oxide coating.

Fig. III 13. Photomicrograph of nickel wire (cathode No. 13) showing the metal deposit on the oxide coating. The oxide coating is not visible.

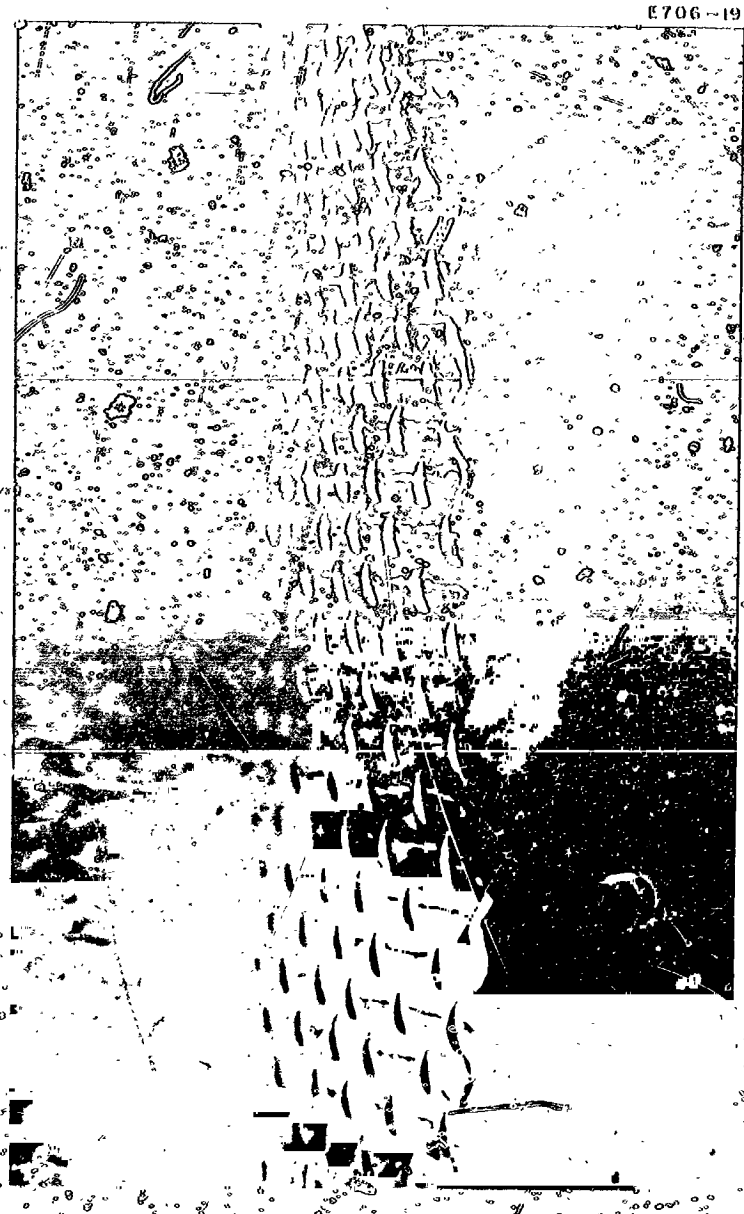

Fig. III-14. Ends of nickel wire at the open circuit cathode No. 13.

Fig. III-15. Comparison of the nickel wire surface: (a) Before test, (b) After life test, Cathode No. 13.

Fig. III-16. Comparison of the [illegible] nickel wire (UFCO [illegible]) (a) before test and (b) after [illegible]. Orig. No. 13

Performance characteristics of the design 2 and 3 flower cathodes in 10 cm thrustors are shown in Fig. III-17 by the plots of mercury arc discharge current as a function of arc voltage. The dashed portion of curve (a) shows that the arc extinguishes at approximately 29 V. Although the arc characteristics of the flower cathodes in the 10 cm thrustors varied considerably depending on the cathode activity, cathode power, resistive heating in the oxide coating, mercury flow rate, chamber pressure, etc., the curves of Fig. III-17 represent typical performance of active flower cathodes. The magnet current was set at the lowest value obtainable without decreasing arc current for the nominal arc voltage setting.

Flower Cathodes No. 19, 20, 21, 24, and 25

These cathodes were designed and fabricated for evaluation using a Lewis Research Center thrustor, Hughes solar panel-power conditioning equipment, and the Hughes 9 ft cryowall vacuum chamber. The heater supply output was limited to 3.25 V and 50 A. Cathode No. 19, design 4, was heated in a vacuum system for the purpose of establishing the voltage-current and heater power-temperature characteristics. The required heater voltage was slightly greater than desired. Therefore, the design was modified by a 10% decrease in cathode mesh length. This modified cathode design was labeled design 4A. All remaining cathodes of this series, Nos. 20, 21, 24, and 25 were of design 4A. The dimensions of these cathode designs are listed in Table II. All of these cathodes were coated with a triple carbonate multithickness layer of 10, 20, and 30 mg/cm^2. Fig. III-18 is a photograph of one of the design 4 cathodes, before test. Cathodes No. 20 and 21 were tested for less than 10 hours each. The purpose of these tests was to establish thrustor and power conditioning performance. Life test of this series of cathodes was initiated with cathode No. 24. Cathode voltage-current and power-temperature characteristics for design 4A cathodes are shown in Figs. III-19 and III-20. The two curves of Fig. III-20 are for cathodes Nos. 20 and 24. This shown spread in cathode temperature for a given heater power was caused by the varying degrees of cathode darkening.

Life testing of cathode No. 24 was performed with the thrustor operating parameters set as follows:

accel voltage	= 3.5 kV
decel voltage	= 2.5 kV
beam current	= 250 mA
arc voltage	= 36 V
arc current	= 2.3 A
mercury flow	= 300 mA.

The power conditioning equipment was set to increase cathode power to maintain a constant beam current. The resulting variation of cathode power and temperature with life is shown in Fig. III-21. Life testing of cathode No. 24 was terminated after 230 hours. This cathode test was terminated due to its exposure to the atmosphere. This exposure was necessary to replace dam-

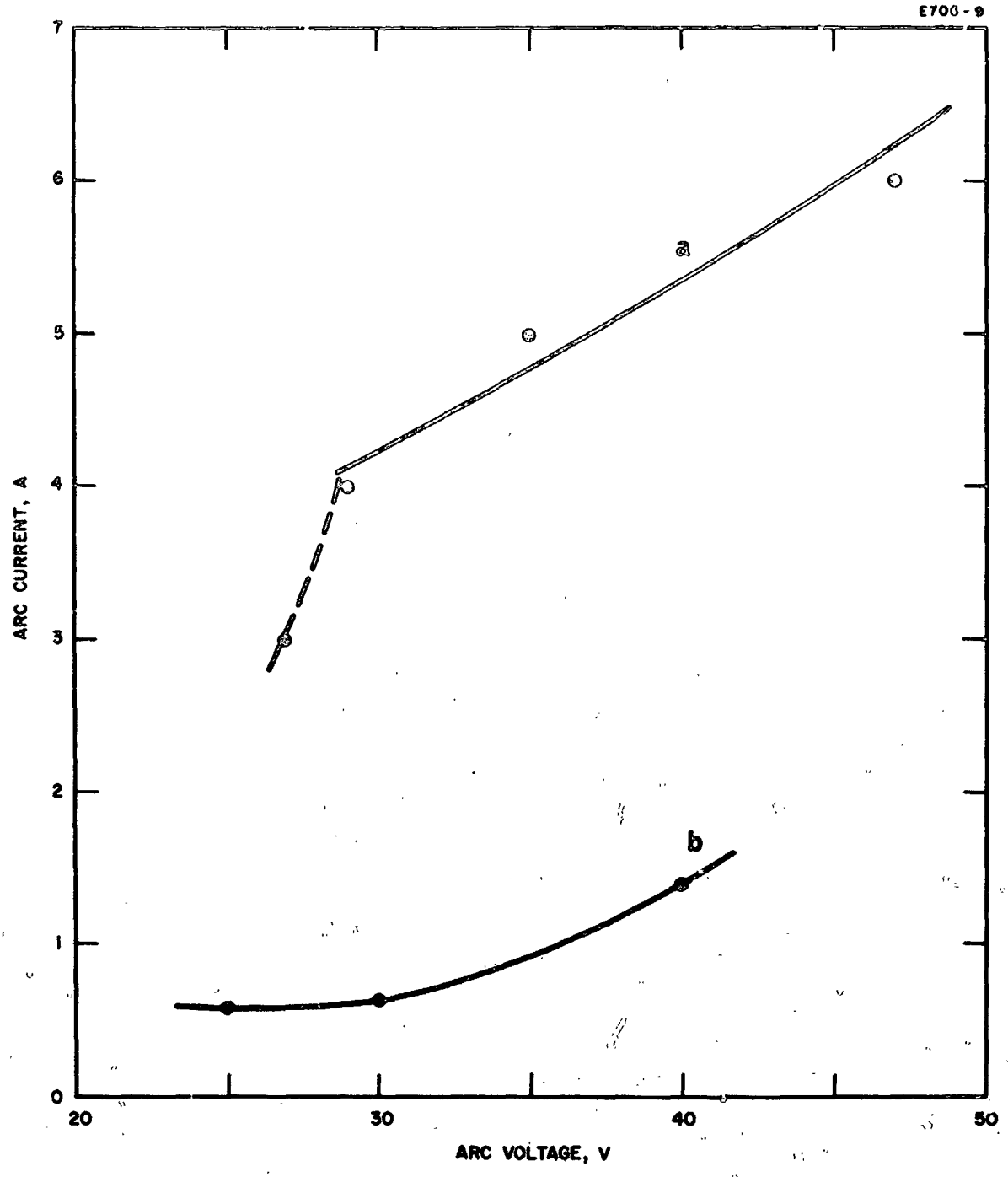

Fig. III-17. Arc current as a function of arc voltage. (a) For flower cathode No. 2, design 2 in a 10 cm thruster with a cathode power of 96 W, mercury flow of 230 mA, and a magnet current of 10 A. (b) For flower cathode No. 13, design 3 with a cathode power of 28 W, mercury flow of 150 mA, and a magnet current of 10 A.

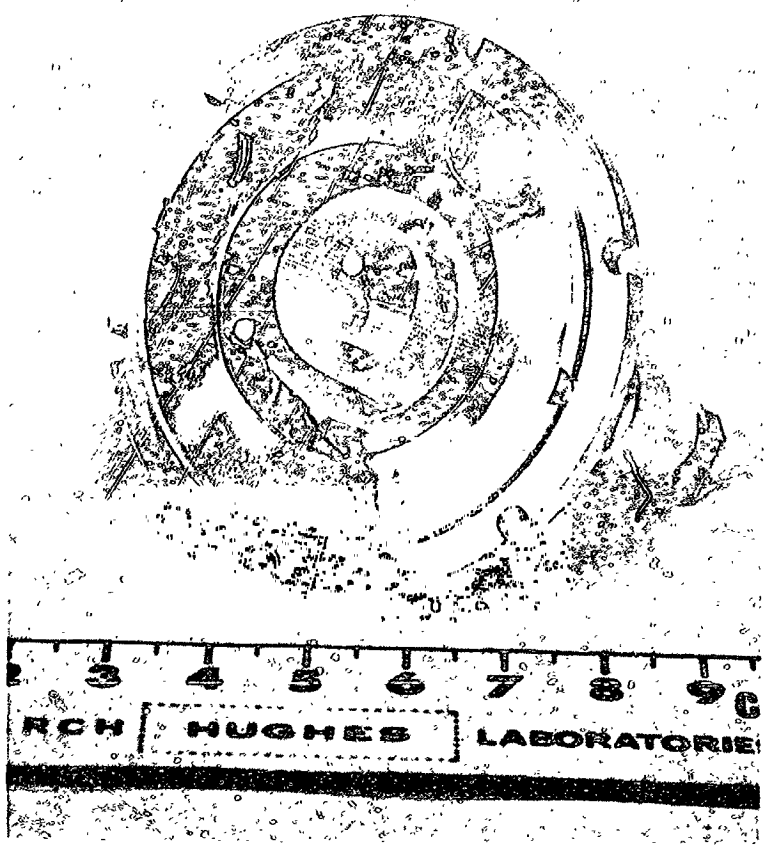

Fig. III-18. Flower pod, design 4A before test.

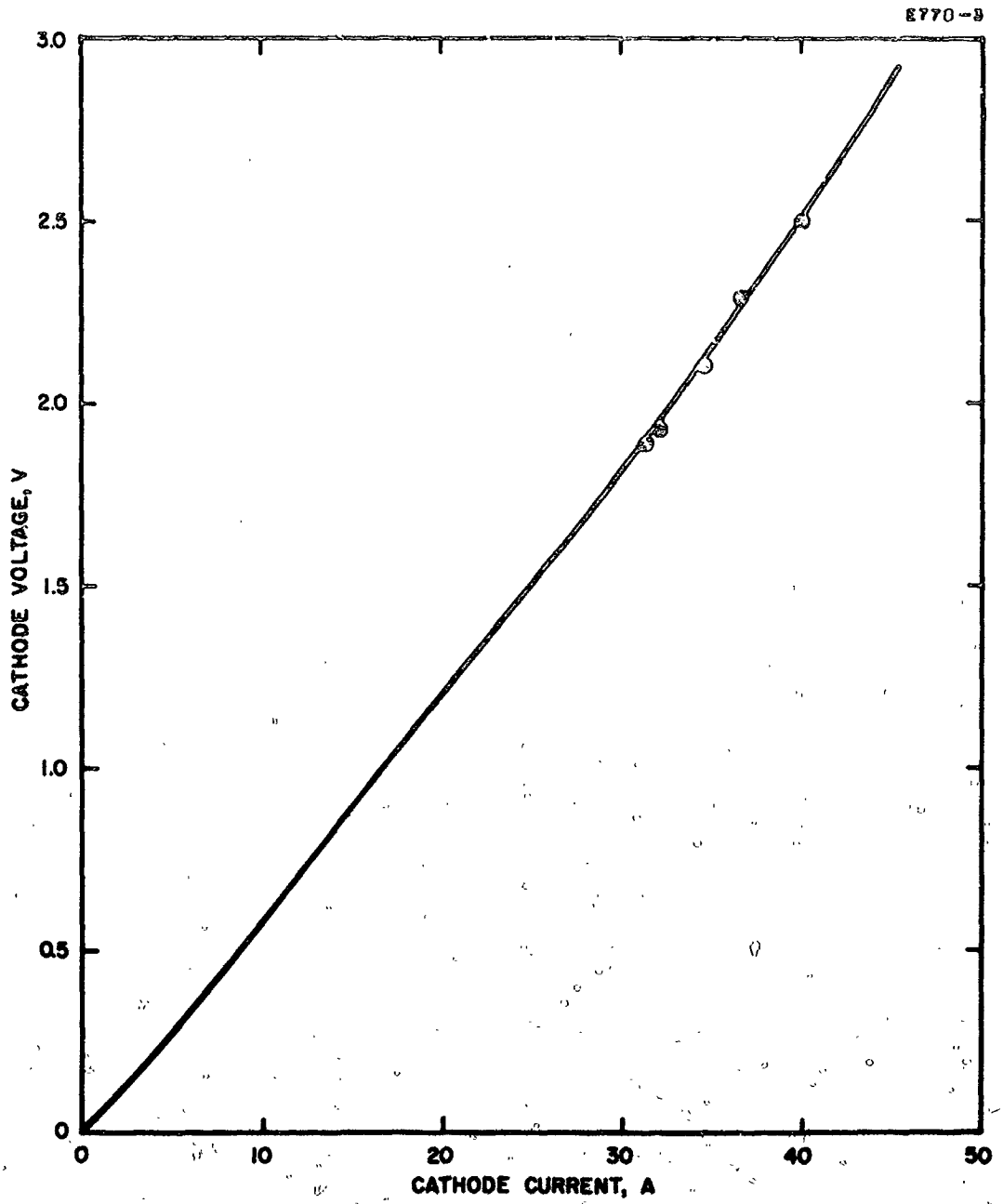

Fig. III-19. Flower cathode No. 24, design 4A.

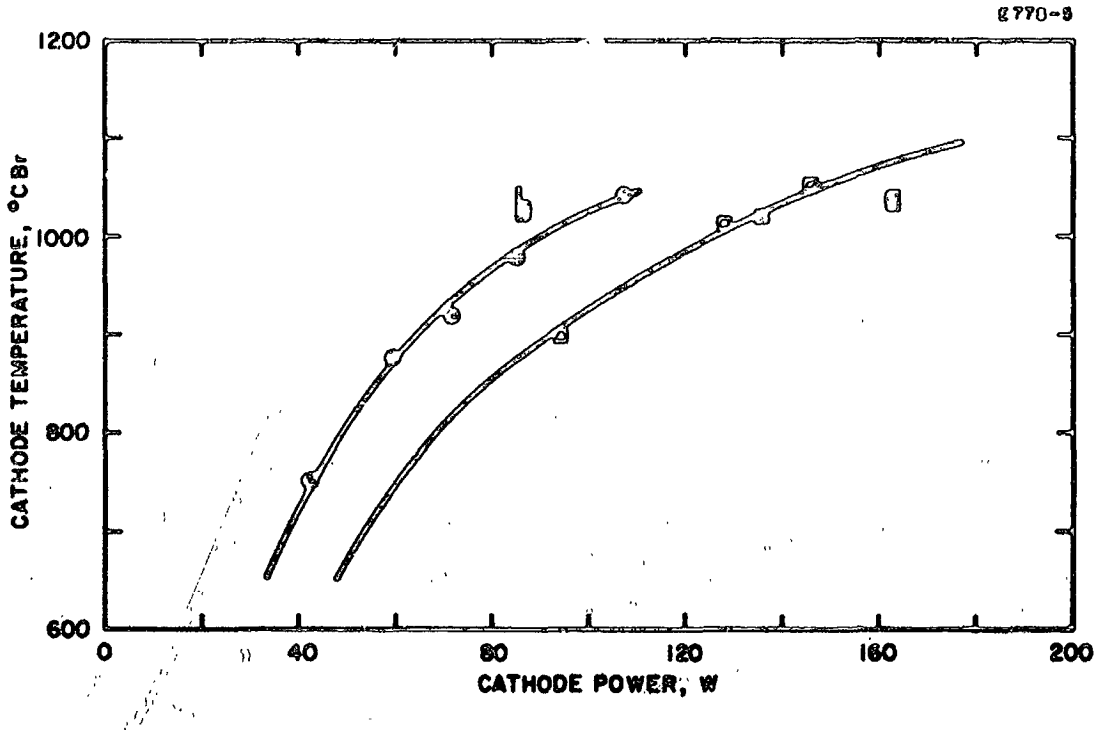

Fig. III-20. Temperature-power relationship for (a) flower cathode No. 20 and (b) flower cathode No. 24, designs 4A.

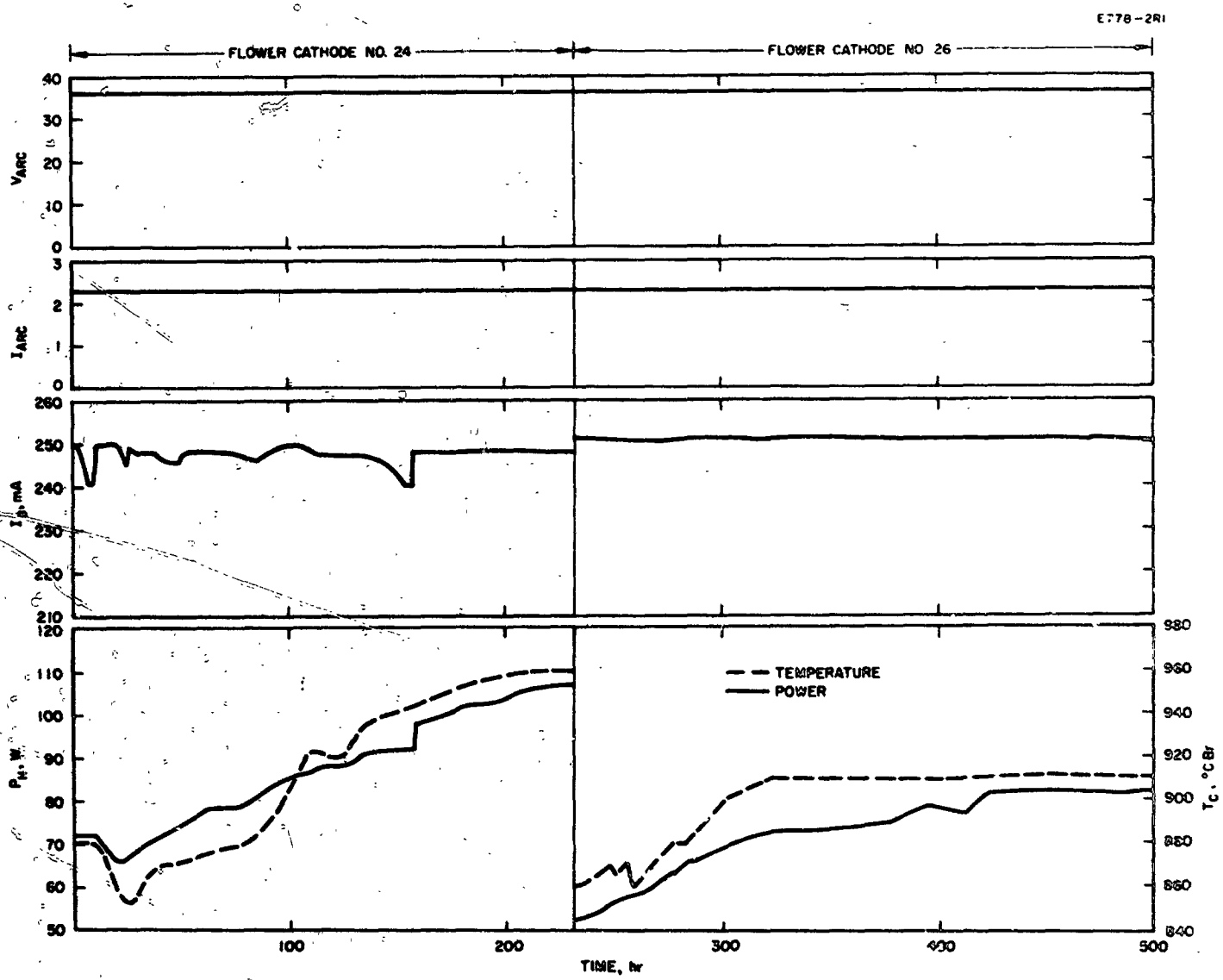

Fig. III-21. Arc voltage, arc current, beam current, cathode temperature, and heater power as a function of life for flower cathode Nos. 24 and 26, designs 4A.

aged filament transformers withinthe vacuum chamber. Upon removal of this cathode from the thrustor, it was noted that the oxide coating was discolored, indicating a carbon deposit. Chemical analysis of the oxide coating indicated that its composition was at least 3% carbon. This carbon deposit undoubtedly was responsible for the increasing cathode thermal emissivity, thereby requiring an increasing heater power with life. Also, the carbon coating probably contributes to decreased cathode emission, thereby requiring an increased cathode temperature. (See Fig. III-21.) The carbon deposit on the cathode was a result, in part, of a layer of diffusion pump oil in the bottom of the 9 ft chamber. This oil had accumulated due to back streaming. This oil film was removed in order to improve cathode performance during the next test. The test was then resumed and successfully completed with cathode No. 26. Because this cathode had an encapsulated powder coating, it will be reported further on, in Section III-F.

Cathode No. 25 was fabricated as a back-up for cathode No. 24. Cathode No. 26 was used for continuation of these tests, therefore, cathode No. 25 was not needed; hence, it has not been life tested.

D. Disk Cathodes

Disk Cathode Nos. 1 and 2.

The disk cathode was the second type of cathode to be evaluated under this contract. This cathode design was to maintain the advantage of the flower cathodes, e.g., the low work function of an oxide coated nickel surface, yet provide greater storage of emitting material and increased reliability with an indirect heater. This cathode contained 50 nickel disks (0.0005 in. thick) coated with a triple carbonate layer of 10 mg/cm^2. This provided a storage of about 7 gm of emitting material. This cathode ready for installation in a 15 cm simulated thrustor, is shown in Fig. III-22. This cathode-thrustor combination was tested in the mercury vacuum station. This test lasted 324 hours for the cathode; the arc was burning during 267 hours. The initial and final cathode temperature-power relationships are shown in Fig. III-23. Heater power, mercury flow rate, arc current and voltage, and magnetic field were varied through this life test. However, the nominal values for these parameters were heater power equal to 52W, mercury flow rate of 370 mA, arc current of 4 A at an arc voltage of 40 V, and a magnetic field of 20 G.

The performance of the disk cathode in the simulated thrustor is best shown by plotting the test data as described below. Figure III-24 shows the arc voltage as a function of cathode temperature for a fixed arc current, mercury flow rate, and magnetic field. The cathode temperature plotted on the abscissa is that temperature resulting from the heater power setting only, that is, the heater power remains constant for each data point and determines the cathode temperature plotted. As the arc voltage is increased (constant arc current) the arc power obviously increases, and part of this increased arc power is used to heat the cathode. The increased arc voltage

M 4204

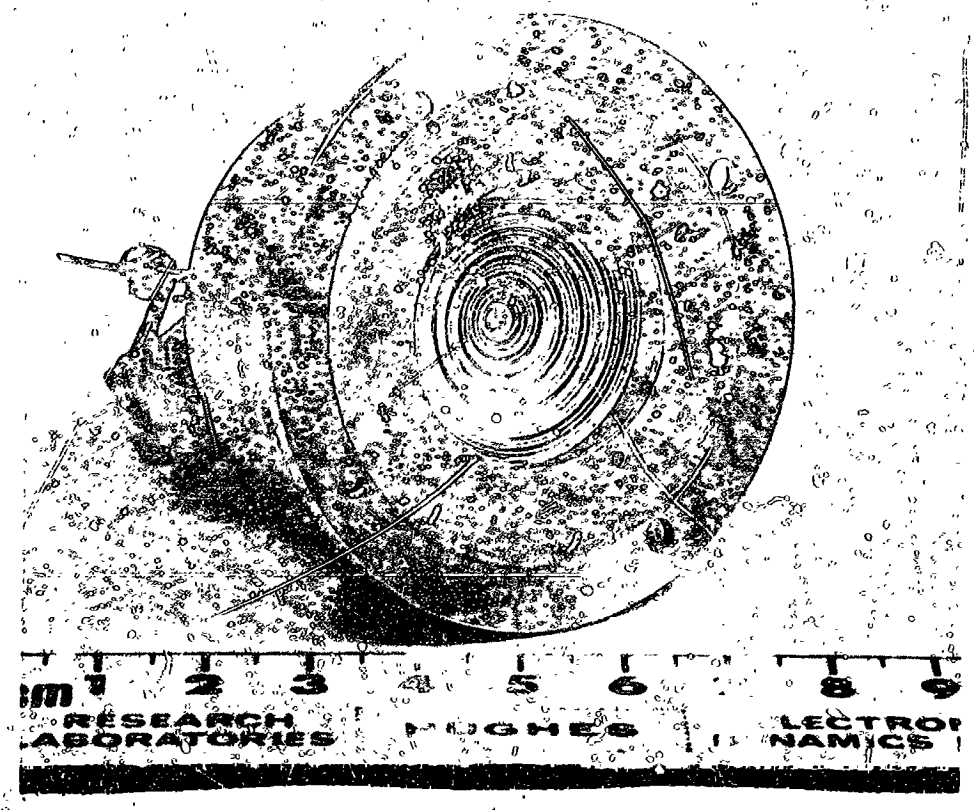

Fig. III-22. Disk cathode assembly No. 1.

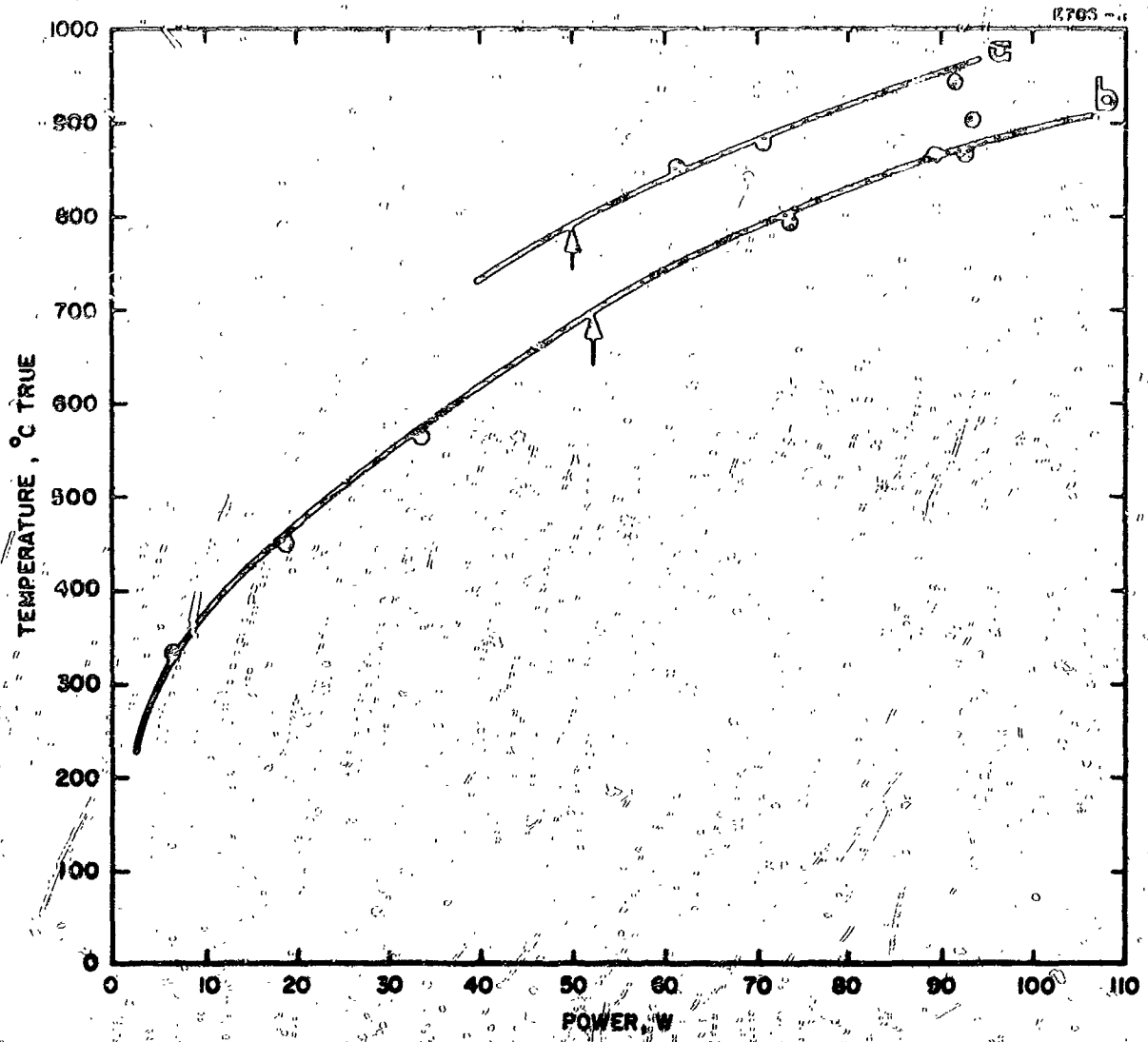

Fig. III-23. Temperature-power relationship for disk cathode No. 1. (a) Initially. (b) At end of life test. Arrows indicate operating temperatures.

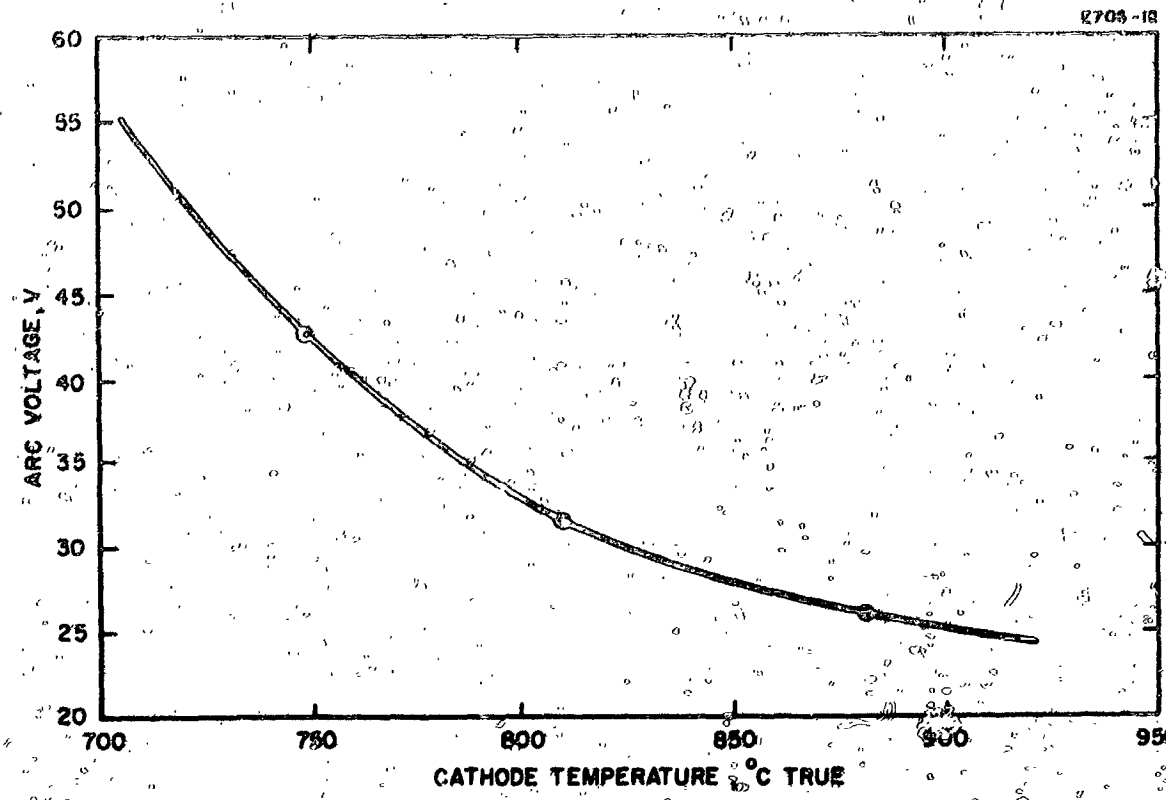

Fig. III-24. Arc voltage as a function of cathode temperature for an arc current of 4 A, mercury flow rate equivalent to 320 mA, and magnetic field of 19 G. Disk cathode No. 1 in simulated thruster No. 1.

increases the Hg ion energy, and ion erosion of the emitting surface should increase. Since the cathode emission level increases (or cathode temperature decreases) with increasing arc voltage, the cathode heating by the arc power more significantly determines the emission level than does the increased ion erosion. This cathode design appears to be quite resistant to ion sputtering damage. Arc current as a function of arc voltage for fixed mercury flow rate, cathode temperature, and magnetic field is shown in Fig. III-25. Figure III-26 shows the arc voltage as a function of magnet current for all other parameters fixed and Fig. III-27 shows the arc current as a function of magnet current for all other parameters fixed. Finally, Fig. III-28 shows the arc voltage as a function of mercury boiler temperature or mercury flow rate, again with all other parameters fixed. The calibration of the mercury feed system is shown in Fig. III-29.

The performance of the disk cathode in the 15 cm simulated thrustor at the end of the 324 hour test was essentially the same as at the beginning. The most significant change in this cathode during test was in appearance; Fig. III-30 shows this cathode after test. The flaking of the coating was caused partly by water absorption upon removal from the vacuum system. The black deposit covering most of the cathode is believed to be carbon (this is based upon previous analysis of darkened cathode coatings). The deposit on the vacuum envelope (see Fig.IV-2) was spectrographically analyzed and found to be 18% chromium, 10% nickel, and iron. Anode and screen are made from 304 stainless steel. Mercury ion sputtering of the screen undoubtedly results in the deposit on the glass envelope.

Weight measurements of the cathode-heater assembly before and after test show a weight loss of 2.18 g. The expected loss from binder and CO_2 is 2.2 g. Loss of nickel sputtered from the front cathode shield is readily apparent from a comparison of Figs. III-22 and III-30. This loss of nickel could balance the gains resulting from water absorption and "carbon" deposition. It is concluded that the loss of oxide coating due to mercury ion sputtering is not significant.

Disk cathode No. 1 was subjected to a second test. It was placed in the ion-sublimation vacuum chamber which is free of O-rings, greases, and oils. Therefore, hydrocarbons should not be present. The objectives of these tests were (1) to determine to what extent this cathode could be reactivated after exposure to the atmosphere, (2) to investigate removal of the black coating by mercury ion sputtering and (3) to extend the life testing of the heater-cathode assembly. As compared with the first test of this cathode, a further increase of heater power is required for a given cathode temperature, as is shown in Fig. III-23. During this second test, the cathode never fully activated. The performance was characterized by operation at either low arc voltage and high current (20 V and 4 A) or high voltage and low current (60 V and 1 A). Stable operation at intermediate voltage and current could not be maintained. The heater power used ranged from 70 to 180 W. At low heater power and high arc current, localized heating or white spots could be observed on the cathode surface. For this second test, the cathode was maintained at operating temperature for 480 hrs. and the arc

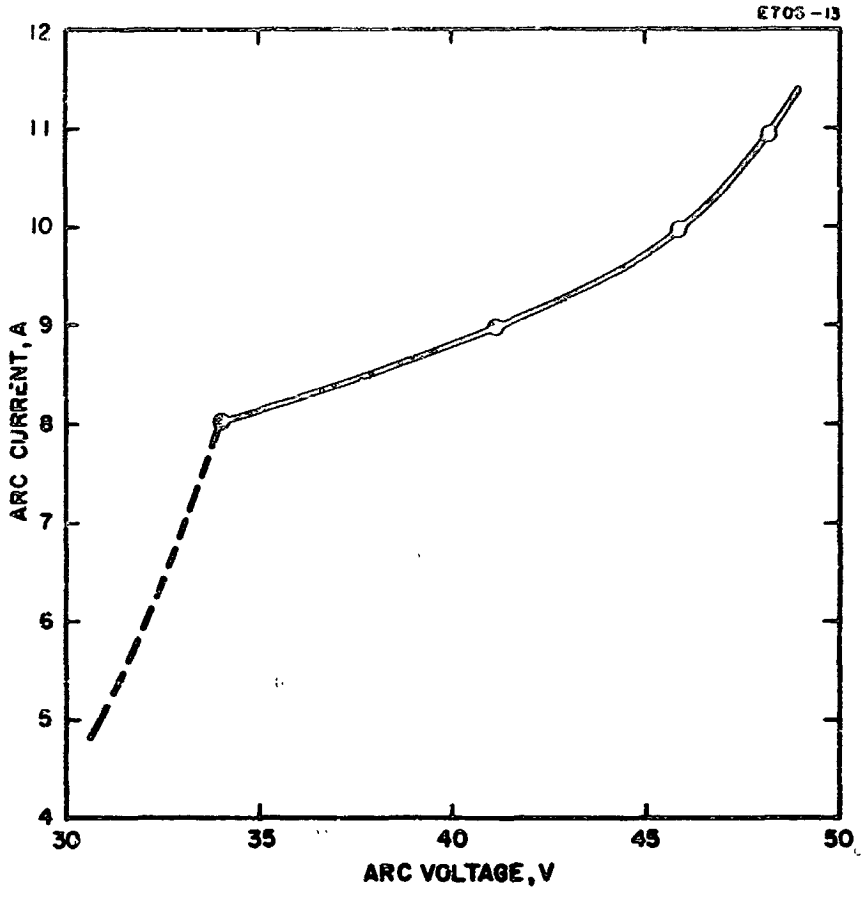

Fig. III-25. Arc current as a function of arc voltage for a cathode temperature of 748°C, mercury flow rate of 335 mA, and magnetic field of 24 G. Disk cathode No. 1 in simulated thruster No. 1.

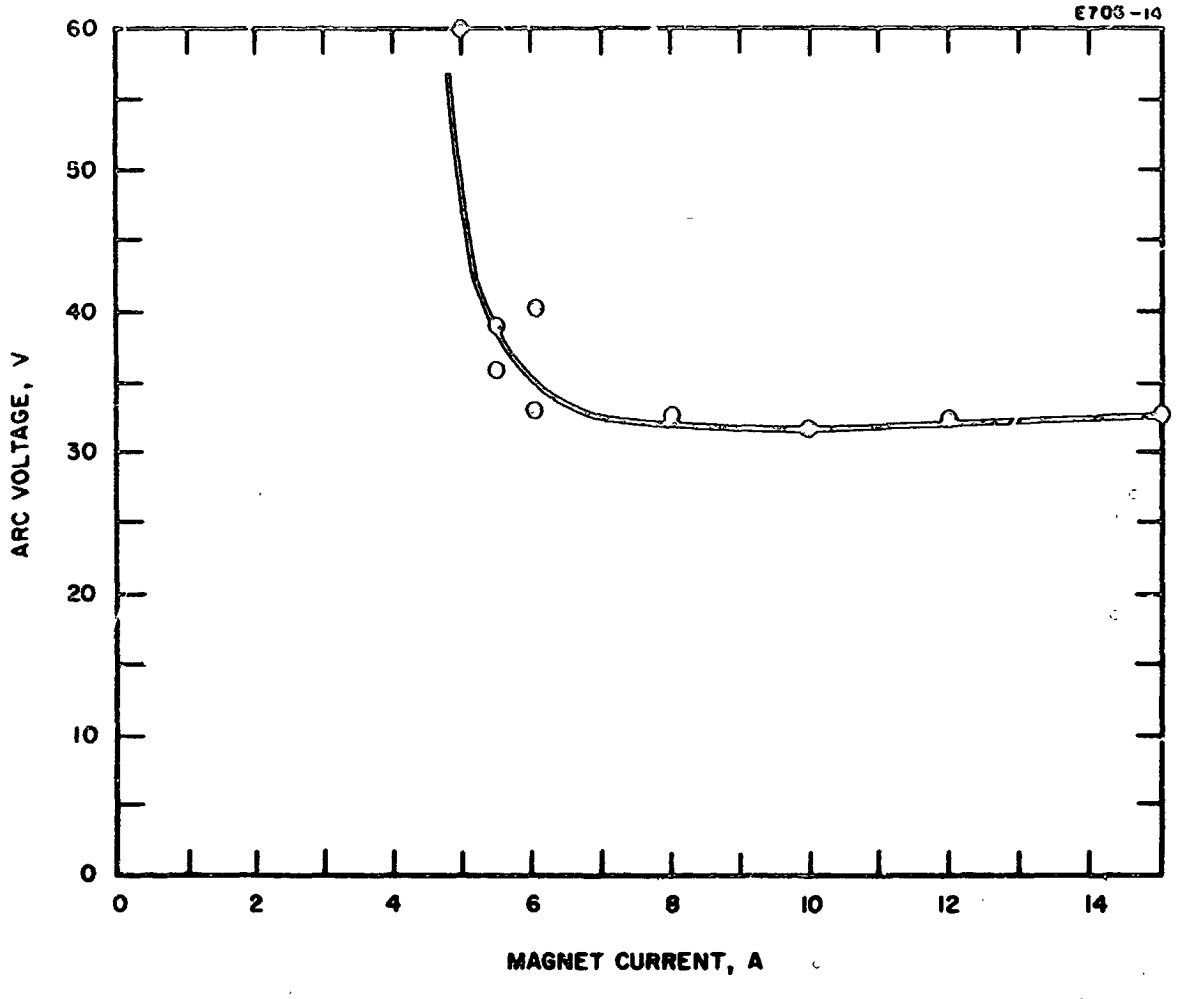

Fig. III-26. Arc voltage as a function of magnet current for a cathode temperature of 748°C, mercury flow rate equivalent to 335 mA, and arc current of 4 A. Disk cathode No. 1.

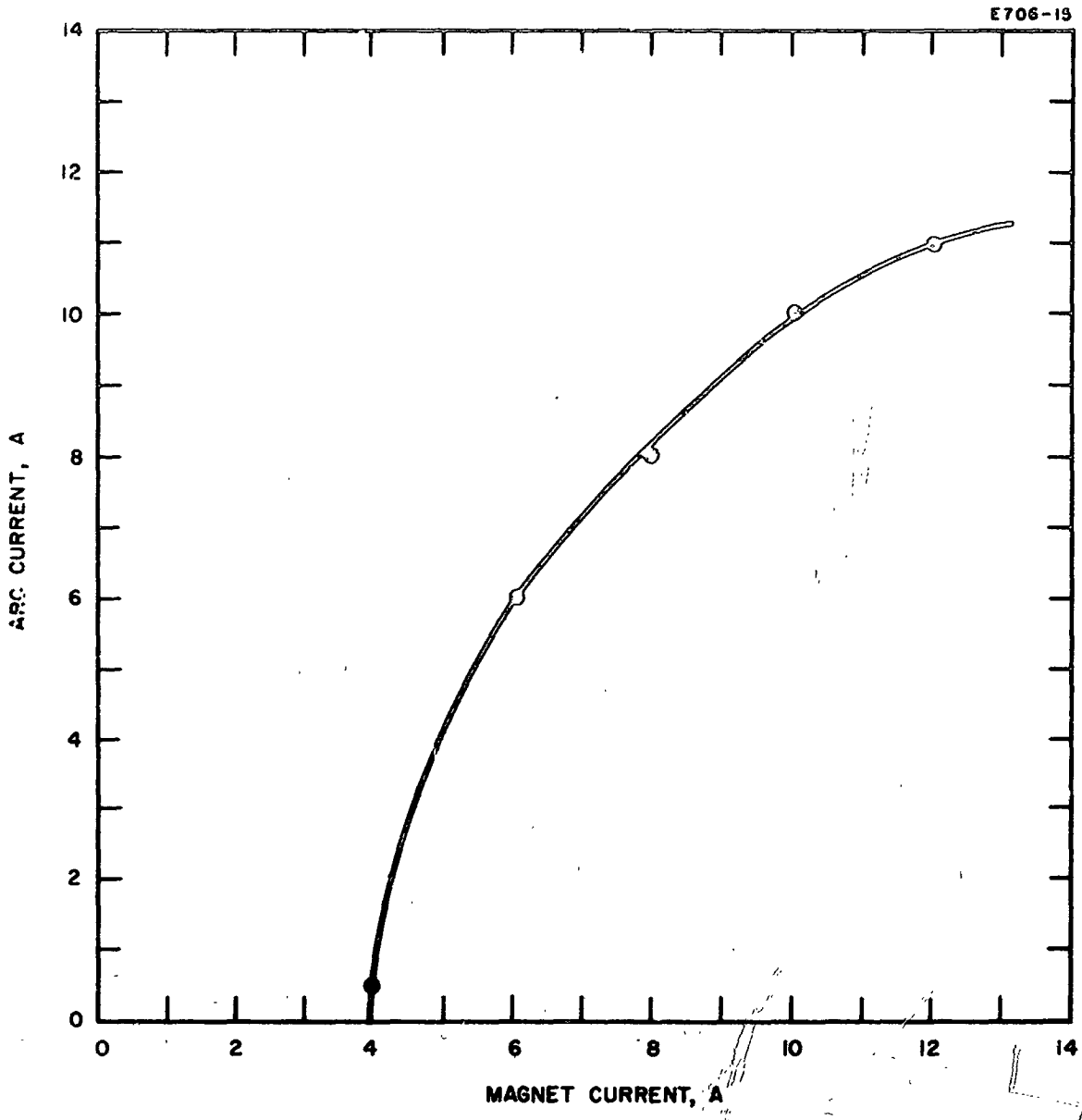

Fig. III-27. Arc current as a function of magnet current for a cathode temperature of 840°C, mercury flow rate of 310 mA, and arc voltage of 40 V. Disk cathode No. 1.

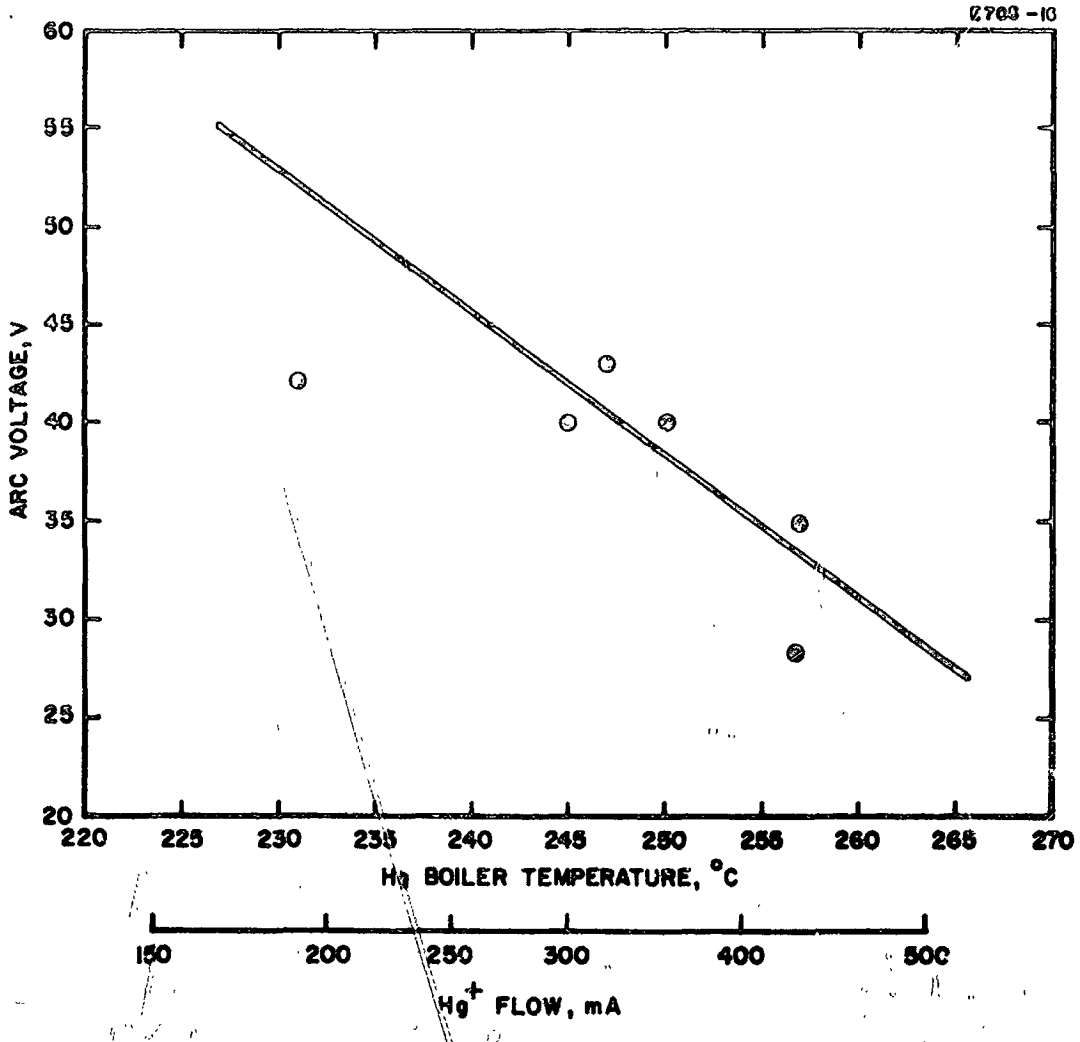

Fig. III-28. Arc voltage as a function of mercury boiler temperature (flow) for an arc current of 4 A, cathode temperature of approximately 750°C, and magnetic field of 19 G. Disk cathode No. 1, simulated thruster No. 1.

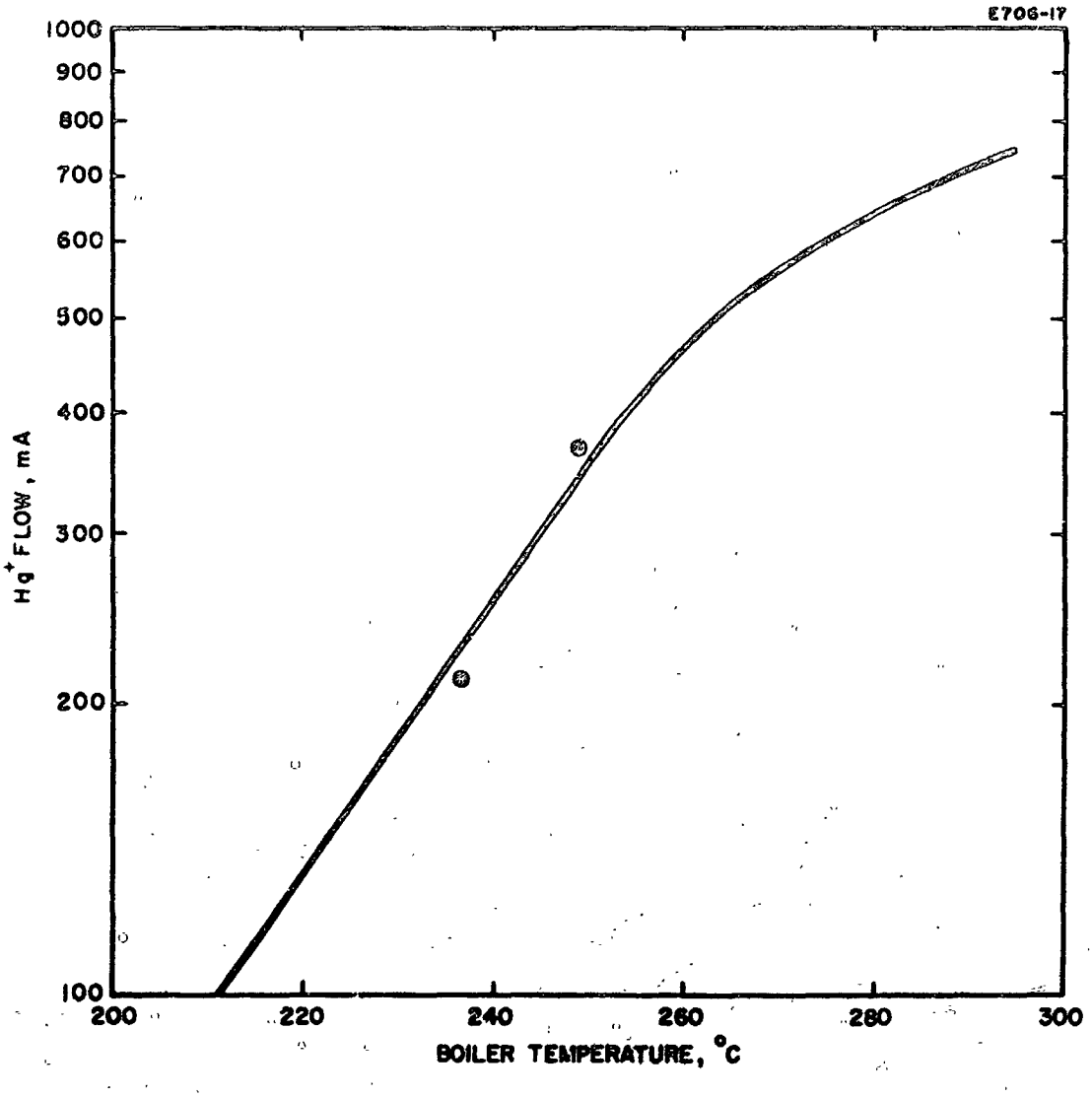

Fig. III-29. Mercury flow in milliamperes of ion current versus boiler temperature for feed system with plug T-3, simulated thruster No. 1.

M 4293

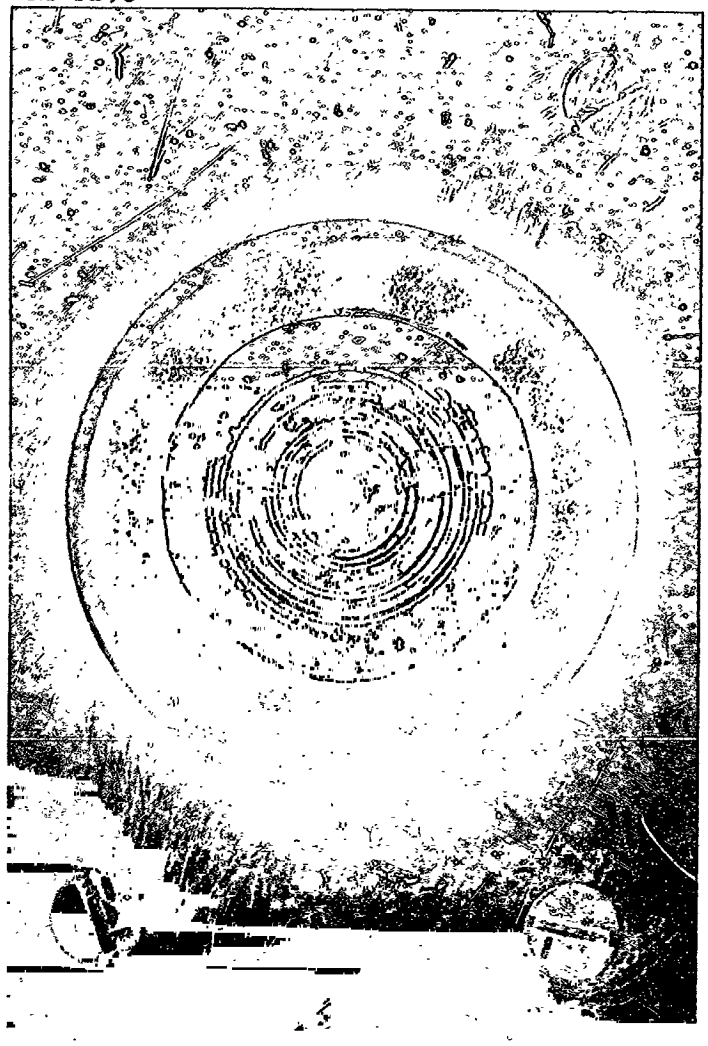

Fig. III-30. Disk cathode No. 1 after 324 hour life test

was on for 460 hours. Most of this arc time was accumulated at the low voltage-high current mode of operation. The mercury flow rate averaged over 600 mA for this second test. The heater remained intact although a heater power of 180 W was used for the last 300 hours of this test. The appearance of the cathode after termination of this second test is shown in Fig. III-31. The weight loss for this 480 hour test was 0.56 g. The emissive coated disks original weight was about 12.5 g. Even at this high loss rate of cathode material, mainly by evaporation at localized overheated regions, sufficient material remains for a life in excess of 10,000 hours. The test was terminated because no increase in cathode activity could be observed. Lack of athode activation was a result of the slower erosion or ion sputtering of the nickel disks as compared to the erosion of the emissive coating. The nickel surfaces shield the fresh oxide coating from the plasma. To overcome this difficulty, or to increase the erosion rate of the disks, a thinner nickel is required.

Since disk cathode No. 2 was already fabricated with 0.0005 in. thick disks, and since it was desired to test a cathode with thinner disks, this cathode was set aside untested.

Disk Cathode No. 3

This cathode was fabricated using nickel foil as thin as 0.0002 in. and 50% transparent. The nickel disks for cathodes Nos. 1 and 2 were 0.0005 in. thick solid foil. This factor five decrease in nickel content was for the purpose of matching the erosion rates for the nickel and the oxide coating. Fig. III-32 shows this disk cathode. This cathode was used in a complete 15 cm thrustor and was tested in the 2 ft cryowall vacuum chamber. The cathode temperature power relationship is compared with that for other disk cathodes in Fig. III-33. The increased heater power of 100 W required for a temperature of 850°C Br, as compared to 70 W for cathode No. 1, results in part from separation of the disks. The thinner nickel disks deformed on heating and the lack of good contact between disks results in a lower temperature for the top disk for a given heater power. In the first portion of this life test, satisfactory thrustor performance could be obtained and was as follows:

heater power	=	50 W
arc voltage	=	35 V
arc current	=	1.5 A
acc voltage	=	6.0 kV
dec voltage	=	0.5 kV
beam current	=	220 mA
mercury utilization	=	85%.

For lower accel voltages in the range of 4 to 4.5 kV, heater power as high as 140 to 150 W was required. Intermittent increases in chamber pressure to above 10^{-5} Torr were observed during this test. After 260 hours of cathode life, a heater power of 180 W was insufficient to maintain a stable arc. A vacuum leak was found and eliminated by replacing the O-ring on the thermocouple feed through port. The notable change in cathode appearance during test was the separation of disks, previously described.

M 4438

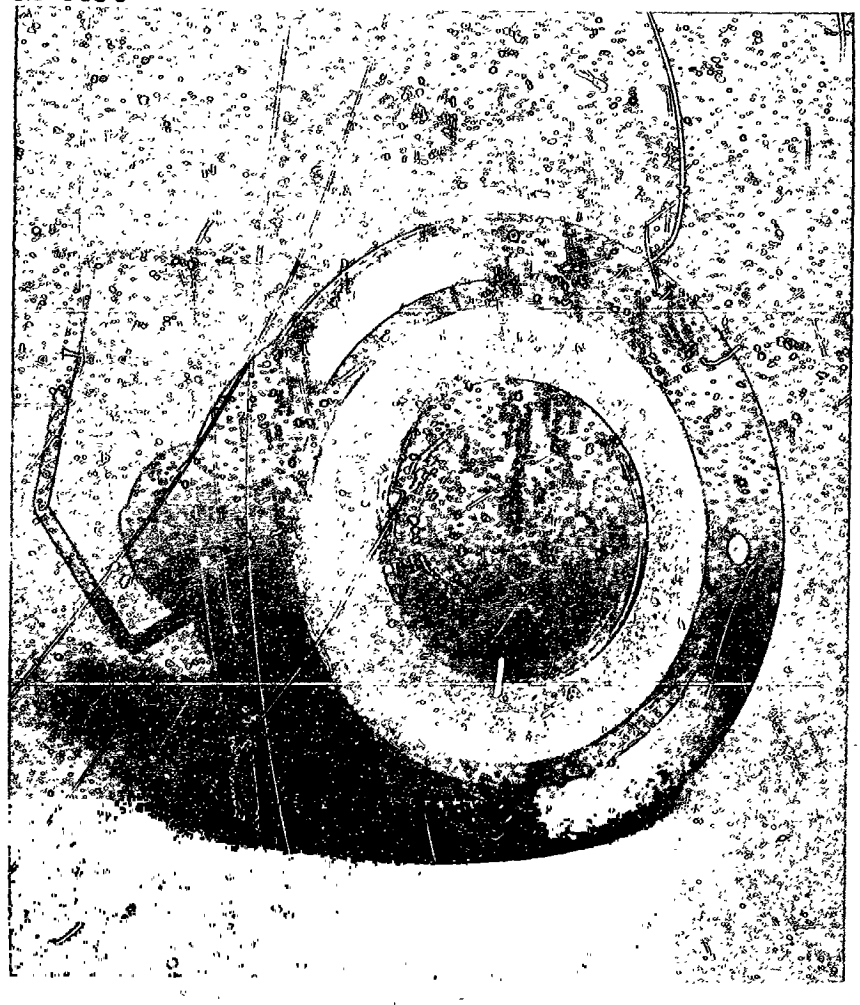

Fig. III-31. Disk cathode No. 1 after the second test of 480 hour duration.

M 4616

Fig. III-32. Disk cathode No. 3 before test.

Disk Cathode No. 4

This cathode was fabricated using a different technique in assembly of the disks. The disks were stacked while still wet with binder. Also, a nickel ring was spot welded in position to prevent disk separation. This cathode was installed in a complete thrustor and life testing commenced in the 2 ft cryowall vacuum chamber. The cathode temperature-heater power relationship is shown in Fig. III-33. The heater power required was greater than expected, again indicating disk separation. Life testing continued for approximately 190 hours with a typical operating point as follows:

heater power	=	150 W
arc voltage	=	40 V
arc current	=	1.6 A
acc voltage	=	5.0 kV
dec voltage	=	1.0 kV
beam current	=	220 mA
mercury utilization	=	85%.

Intermittent increases in chamber pressure were observed during this test period. The test was terminated after 190 hours to replace the cathode with a design requiring lower heater power. Upon cathode removal, separation of the disks was confirmed. The chamber was made completely leak tight eventually by replacing a portion of the cryowall. Further tests with disk cathodes were not attempted, however, because of the success experienced in the meantime with encapsulated coating on flower cathodes. Therefore, during the remaining period of the contract, effort was concentrated on cathodes with encapsulated coating.

E. Impregnated Cathodes

NASA Lewis Research Center supplied, for evaluation in simulated thrustors, impregnated cathodes in two geometries: (1) cylindrical and (2) hollow. These geometries with some outline dimensions are shown in Fig. III-34. The emitting region of these cathodes consist of porous tungsten (2 to 5 μ pore size and approximately 80% of theoretical tungsten density) impregnated with a barium-calcium aluminate. The emittering areas of the cylindrical and hollow cathodes are about 8.5 cm^2 and 10 cm^2, respectively.

Three of these impregnated cathodes were tested; two cylindrical and one hollow. The activation procedure for these cathodes consisted of baking the ion-sublimation chamber at 200°C for approximately 10 hours with the cathodes held at about 500°C. The chamber was cooled to room temperature and if the ultimate system pressure of approximately 10^{-8} Torr was reached, activation continued by increasing the cathode temperature to 1150°C. Cathode temperatures were measured with both thermocouples and an optical pyrometer. The measured cathode temperature-heater power requirements are shown in Fig. III-35.

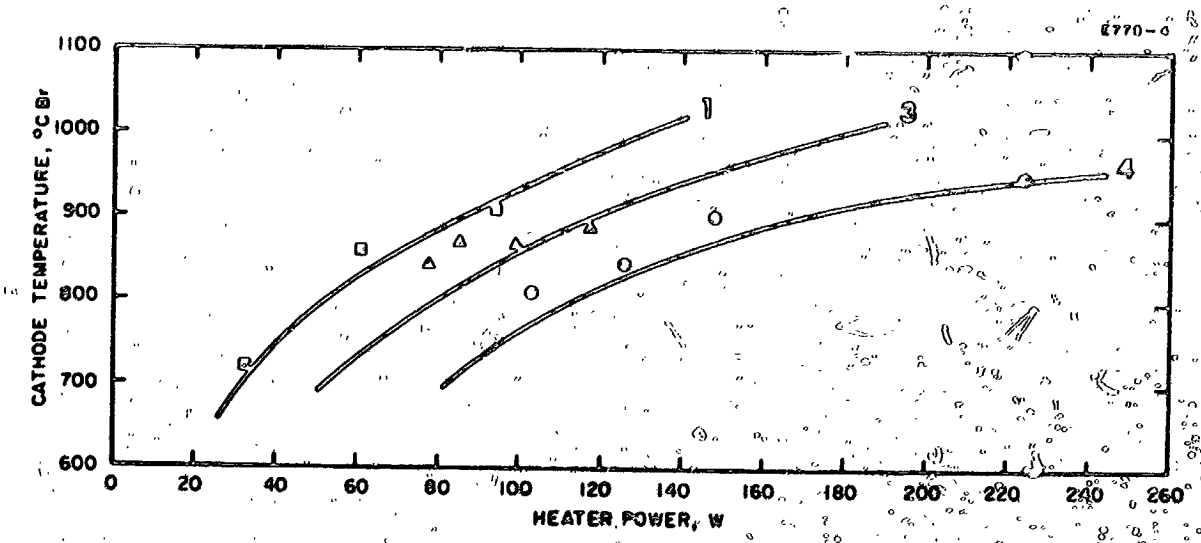

Fig. III-33. Temperature-power relationships for disk cathode Nos. 1, 3, and 4. (These data represent the cathode characteristics near the beginning of the test period.)

E 778-12

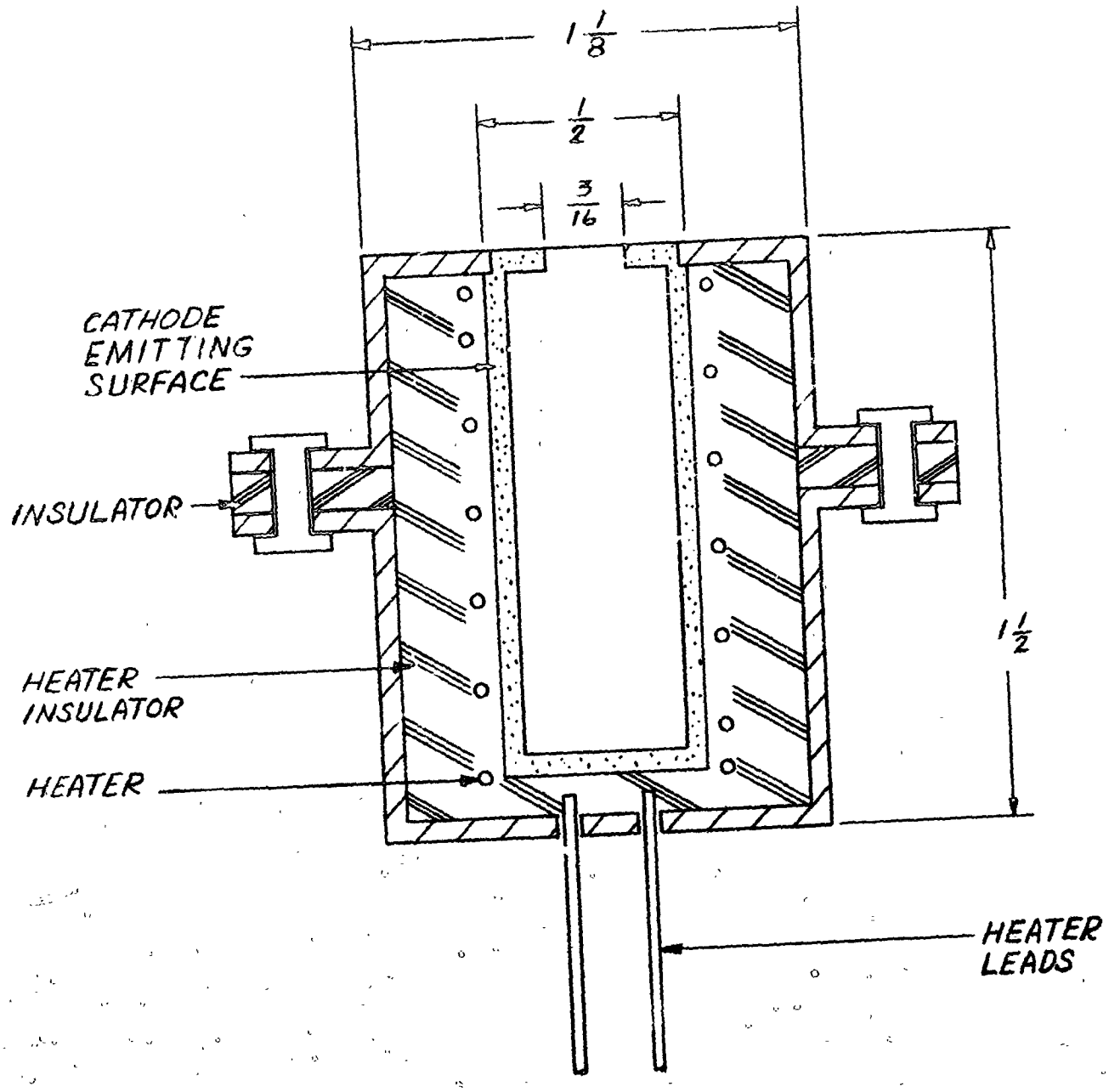

(a) Cylindrical

Fig. III-34. Impregnated cathode geometries

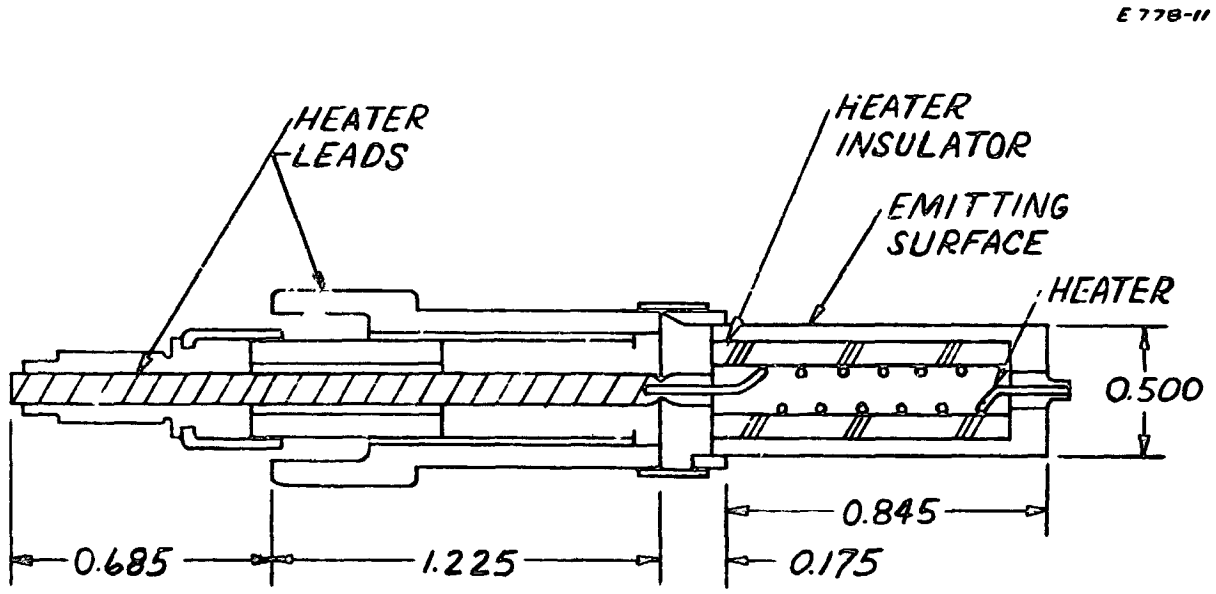

(b) Hollow

Fig. III-34. Impregnated cathode geometries.

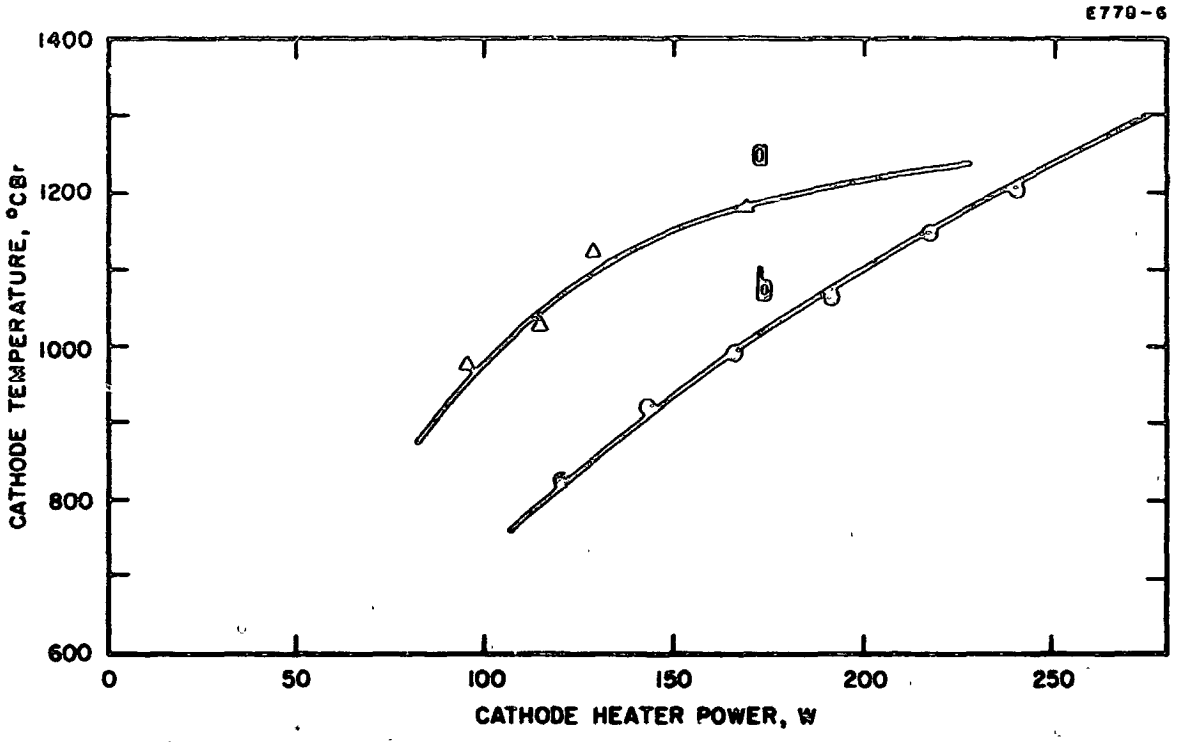

Fig. III-35. Temperature-power relationships for the impregnated cathodes (a) cylindrical and (b) hollow.

Cylindrical Cathode No. 1 (Tungsten density = 82%)

The mercury thrustor arc characteristic using this impregnated cathode was similar to that obtained with a poorly activated oxide cathode. This is, an arc current of 4 A could be obtained at 20 V or a fraction of an ampere resulted for 100 V, but stable operation at intermediate values of current and voltage was unattainable. With normal values for the thrustor operating parameters of magnetic field, cathode temperature, arc voltage and mercury flow rate (Hg vapor pressure), the arc current was intermittent with time. The time variation of arc voltage, arc current and heater power is shown in Fig. III-36. From time equal to 1 to 3 hrs., and 37 to 41 hrs., the arc voltage and current were 15 V and 4-8 A, respectively which was typical of operation at high mercury vapor pressure. The arc power supply can be set to be either current or voltage limited, for example, in the period of 37 to 41 hours, the arc current was limited to about 8 A and when this current was obtained the voltage automatically decreased as is shown in Fig. III-36.

From time equal to 42 hrs. to end of test, the arc current variation of Fig. III-36 occurred with a normal mercury flow rate of about 200 mA. These latter variations of arc current were not related to changes in test conditions such as the heater power setting. For fixed test conditions, the arc current periodically increased to several amperes and decayed to zero. This behavior indicates that the cathode activity is periodically increased by diffusion of barium to the cathode surface. With an active cathode, emission and ion formation result, the mercury ions then sputter the barium from the cathode surface within about 1/2 to 1 hr. and the emissions drop to zero again. In attempts to obtain continuous arc current, the heater power was increased in steps to 170 W, where heater failure occurred. This heater failure occurred after 97 hrs. of life. The failure consisted of a melted heater lead as shown in Fig. III-37. A change in cathode weight or appearance due to ion sputtering is not evident. The small weight change measured is probably the result of vaporized material at the vicinity of the melted heater lead. During this test, a leakage current in the ion pump (which was used to monitor pressure) or a vacuum leak developed. To insure that this type of cathode was properly evaluated, an ionization gauge was installed in the ion-sublimation chamber and another cylindrical cathode was tested.

Cylindrical Cathode No. 2 (Tungsten density = 75%)

This cathode was activated using the standard procedure as previously described. The ionization gauge and ion pump indicated essentially the same chamber pressure, and this pressure remained at about 10^{-7} Torr or below for most of this test period. Initially, the arc characteristics using this cathode were similar to those observed with the first cylindrical cathode. The recorded arc voltage and current for a portion of this test are shown in Fig. III-38. At first, the only operation obtainable was at low arc voltage and high current with an excessive mercury vapor pressures. After about 45 hrs. of cathode operation, an arc could be maintained at about 1 A and 40 V. The performance of this cathode was improved considerably over that for cylindrical cathode No. 1. This performance is presented by plotting arc current as a function of arc voltage for various values of cathode temperature (Fig. III-39), magnetic field (Fig. III-40),

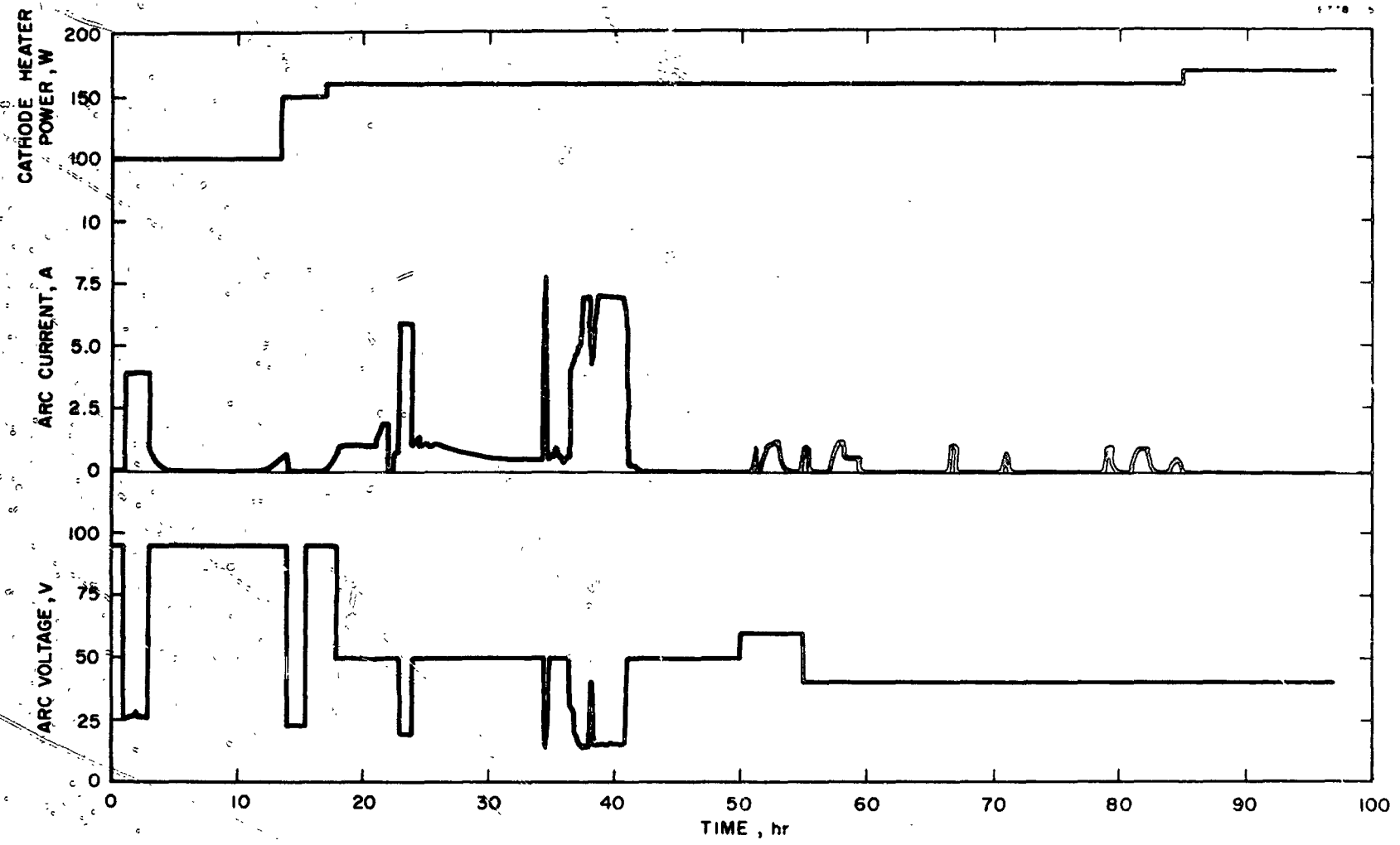

Fig. III-36. Cathode heater power, arc current, and arc voltage as a function of time for the test of impregnated cylindrical cathode No. 1.

M 4922

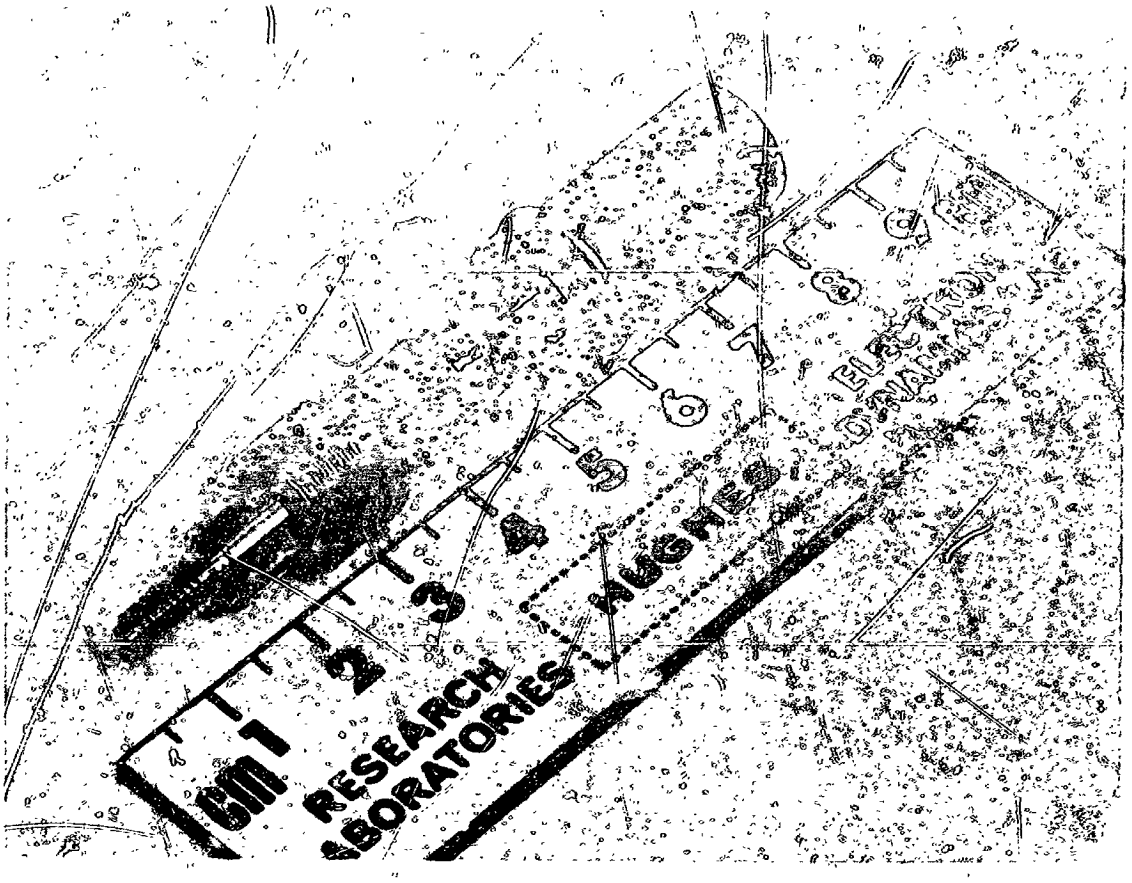

Fig. III-37. Impregnated cylindrical cathode No. 1 after test, showing the melted heater lead.

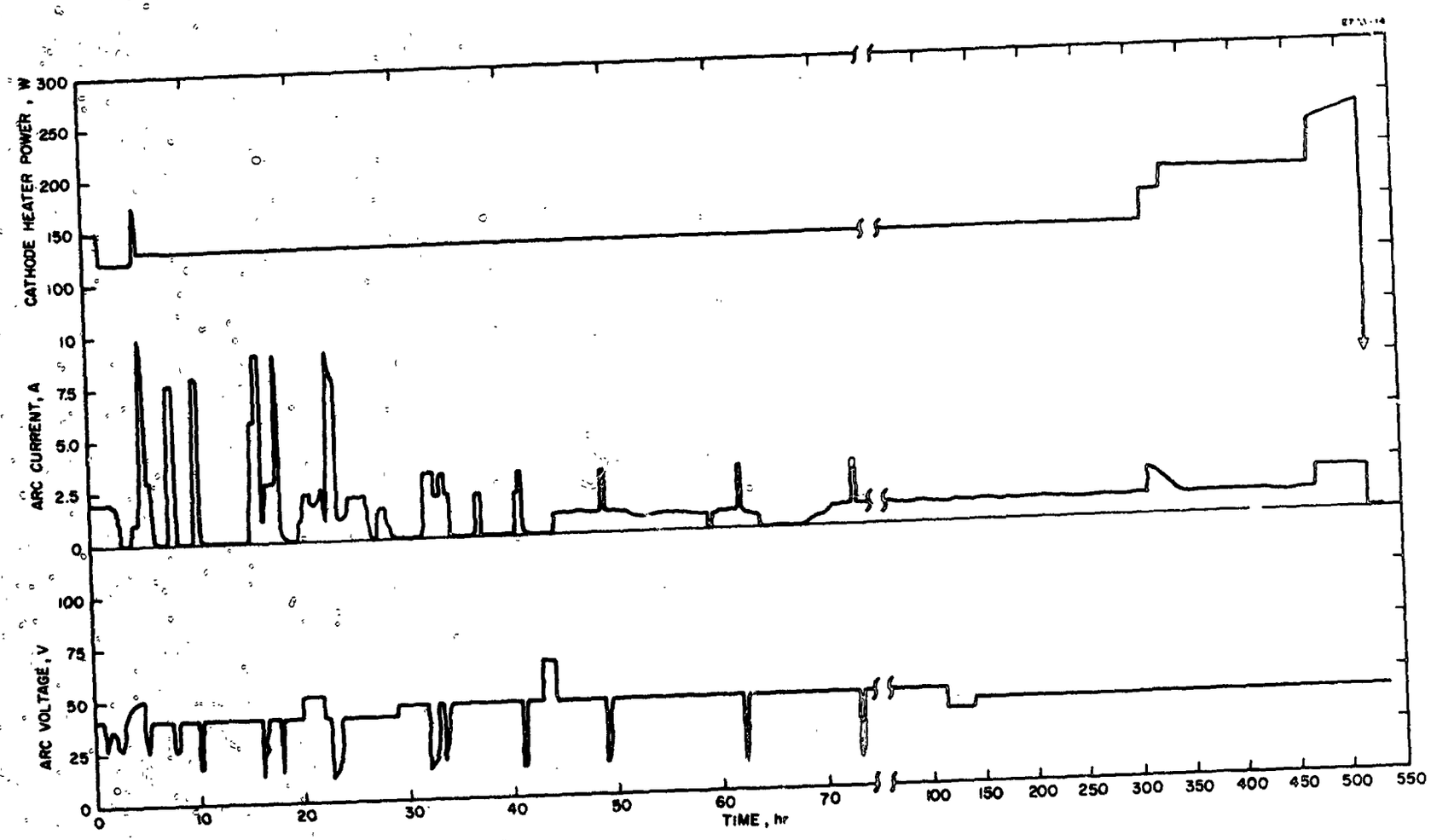

Fig. HI-38. Cathode heater power arc current, and arc voltage as a function of time for the test of impregnated cylindrical cathode No. 2.

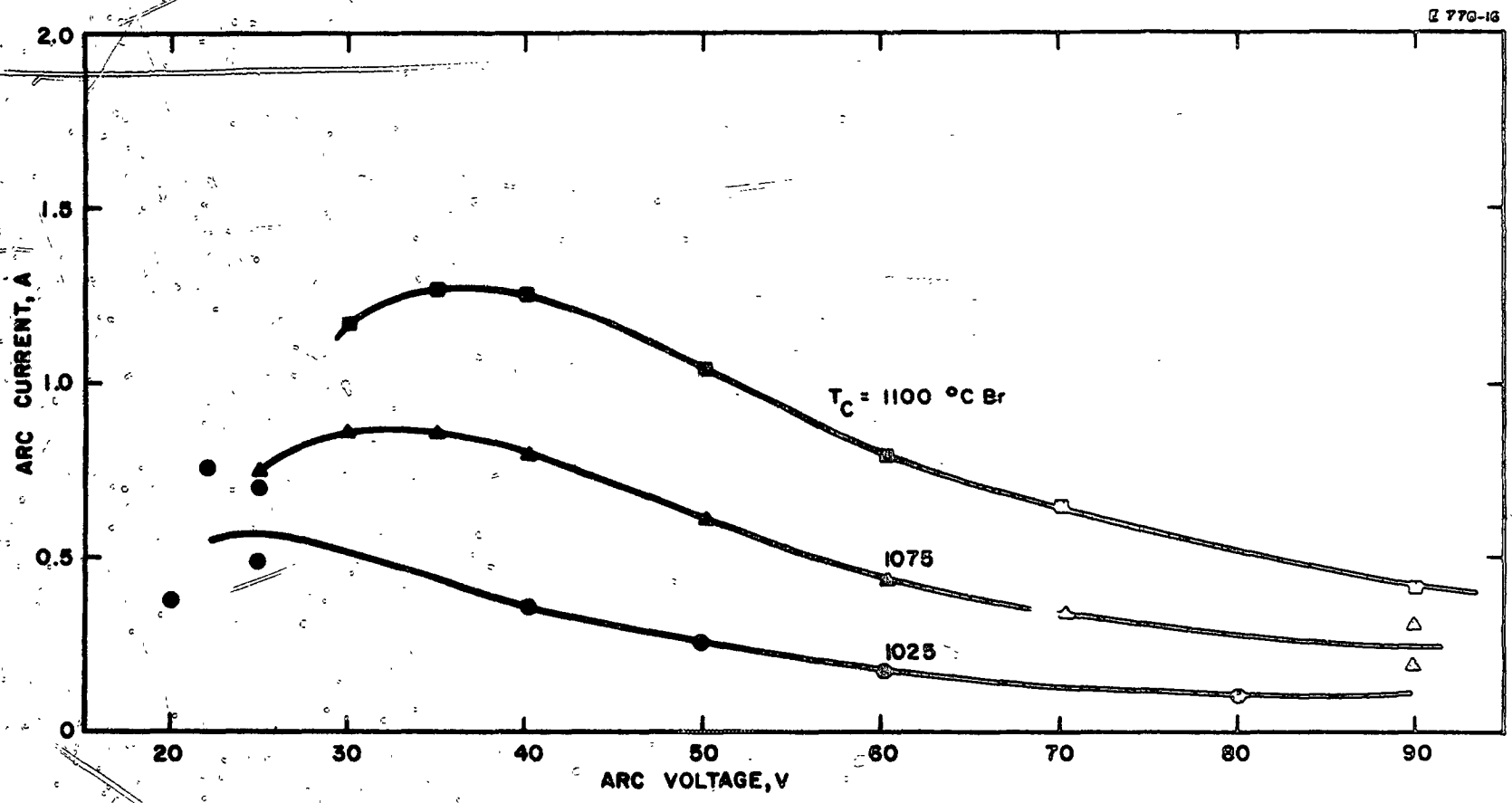

Fig III-39. Arc current as a function of arc voltage with cathode temperature as a parameter. Impregnated cylindrical cathode No. 2. Mercury flow = 230 mA, magnet current = 5 A.

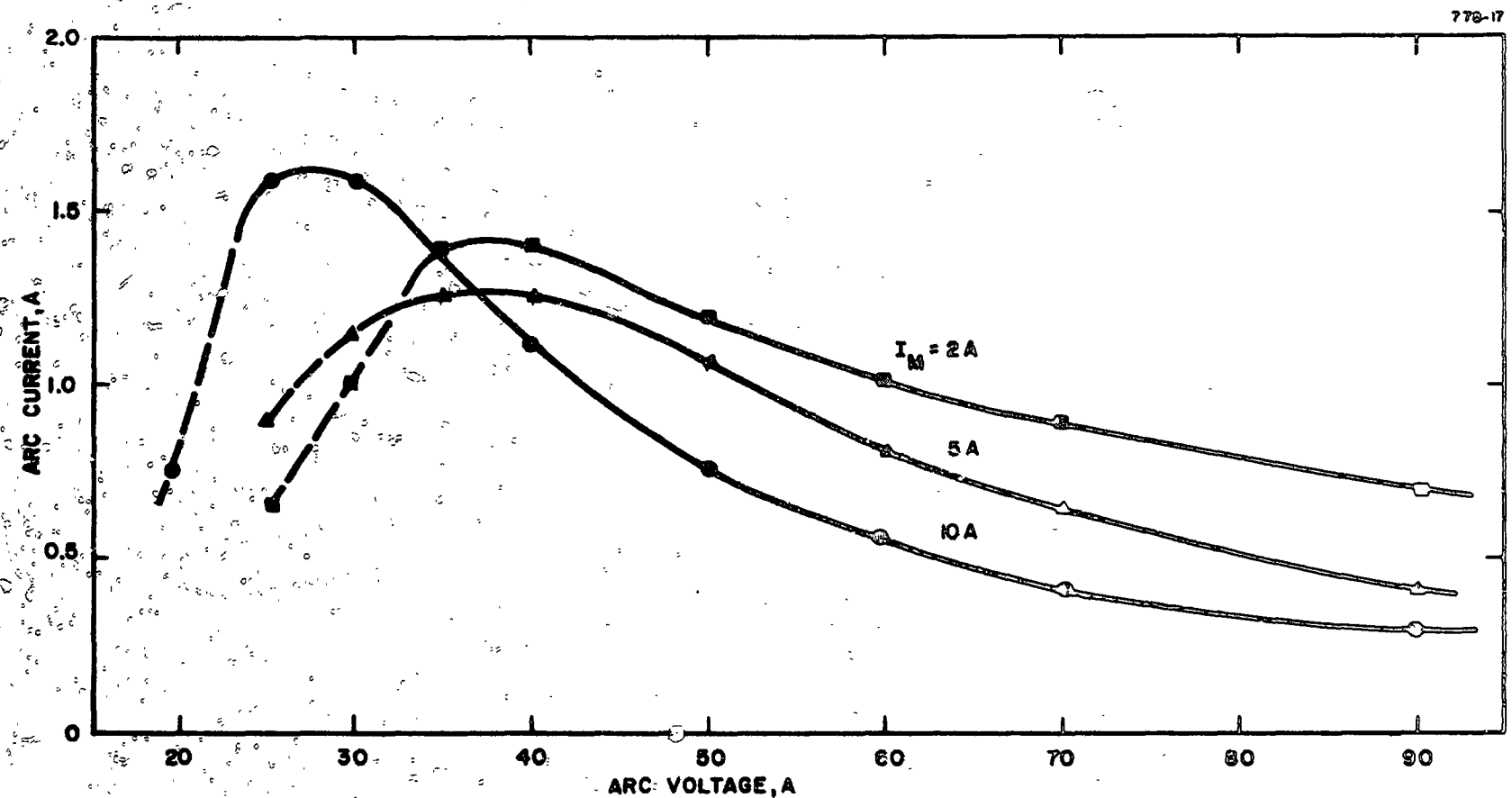

Fig. III-40. Arc current as a function of arc voltage with magnet current as a parameter. Impregnated cylindrical cathode No. 2. Mercury flow = 230 mA, cathode temperature = 1100°C Br.

and mercury flow rate (Fig. III-41). The performance of this cathode appears satisfactory except for the high heater power required for relatively low arc current. After 500 hrs. of life testing were completed, the cathode temperature was increased slightly above 1100°C Br, in an attempt to increase the arc current, and the heater failed. The heater failure consisted of a melted open heater lead as occurred on cylindrical cathode No. 1. The cathode weight or appearance did not change significantly during this 500 hr. test.

Hollow Cathode No. 1

This cathode geometry was devised to lessen the deleterious effects of mercury ion sputtering of the emitting surface. The emitting surface for this cathode is partially shielded from ion bombardment. This cathode was evaluated in a 15 cm simulated thrustor within the ion-sublimation vacuum system. The previously described standard activation procedure was followed. As shown in Fig. III-42, the heater power requirement of 200 W for an operating temperature of 1100°C Br results in an excessive watt per ampere requirement. With this cathode, a stable arc at various voltages and currents could not be maintained. The time variation of arc voltage and current is shown in Fig. III-43. An arc could be obtained only with excessive cathode temperature (1200°C Br) and mercury flow rate (900 mA). The test period was 70 hrs. The test was terminated as a result of heater failure. Again, this failure consisted of a melted open heater lead. The lead failed near its entrance point to the cathode body. Typical vacuum pressure during test was 10^{-7} Torr. After test, the appearance of the cathode was normal. The poor performance of this cathode probably results from lack of plasma sheath penetration within the hollow region.

Test Diode

A test diode (Fig. III-44) was used during the life testing of disk cathodes Nos. 3 and 4 and flower cathode No. 22. This test diode was for the purpose of evaluating the environmental conditions within the 2 ft vacuum chamber. By monitoring the test diode emission current, emission poisoning phenomena affecting only the thrustor cathode could be separated from poor vacuum conditions affecting emission from both the thrustor and test diode cathodes. The test diode used an indirectly heated cathode and planar geometry. The cathode emitting area consisted of oxide coated nickel disks similar to those of the disk cathodes. These coated disks were spot welded to the sides of a tungsten cylinder which surrounded the cathode heater.

When vacuum chamber leaks were encountered during tests of the disk cathodes, the test diode current dropped to essentially zero. During the test of flower cathode No. 22, after the cryowall leaks were eliminated, the diode was operated temperature limited and the emission remained constant at approximately 1 mA for an anode voltage of 25 V.

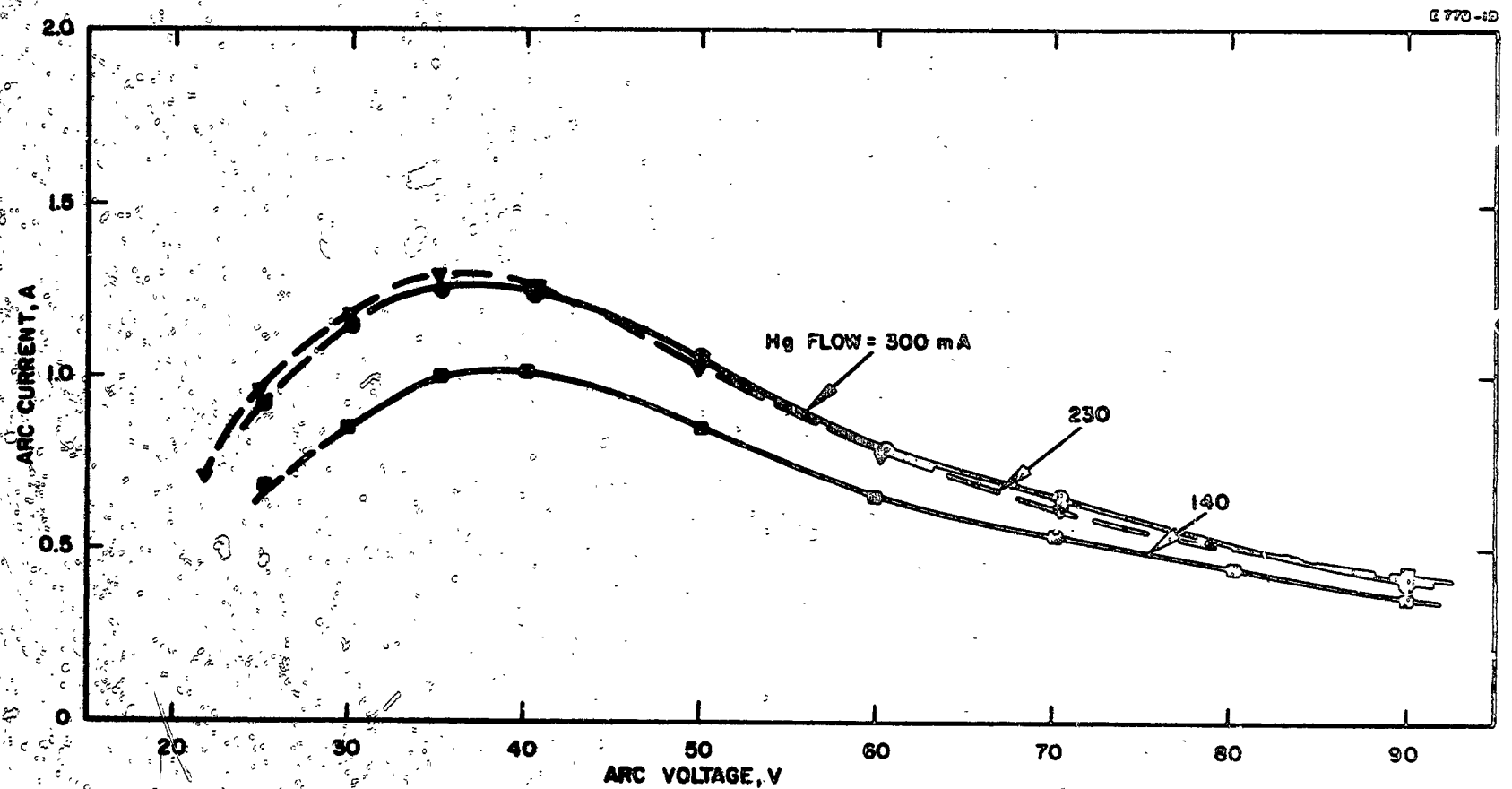

Fig. III-41. Arc current as a function of arc voltage with mercury flow as a parameter. Impregnated cylindrical cathode No. 2. Magnet current = 5 A, cathode temperature = 1100°C Br.

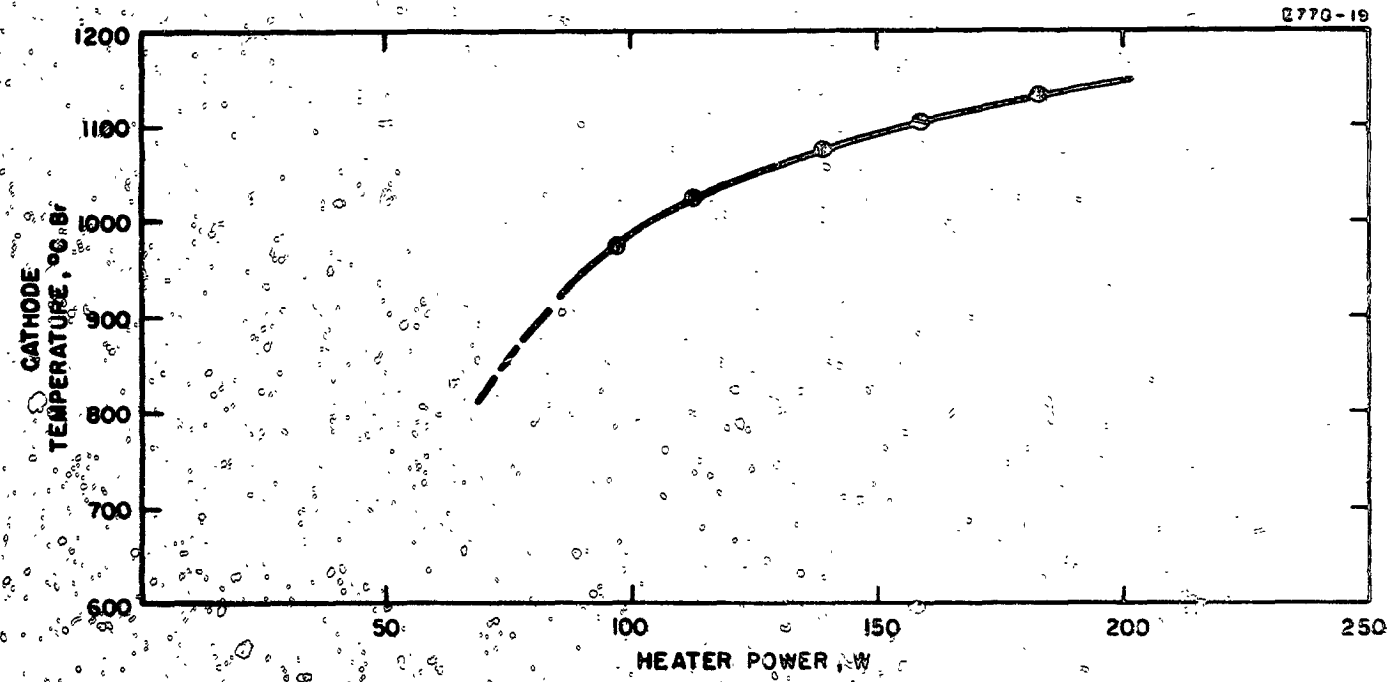

Fig. III-42. Temperature-power relationship for impregnated hollow cathode No. 1.

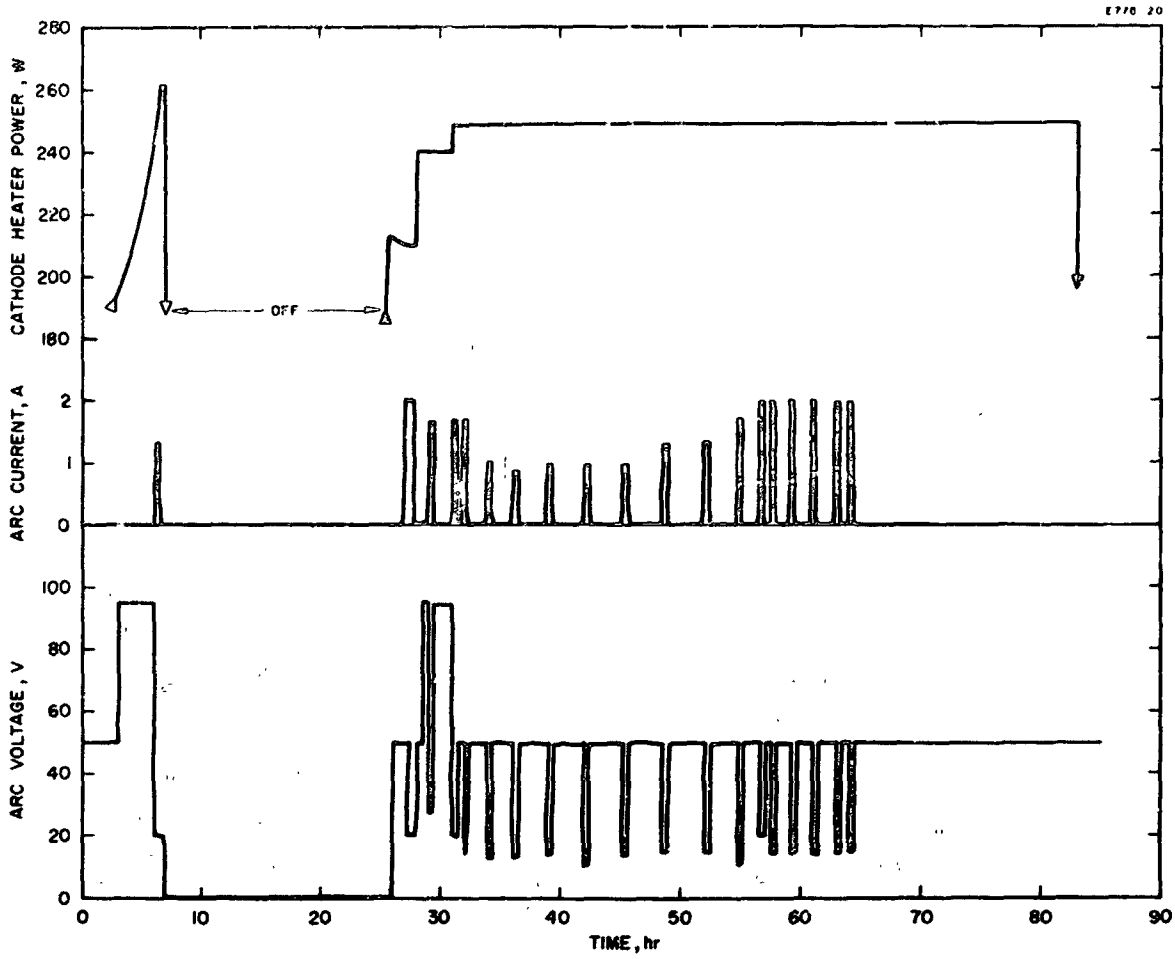

Fig. III-43. Cathode power, arc current, and arc voltage versus time for impregnated hollow cathode No. 1.

M 4622

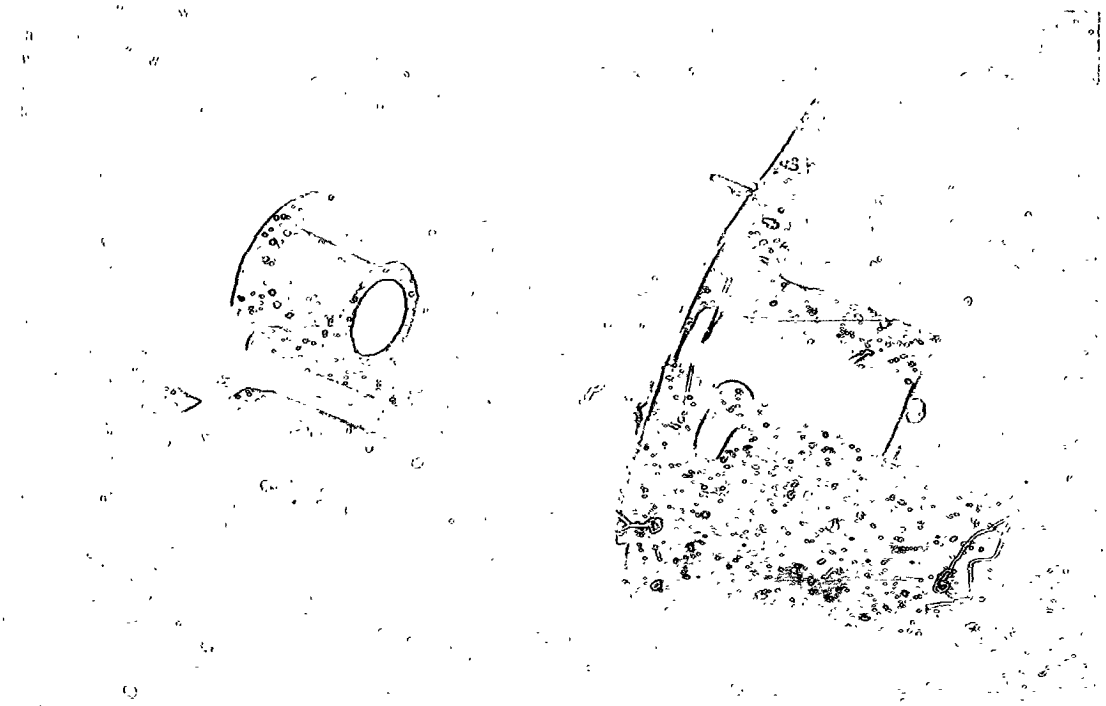

Fig. III-44. Test diode used during life testing of disk cathodes Nos. 3 and 4, and flower cathode No. 22.

F. Nickel Encapsulated Powder Cathodes

The cathode carbonate particles were nickel encapsulated to improve the adhesion and reduce the resistance of the cathode coating. Thick cathode coatings are required to provide sufficient emitting material to withstand long periods of mercury ion bombardment. Two problems associated with thick oxide cathode layers are flaking, or poor adhesion, and resistive heating in the oxide layer, or autocathoding. The objective is to encapsulate each particle of carbonate with a thin layer of nickel so that the nickel surfaces fuse together on heating thereby providing adhesion and current paths of low resistance.

Nickel encapsulating of the carbonate particles is accomplished by using nickel carbonyl vapor. This encapsulating technique has been discussed by Maurer and Pleass.[20] The apparatus used for nickel encapsulating the carbonate powder is schematically illustrated in Fig. III-45. A measured amount of liquid nickel carbonyl $Ni(CO)_4$ is dispensed into the graduated beaker, and then the carrier gases (H_2 and N_2) transport the $Ni(CO)_4$ vapor to the heated reaction vessel containing the (Ba Sr Ca) CO_3 particles. With the reaction chamber heated to 120-150°C, the $Ni(CO)_4$ decomposes with the Ni encapsulating the (Ba Sr Ca) CO_3 particle and CO leaving as exhaust. Any $Ni(CO)_4$ that is not decomposed within the reaction chamber decomposes in the heated (250°C) residual decomposer.

The carbonate particles are in the 2 to 3 μ size range. The desired nickel encapsulant is about 2% by weight. This amount of nickel provides an encapsulant thickness less than 0.05 μ which is below the resolution limit of a light microscope. Hence, the nickel encapsulant can not be observed. X-ray spectrographs, arc spectrographs, and chemical analyses were made to determine the nickel content of the encapsulated carbonates. The measured nickel content ranged from about 0.1 to 2%, depending on the sample and measurement technique used. Chemical analysis (gravimetric method using dimethlyglyoxime) yielded the higher values of nickel content, and arc spectrographic measurements yielded the lower values.

Measured values of the resistivity of nickel encapsulated and uncoated carbonate powders were not of the order of 0.1 and 100 Ω-cm that would be expected for active emitting coatings using these powders. The carbonates must be dissociated into oxides and the powder sintered in order to obtain the expected resistivities. After activation and removal of the oxide coated surfaces from the vacuum system, the oxides are converted to hydroxides and hydrates. This water absorption and problems with contact resistance still prevent meaningful resistivity measurements. Performance of the 2 mm thick cathode coating on the cup cathode, and the 0.2 to 0.4 mm thick coatings on the flower cathodes indicate that indeed the nickel encapsulate lowers the resistance of the oxide layer. But it should be noted that some flaking of the 2 mm thick coating on the cup cathode did exist.

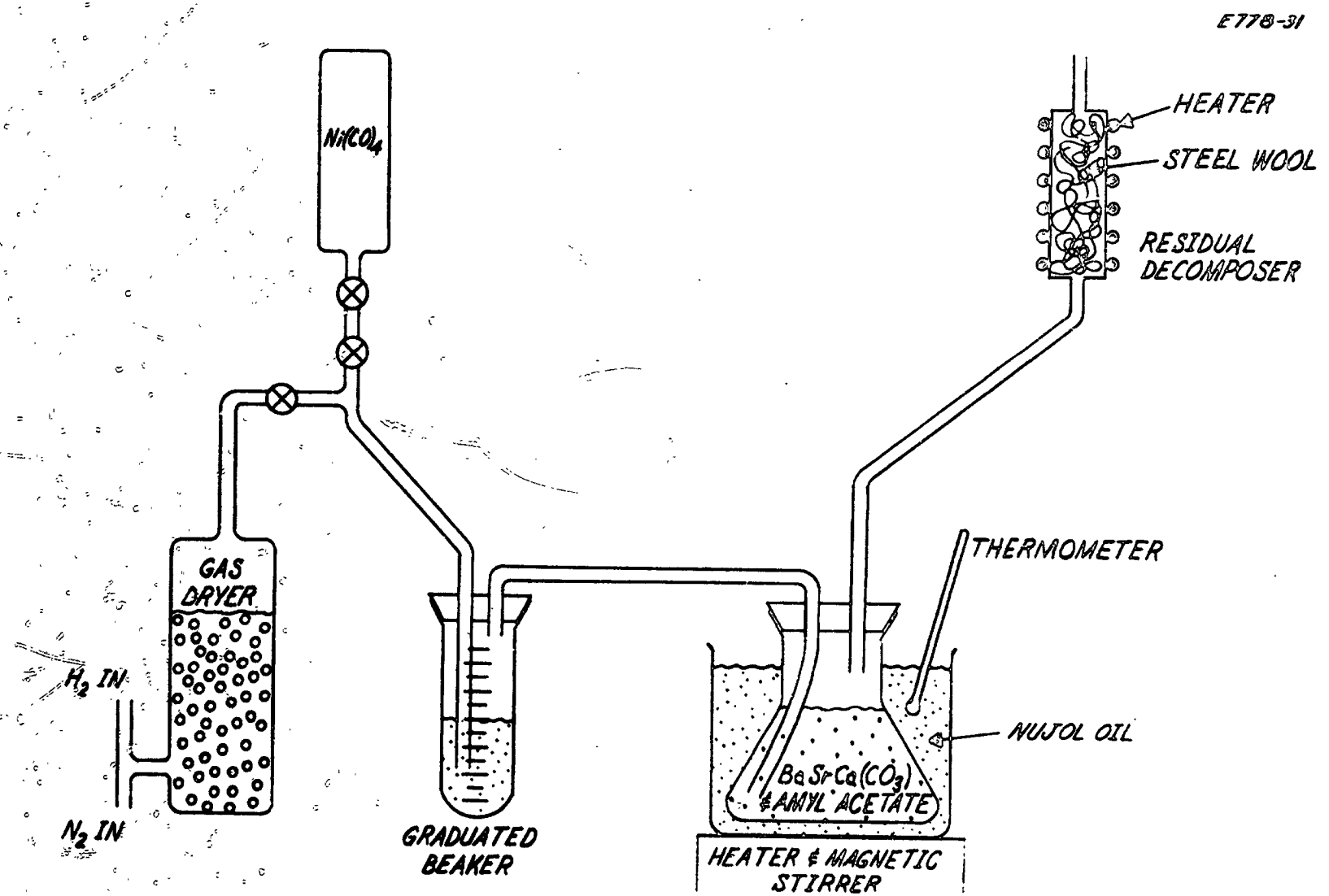

Fig. III-45. Schematic representation of the apparatus used for nickel encapsulating carbonate powder.

Flower Cathode No. 18

The purpose of flower cathode No. 18 was to evaluate, during a 200 hour test, the emitting properties of nickel encapsulated barium carbonate. This first cathode using the nickel encapsulated barium carbonate was sprayed with a multithickness coating of 10, 20, and 30 mg/cm^2. The appearance of a portion of this coated mesh, before test, is shown in Fig. III-46. The dimensions of this cathode were those of design 2. This cathode was tested using a 15 cm simulated thrustor installed in the 6 in. mercury diffusion vacuum system. The performance of this cathode is described by the following test results. Fig. III-47 shows the cathode temperature-power relationship. As compared with the heater power required initially for a design 2 cathode sprayed with carbonates only (75 W for 850°C Br, -see Fig. III-4), this cathode sprayed with nickel encapsulated carbonate required an increased heater power (120 W for 850°C Br). This result is consistent with the darker appearances (increased emissivity) of the nickel encapsulated carbonate. Arc current as a function of arc voltage is shown in Fig. III-48, for a cathode power of 100 W, magnet current of 10 A, and a mercury flow rate of approximately 300 mA. The increase in arc current with arc voltage most likely is a result of cathode heating by the increased arc power. There is also the possibility that the cathode activity is increased by the enhanced ion bombardment. Arc current as a function of arc power for a fixed cathode power of 74 W is plotted in Fig. III-49. Also, the arc current is a function of the heater power and this relationship is shown in Fig. III-50, where the arc power is held constant at 212 W. The relationship of arc power to cathode power, for a constant arc current of 4 A, is shown in Fig. III-51. Since the sum of arc power and heater power does not remain constant for a given arc current, it can be concluded that the arc power is more effective in determining the cathode temperature or emission level than is the heater power.

The test period for this cathode was intended to be 200 hours. The cathode was maintained at operating temperature for 317 hours, and an arc voltage and current of 40 V and 4 A were maintained for 215 hours. The test was terminated as a result of an open circuit in the cathode mesh. The appearance of the cathode mesh in the vicinity of the open circuit is shown in Fig. III-52. The loss of cathode coating and nickel mesh by evaporation and/or sputtering is readily apparent. In the lower portion of Fig. III-52, the nickel has agglomerated, indicating that the temperature had reached the melting point of nickel (1453°C). Two unfavorable conditions associated with these tests were (1) the mercury flow rate was lower than expected and (2) the chamber pressure increased above the normal operating range of 10^{-6} to 10^{-8} Torr. The mercury feed system was held at a temperature for a flow rate of 250 mA, but the mercury expended as calculated from weight measurement before and after test indicated that the flow rate was about 100 mA. Either the apertured plug in the feed system was partially closed, or the feed system thermocouple was in error. The vacuum system used for this test contains an automatic pneumatic valve that isolates the test chamber from the pumping system on momentary power failures. After the cathode failed, it was observed that this valve was closed. The time lapse between valve closure and cathode failure is not known. The ionization gauge indicating the pressure is located on the pump side of the valve. Therefore, the vacuum

M 5162

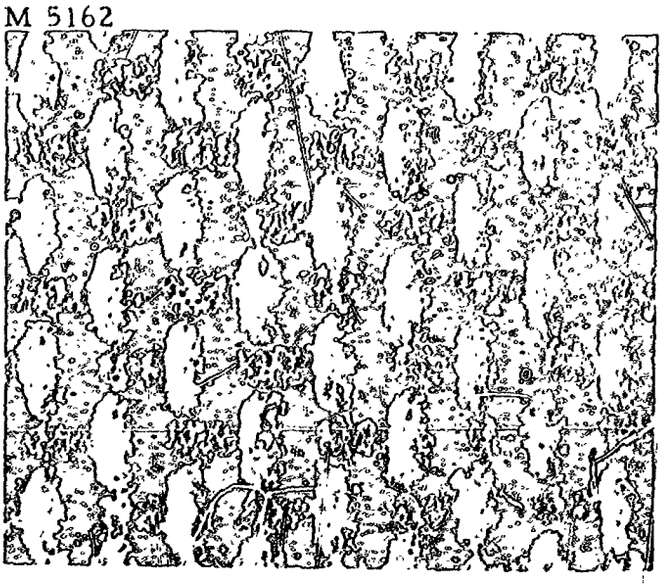

M 5163

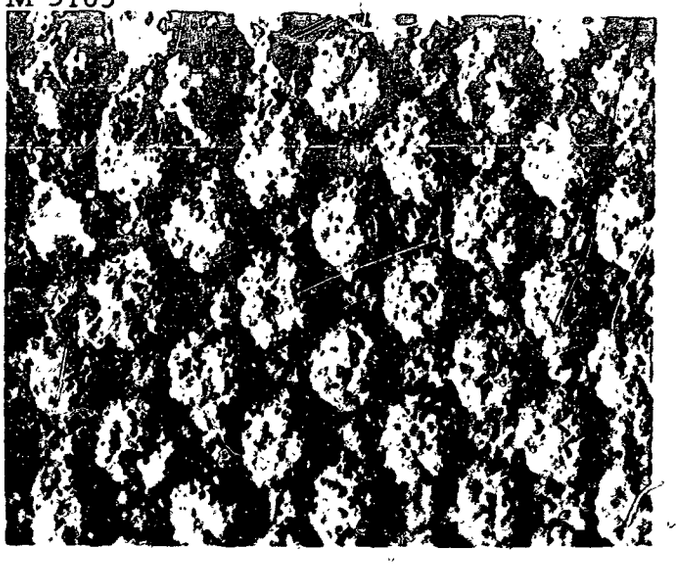

Fig. III-46. Nickel encapsulated cathode powder coating the emitting mesh of flower cathode No. 18, before test.

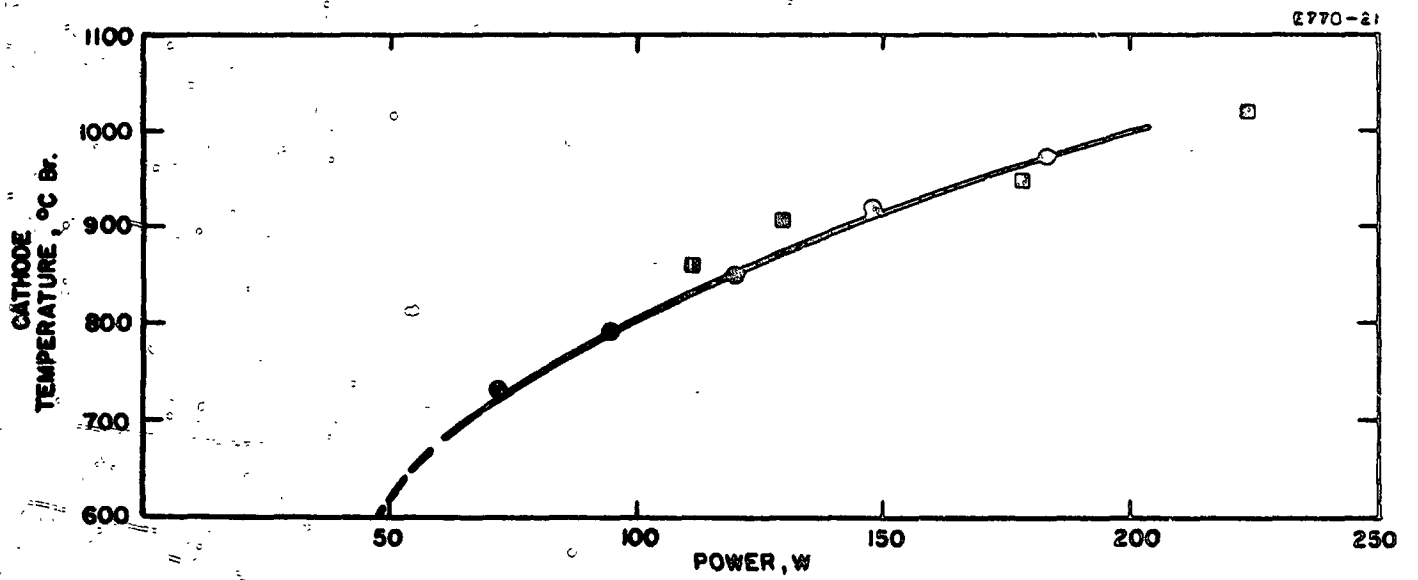

Fig. III-47. Temperature-power relationship for flower cathode No. 18, design 2 at beginning of test.

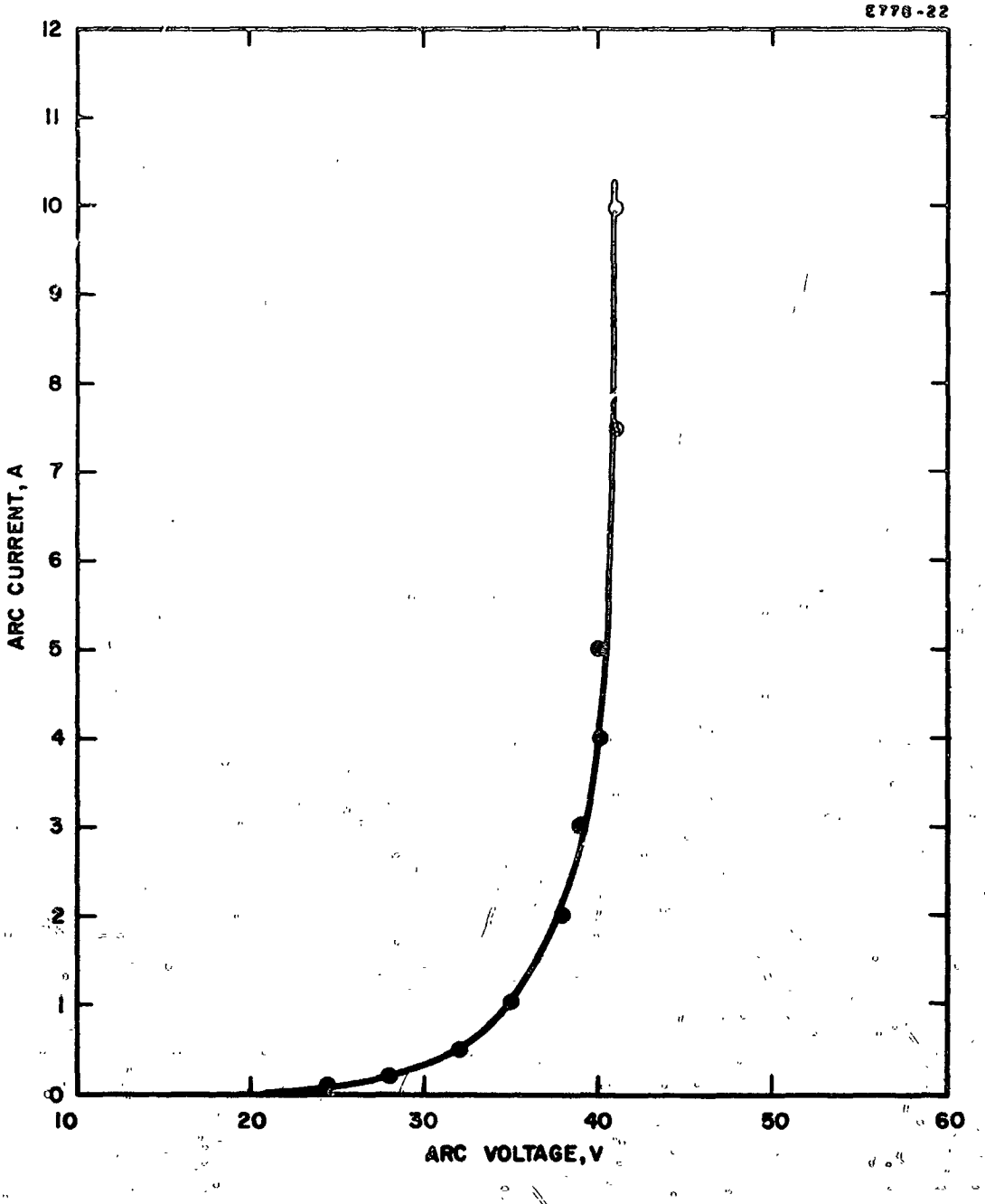

Fig. III-48. Arc current as a function of arc voltage for flower cathode No. 18, design 2, heater power = 100 W, magnet current = 10 A, mercury flow rate ≅ 300 mA.

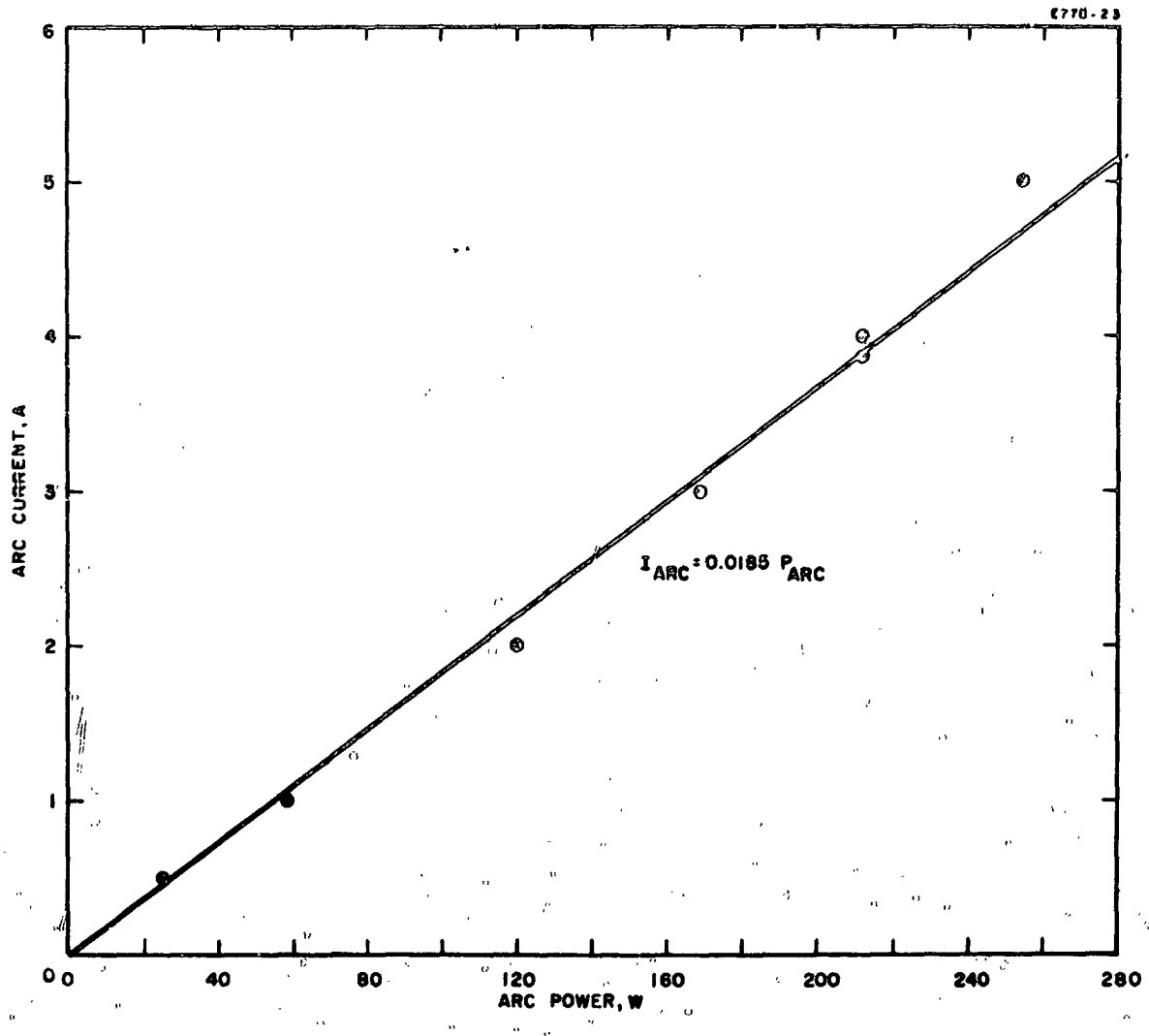

Fig. III-49. Arc current as a function of arc power for a fixed cathode power of 74 W. Flower cathode No. 18, design 2.

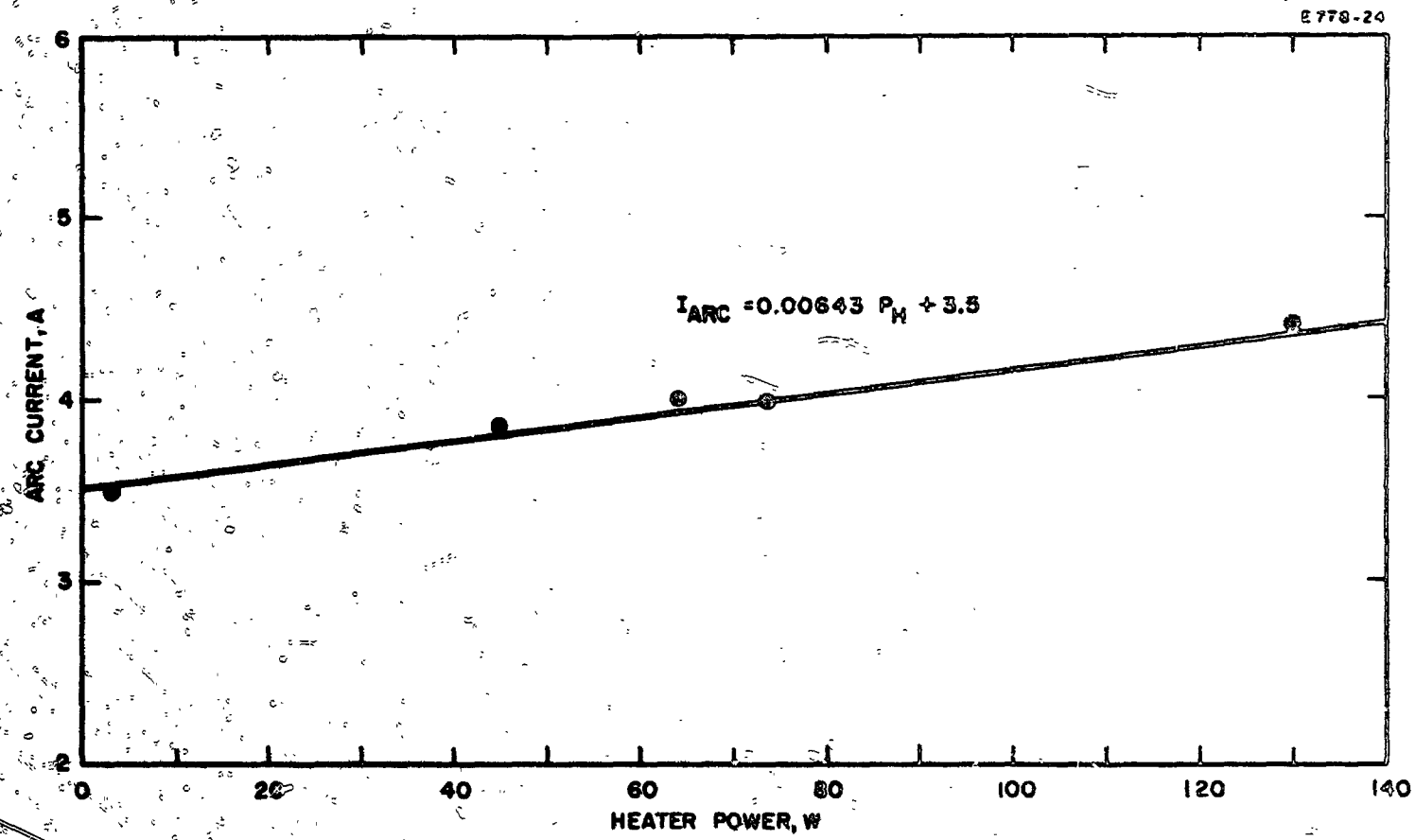

Fig. III 50. Arc current as a function of heater power for a constant arc power of 212 W. Flower cathode No. 18, design 2.

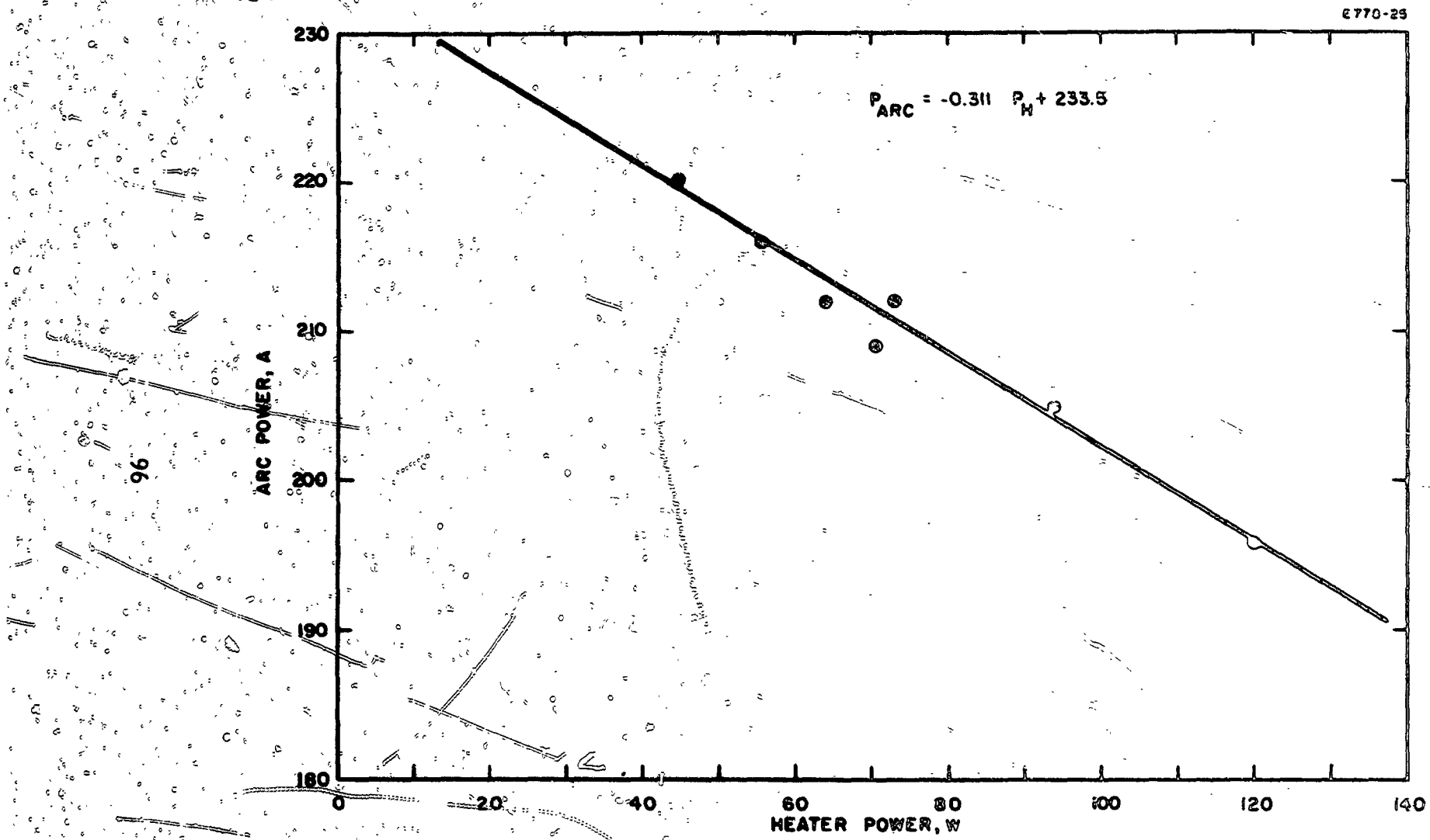

Fig. III-51. Relationship of arc power to cathode power for a constant arc current of 4 A. Flower cathode No. 18, design 2.

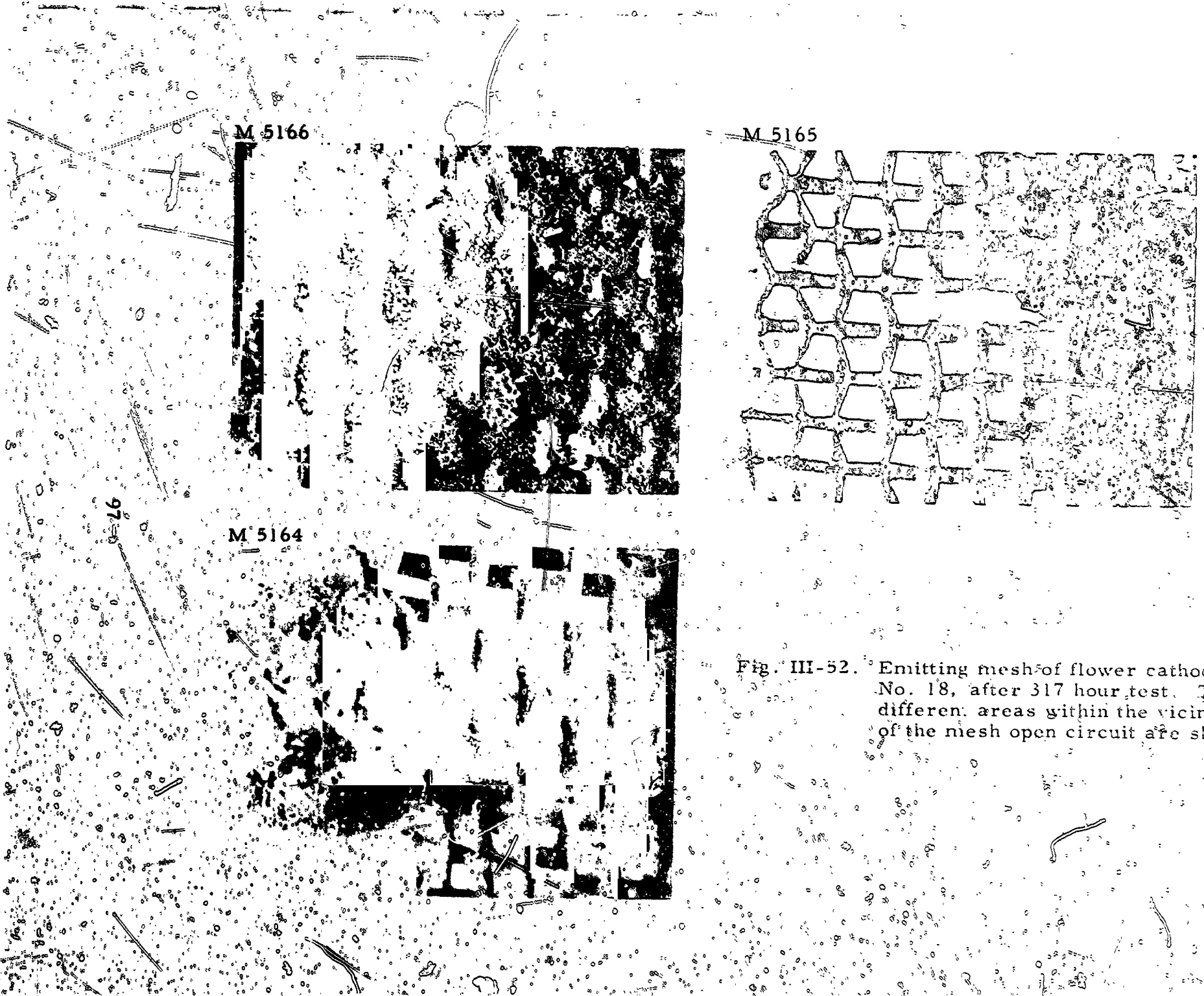

Fig. III-52. Emitting mesh of flower cathode No. 18, after 317 hour test. Three different areas within the vicinity of the mesh open circuit are shown.

pressure readings to the cathode failure point were normal. This ionization gauge will be relocated for future tests. An increased chamber pressure can partially poison the emission and cause localized heating. This cathode failure could be a result of this unfavorable test condition. The over-all appearance of this cathode, after test, is shown in Fig. III-53. The open circuit is at the upper left. Most of the cathode coating is intact. The coating, remaining on a section of the mesh that was removed after test, amounted to 12.3 mg/cm^2 or 71% of the original coating weight density. On this basis, this cathode coating would have a projected life of only 1100 hours. But from Fig. III-53, it is obvious that most of the cathode coating remains on the mesh. However, it should also be noted that the cathode coating is completely eroded or evaporated from the mesh in the vicinity of the open circuit (Fig. II-52).

Flower Cathodes Nos. 22 and 23

Cathode No. 22 was fabricated for a 1000/3000 hour life test. This cathode was of design 4B, and the pertinent dimensions are listed in Table II. The cathode emitting layer consisted of nickel encapsulated barium, strontium, calcium carbonates. The top half of this cathode mesh was coated with a 20 mg/cm^2 layer and the bottom half was coated with a 40 mg/cm^2 layer. The cathode was installed in a complete thrustor and was life tested in the 2 m cryowall vacuum chamber.

This cathode was at operating temperature 1650 hours and a beam current of 200 to 250 mA was maintained for 1013 hours. After testing for 1013 hours of beam life, this cathode and thrustor performance was essentially identical with initial performance. The test was interrupted at this time because of lack of contract provision for more extensive life testing. During life test, the cathode power was increased from 50 W to only 58 W. Typical life testing parameters were as follows:

cathode power	=	58 W
arc voltage	=	40 V
arc current	=	1.7 A
accel voltage	=	5 kV
decel voltage	=	0.6 kV
beam current	=	227 mA

mass utilization efficiency $\cong$ 85%.

After 810 hours of beam life, a seal in the mercury feed system opened and the reservoir was emptied. Thus, it was necessary to expose the cathode to atmosphere during the repair and refilling of the mercury feed system. By visual inspection of the cathode at this time, it was estimated that the ion sputtering of the oxide coating was negligible. To minimize Ba, Sr, Ca hydroxide-hydrate formation during cathode exposure, the cathode temperature was held at about 150°C during exposure to air. After the thrustor was reinstalled in the vacuum chamber and a 10^{-7} Torr pressure

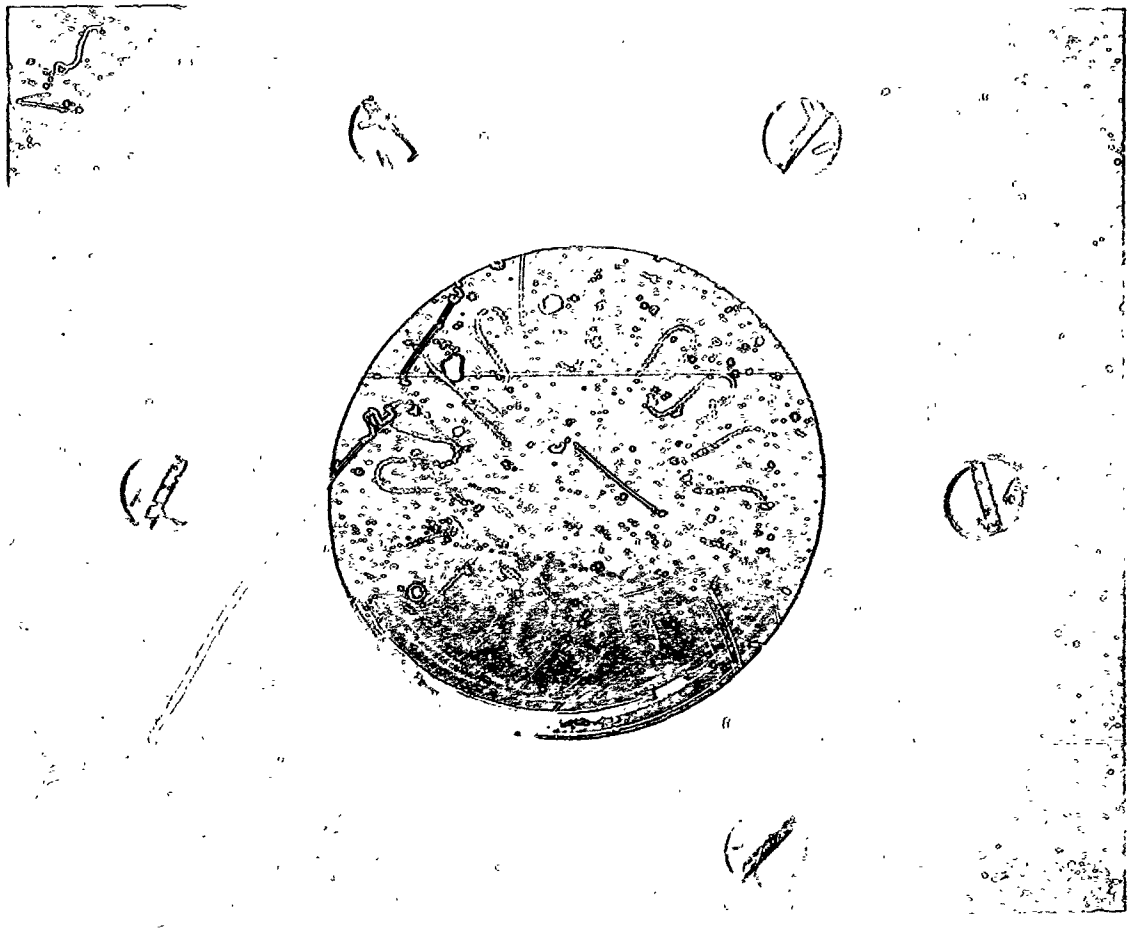

Fig. III-53. Flower cathode No. 18 after test. Open circuit is at upper left.

was obtained, the cathode reactivated readily and the thrustor operating parameters were re-established as listed above.

A more complete description of the cathode-thrustor performance is shown by the following graphs. Fig. III-54 shows the cathode temperature-power relationship. As this cathode was installed in the 2 ft cryowall vacuum chamber, it was necessary to measure its temperature optically from its reflected image. Therefore, the actual temperature was probably higher than that shown in Fig. III-54. Nevertheless, the low operating temperature, in the range of 800°C Br for cathode powers of 50-60 W, indicates that this cathode has remained an active emitter throughout this life testing. Arc current as a function of arc voltage is shown in Fig. III-55. These data are for mercury flow rates of 220, 300, and 340 mA. The numbers on the curves are the values of measured beam current. Arc current as a function of arc voltage with cathode power as a parameter is plotted in Fig. III-56. A considerable decrease in arc current is not evident until the cathode power and arc voltage are decreased below 50 W and 35 V, respectively.

This cathode, after test, is shown in Fig. III-57. The cathode mesh appears in good condition without excessive ion sputtering, but the back support plate has been partially sputtered away. The loss of support plate has permitted the cathode mesh to sag from its original shape. To withstand the ion sputtering, this back plate thickness can be increased without difficulty or without changing the cathode characteristics. A portion of the mesh was removed and the oxide coating remaining after test was measured. A coating loss of 34% was calculated from these weight measurements, but considerable oxide coating was lost in the process of removing a portion of the cathode mesh. Therefore, these weight measurements do not serve as an accurate measure of the oxide coating lost as a result of life testing. From visual inspection, there is no significant loss of oxide coating. The nickel encapsulated powder was applied to the cup cathode emitting surface to a thickness of 2 mm (150 mg/cm^2) without resistive overheating (autocathoding) or sparking problems. Therefore, the oxide coating for the flower cathodes, using nickel encapsulated powder, could be increased by factors of 7.5 to 10. With this increase in oxide coating thickness, sufficient oxide would be available to withstand more than 10,000 hrs. of ion bombardment, even if one assumes that 34% of the coating was lost during this test.

Cathode No. 23 was fabricated as a back up for cathode No. 22. Cathode No. 22 served properly; therefore, cathode No. 23 was not tested.

Flower cathode No. 26

This cathode, using nickel encapsulated powder, was fabricated for use with a LeRC thrustor and Hughes power conditioning equipment. Required testing of this thrustor and power conditioning equipment provided a means of obtaining additional tests of the encapsulated powder cathodes. Cathode life testing was performed with the thrustor operating parameters

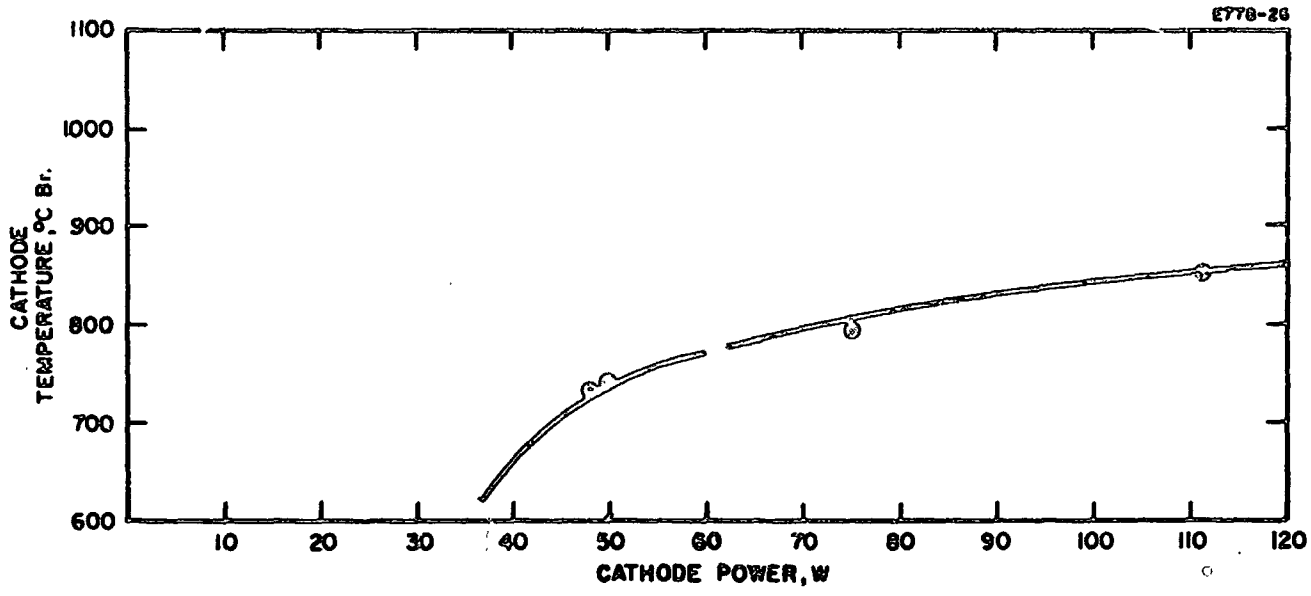

Fig. III-54. Temperature-power relationship for flower cathode No. 22, design 4B at beginning of test. (As measured from a reflecting metal plate.)

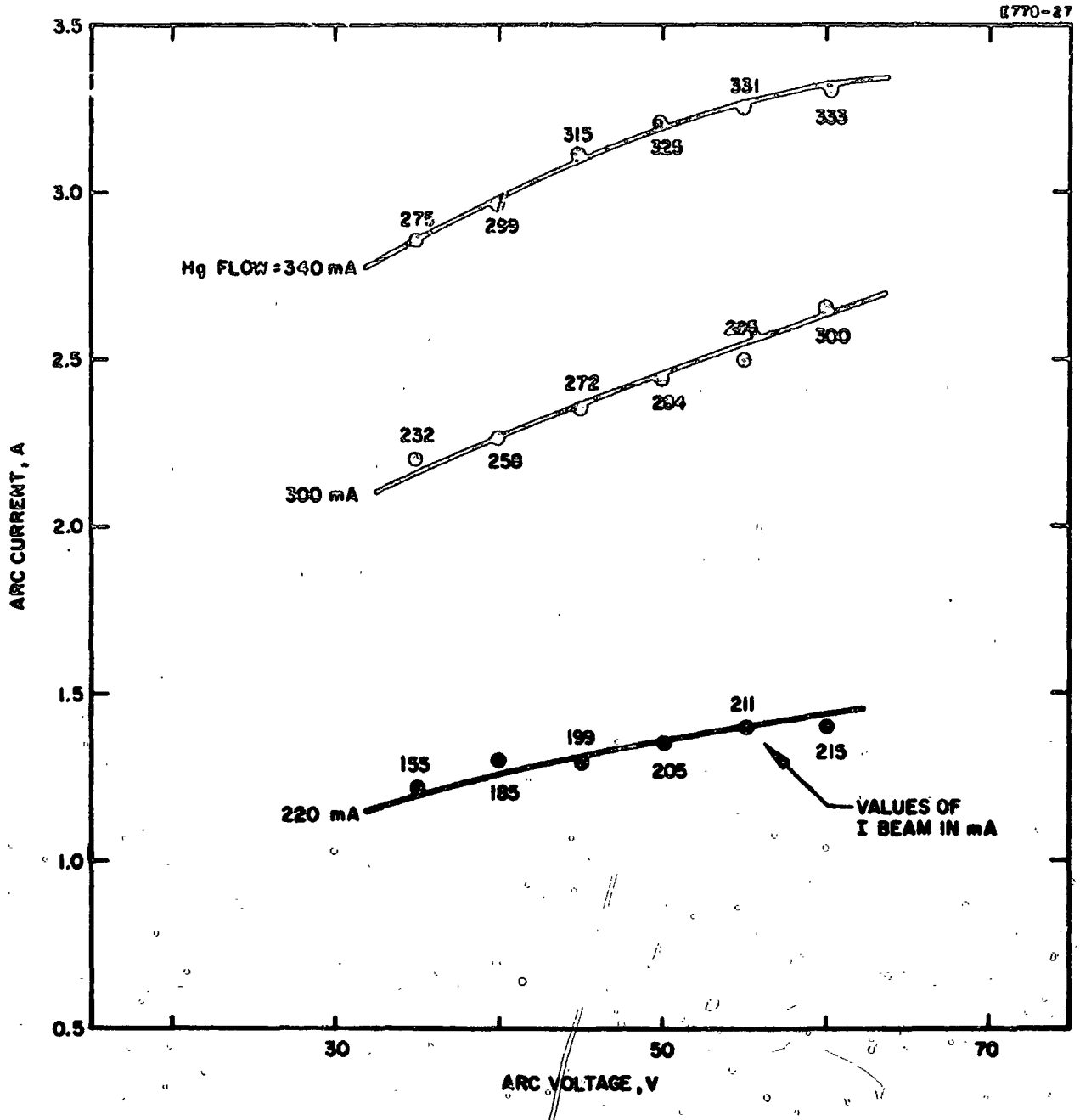

Fig. III-55. Arc current as a function of arc voltage with Hg flow as a parameter. Flower cathode No. 22, design 4B.

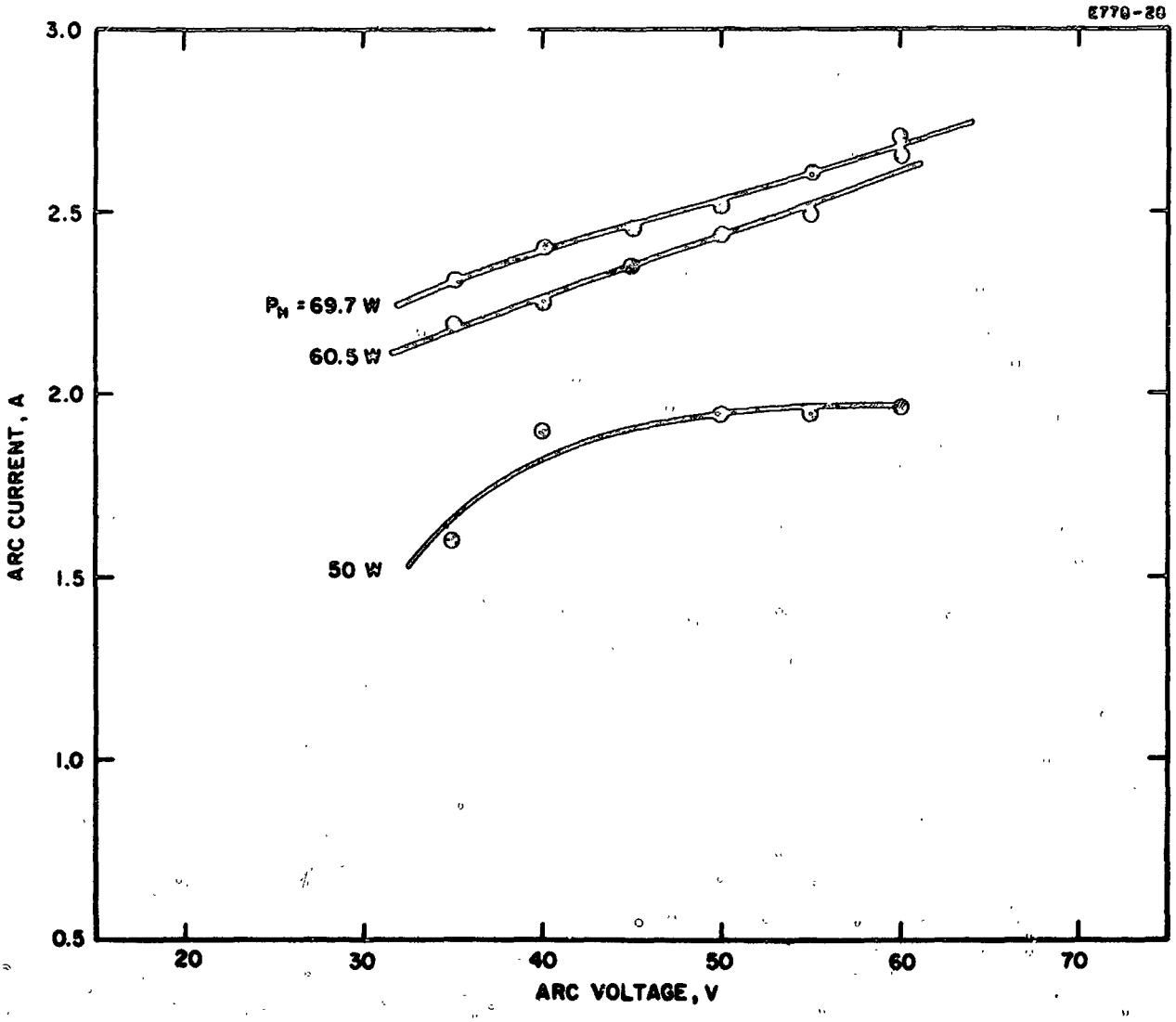

Fig. III-56. Arc current as a function of arc voltage with cathode power as a parameter. Flower cathode No. 22, design 4B. (These data were taken near the beginning of the 1000 hour life test.)

M 4968

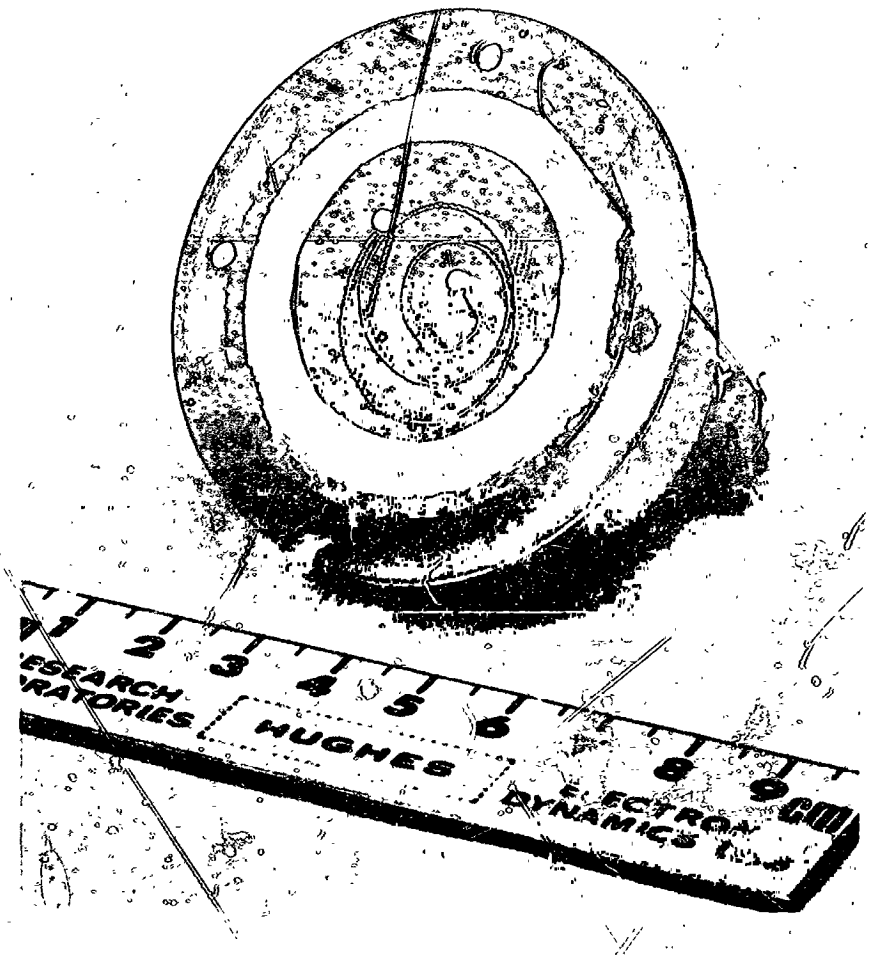

Fig. III-57. Flower cathode No. 22 after 1000 hour life test.

set as previously listed on page 47.

The variation of cathode power and temperature for this test is also plotted in Fig. III-21. The test was terminated after a total of 500 hours for both cathodes No. 24 and 26, as a 500 hour test was the objective set for the thrustor and power conditioning equipment. This cathode performed without a continuing increase in cathode power and temperature. This improved performance was due to the improved environmental test conditions. The cathode appearance after test was a light gray, which is characteristic of active emitters. This test therefore was successful, even though it was too short for reliable extrapolation to very long cathode life.

Cup Cathode

The cup cathode was designed to take advantage of the desirable feature of an indirectly heated cathode and to eliminate the disk separation problem of the disk cathode. The desirable feature of an indirectly heated cathode is that the heater need not be exposed to the ion bombardment. As listed in Table II, the emitting area was 8.2 cm and the frontal area was 3.2 cm. For an arc of about 2 A which is the typical requirement for a 15 cm thrustor, the emission density requirement was about 1/4 A/cm^2. The emitting area was sprayed to a coating weight of 150 mg/cm^2 which is equivalent to a thickness of about 2 mm. The emission coating used was the nickel encapsulated triple carbonate. The total amount of emitting material was approximately 1.2 g which should be sufficient to supply the sputter losses for 10,000 hours of operation. Figure III-58 is a photograph of this cathode before test. The essential construction details of this cathode are shown schematically in Fig. II-5. This cathode was tested using a 15 cm simulated thrustor in the 6 in. mercury diffusion vacuum system. The heater power required for various cathode temperatures is shown in Fig. III-59. For a normal cathode operating temperature of 850°C Br, an emission current of 2 A was obtainable with an arc voltage of 75 V. This results in an acceptable power-to-emission ratio of 16 W/A. Arc current as a function of arc voltage with cathode power as a parameter is shown in Fig. III-60. An arc current of only 1.0 A was obtainable with the desired operating arc voltage and heater power of 45 V. A typical life test operating point was as follows:

heater power	=	38.8 W
arc voltage	=	45 V
arc current	=	1 A
mercury flow	=	200 mA
magnet current	=	20 A.

With the cup cathode operating at 2.5 A, the average current density was approximately 0.3 A/cm^2; and although some resistive heating was evident, the heater power setting remained the controlling parameter for the emission current. The life test period consisted of 96 hours for the cathode at operating temperature and 65 hours for the arc on time. The test was terminated as a result of an open circuit heater. The heater power was increased to 75 W in attempts to further activate the cathode for increased emission at 45 V of arc voltage. For long life, this 75 W of heater power was too large

M 4851

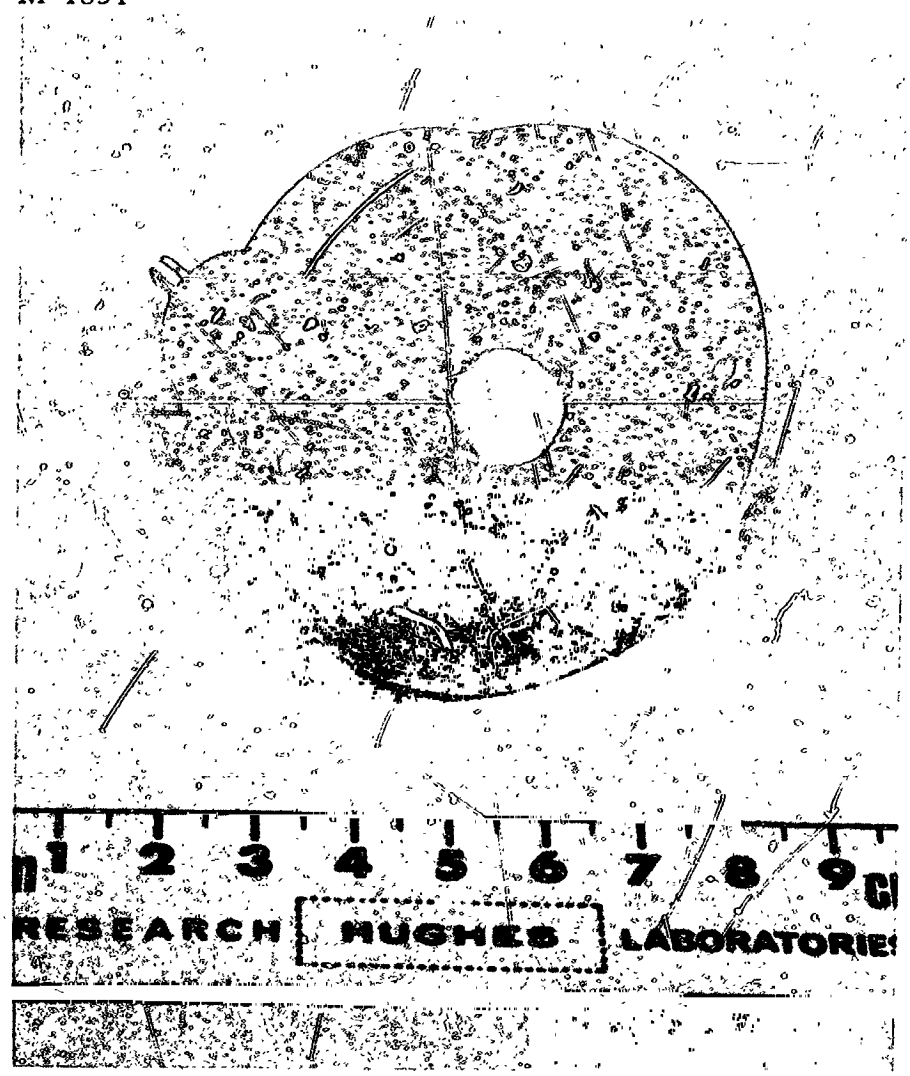

Fig. III-58. Cup cathode before test.

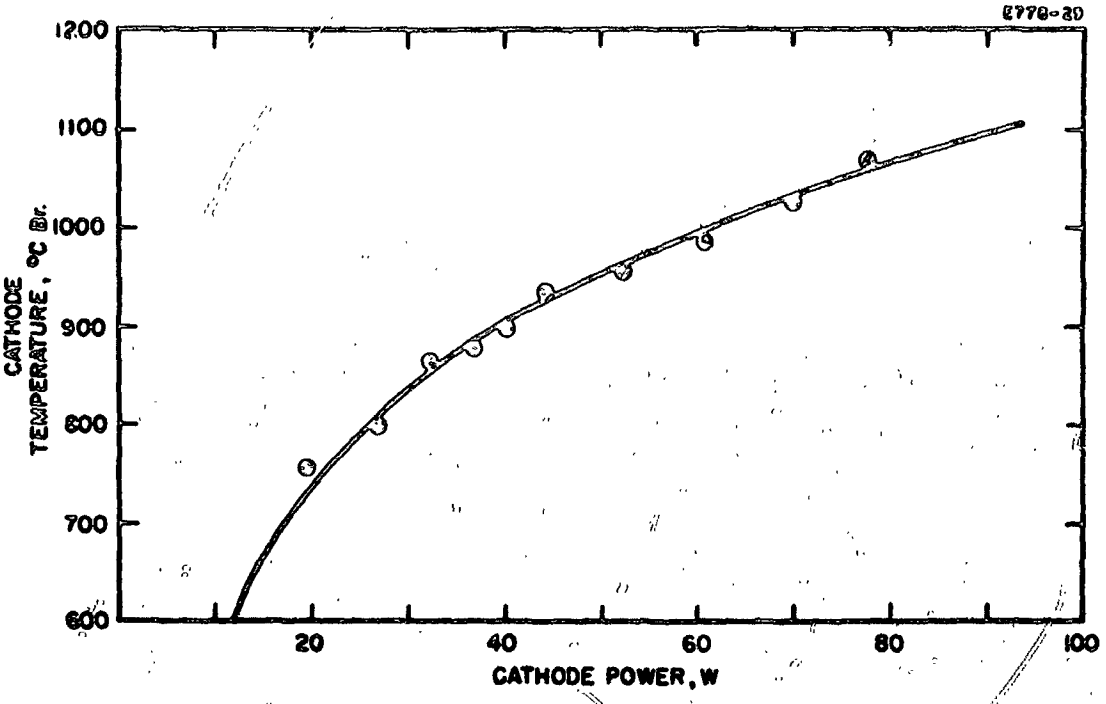

Fig. III-59. Temperature-power relationship for cup cathode No. 1.

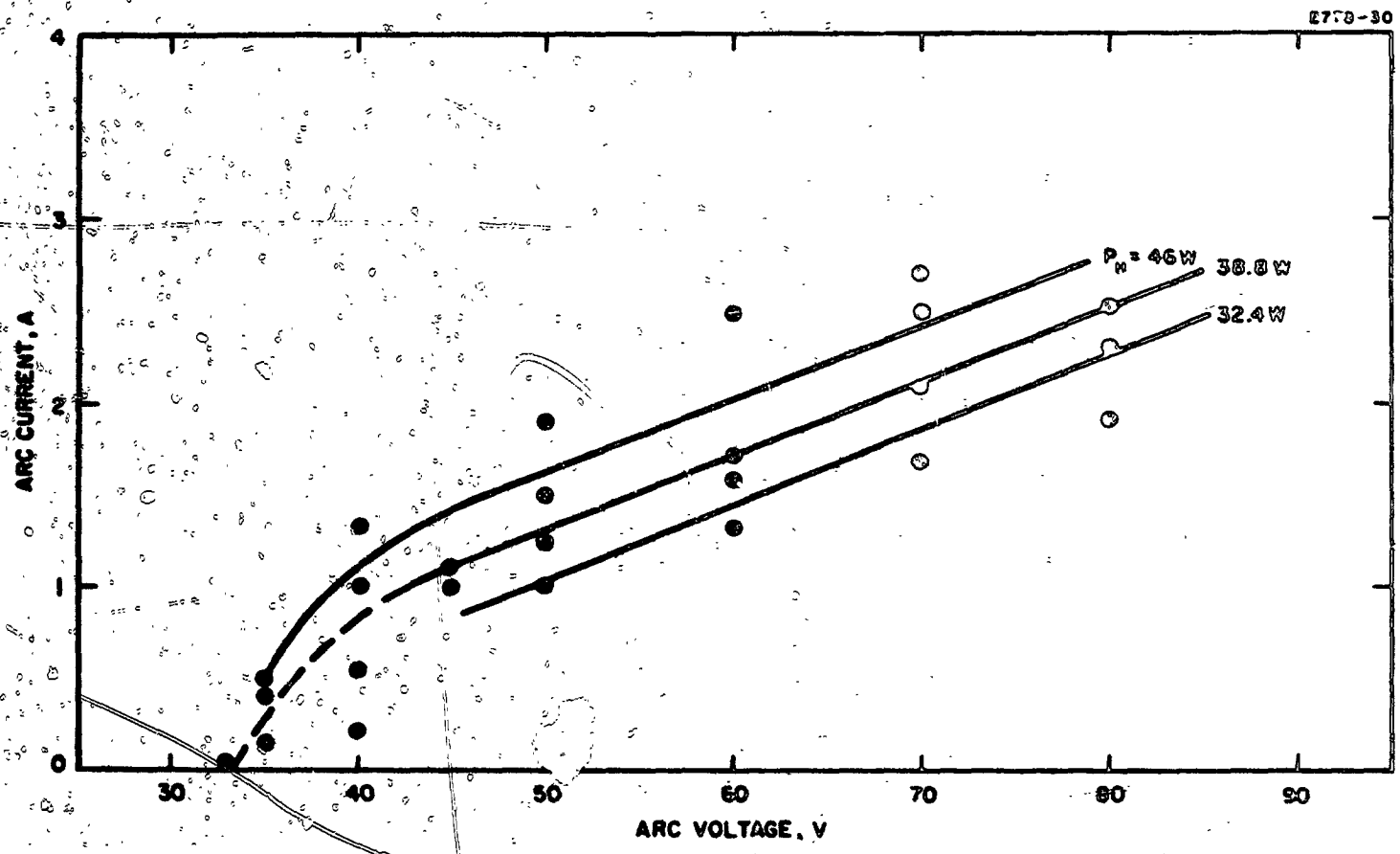

Fig. III-60. Arc current as a function of arc voltage with cathode heater power as a parameter. Magnet current = 20 A, Hg flow ≅ 350 mA. Cup cathode.

an increase over the design operating heater power of about 35 W. The heater opened near one lead by melting of the tungsten coil. The appearance of this cathode after test is shown in Fig. III-61. The emissive coating missing from the cathode top flaked off after removal from the vacuum system. Water absorption from the atmosphere undoubtedly contributed to this flaking phenomenon. The cup cathode test results indicate that (1) the emissive coating of 2 mm thickness does not result in undue cathode self heating or autocathoding when nickel coated carbonates are used, and (2) the emitting area and heater size were too small to provide the desired arc current and heater life. In addition, the amount of nickel used to encapsulate the carbonates was probably near optimum for emissive layers of 20 to 40 mg/cm^2, but for this layer of 150 mg/cm^2 the amount of nickel encapsulating on the carbonates should undoubtedly be increased. The optimum amount of nickel encapsulate for various emission layer thicknesses should be investigated further.

The fact that controlled operation (no arcing nor autocathoding) could be obtained with a 2 mm thick coating is a good indication that a 10,000 hour cathode of this type is feasible.

M 4872

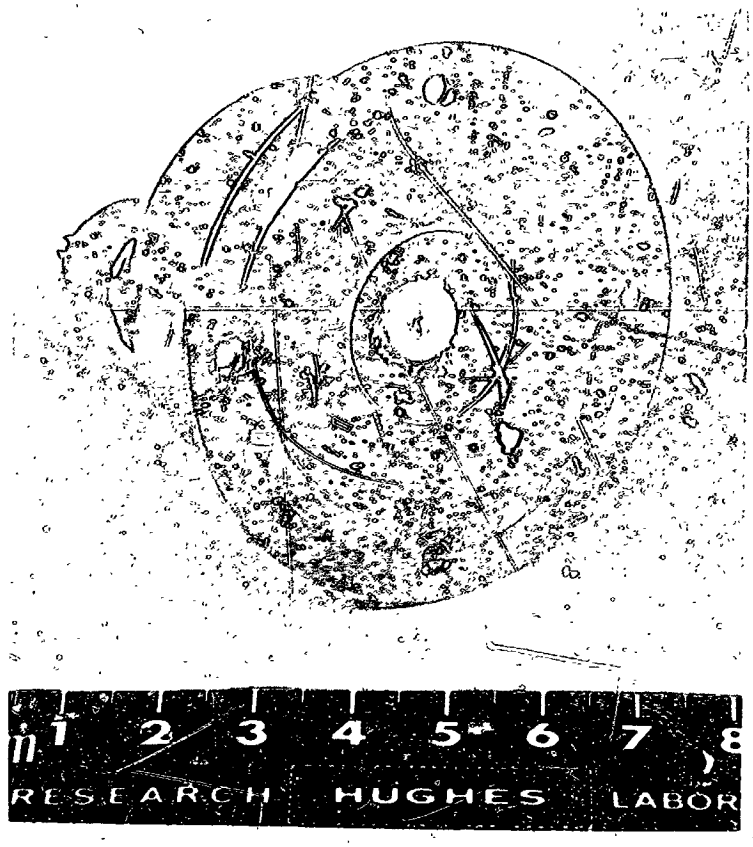

Fig. III-61. Cup cathode after test.

G. Heaters

At the higher cathode operating temperatures, the heater failure rate approaches that for cathodes. Typical life data from Beck[3] indicate that problems with long life (3000 hours +) heaters are encountered at cathode temperatures of about 1200°C. This was another reason for concentrating our efforts on the low temperature oxide cathodes.

For the directly heated cathode, our previous experience had shown that a failure problem was concerned with the connection for the flower cathodes fabricated under this contract. A nickel sheet was welded in good contract with the cathode mesh (before coating). To date, no failures have been encountered for this heater lead to mesh connection.

The heater design for the indirectly heated cup cathode is shown in Fig. III-63. The tungsten heater wire was alumina coated to minimize tungsten evaporation onto the alumina support. Fig. III-63 also illustrates the design features of the heaters used with the disk and impregnated cathodes, although the disk cathodes used a flat heater geometry and the heaters for the impregnated cathodes were potted or entirely enclosed in insulation.

As mentioned under the test results for each cathode, the heater leads failed for the impregnated cathodes, and for the cup cathode the heater failed near a lead. Obviously, the lead failure can be minimized by increasing the lead diameter, and method of increasing heater reliability can be seen from the following analysis.

The heater power is transferred from the enclosed surface (heater) to the enclosing surface (cathode) primarily by radiation; this transfer is governed by the relation[21]

$$P_{1-2} = \frac{\sigma A_1 \left(T_1^4 - T_2^4 \right)}{\frac{1}{\epsilon_1} + \frac{A_1}{A_2}\left(\frac{1}{\epsilon_2} - 1\right)}$$

where

A_1 ≡ effective heater radiating area

A_2 ≡ total cathode radiating area

ϵ_1 and ϵ_2 ≡ emissivities of A_1 and A_2

T_1 and T_2 ≡ heater and cathode temperatures.

The heater temperature for a given power transfer is minimized as A_1/A_2

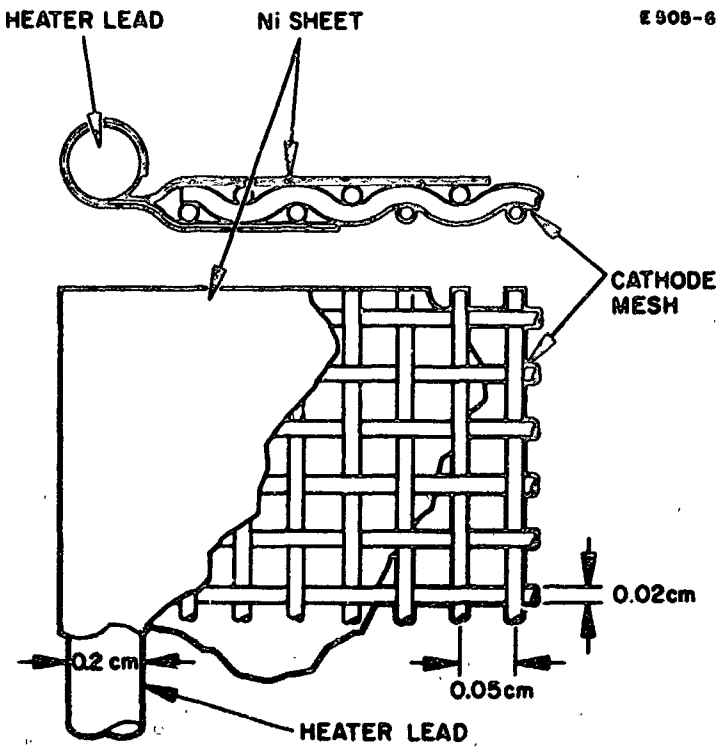

Fig. III-62. Heater connection for directly heated flower cathode.

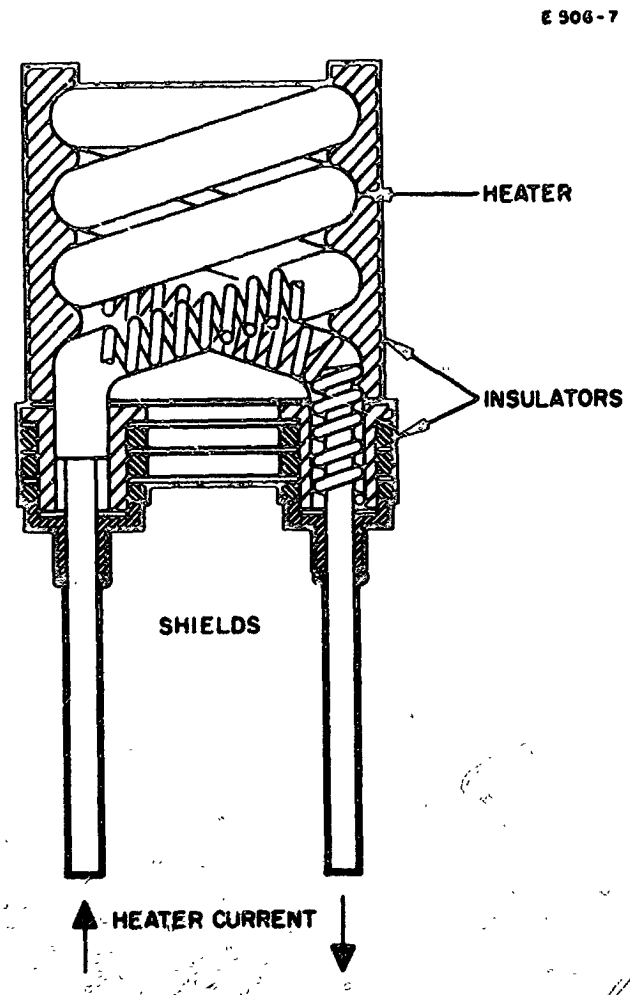

Fig. III-63. Heater design for indirectly heated cup cathode.

approaches unity. Therefore, the design changes for future cup cathodes would include an increased heater area in relation to the cathode area.

IV. FACILITIES

The major facilities needed for this cathode study program were thrustors, vacuum chambers and power conditioning equipment. Chemical and metallurgical laboratories, cathode spray room, furnaces, and other general purpose facilities also were used as required. Some of the earlier cathode tests were completed using 10 cm diameter thrustors that were available at the HRL. For later cathodes tests, two 15 cm simulated thrustors and one complete 15 cm thrustor were fabricated. A simulated 15 cm thrustor along with a mounting plate and a disk cathode is shown in Fig. IV-1.

A 6 in. diameter oil diffusion vacuum station was converted to a mercury diffusion system. The water cooled baffle and roughing lines were converted to refrigeration cooling. In addition, the liquid nitrogen trapping system was rebuilt to provide optically tight baffling. The power conditioning equipment for the simulated thrustor tests consisted of cathode heater supplies, dc magnet supplies, boiler heater supplies and controllers, and arc supplies. Two consoles containing one of each of these listed supplies were fabricated. A simulated thrustor, power conditioning console and mercury diffusion vacuum station are shown in Fig. IV-2. A schematic diagram of the simulated thrustor-cathode test set-up is shown in Fig. IV-3.

An ion-sublimation pumping system was manufactured to provide a bakable vacuum-chamber which produces a very high vacuum, completely hydrocarbon free. All seals are metal to metal, thereby eliminating all greased o-rings. The sublimation pump is a Varian Model 956-5030 and the ion pump is a Hughes Vacuum Tube Products 30 liter/sec pump. A typical pressure during cathode test, using this system, was 10^{-8} Torr. This system, including a simulated thrustor mounted on the end plate, is shown in Fig. IV-4.

The complete thrustor, fabricated as part of this Contract, consisted of the accelerator optics, thrustor discharge chamber, isolator, flow meter, vaporizer, and mercury reservoir. These items and the test equipment are shown schematically in Fig. IV-5. A photograph of this complete thrustor as it was installed in the 2 ft. chamber is shown in Fig. IV-6. The power conditioning equipment for the complete thrustor tests, and the 2 ft chamber were available prior to this Contract. These latter two items required only modifications in order to complete these cathode-thrustor tests. Fig. IV-7 shows the thrustor power conditioning equipment and 2 ft. vacuum chamber.

M 4203

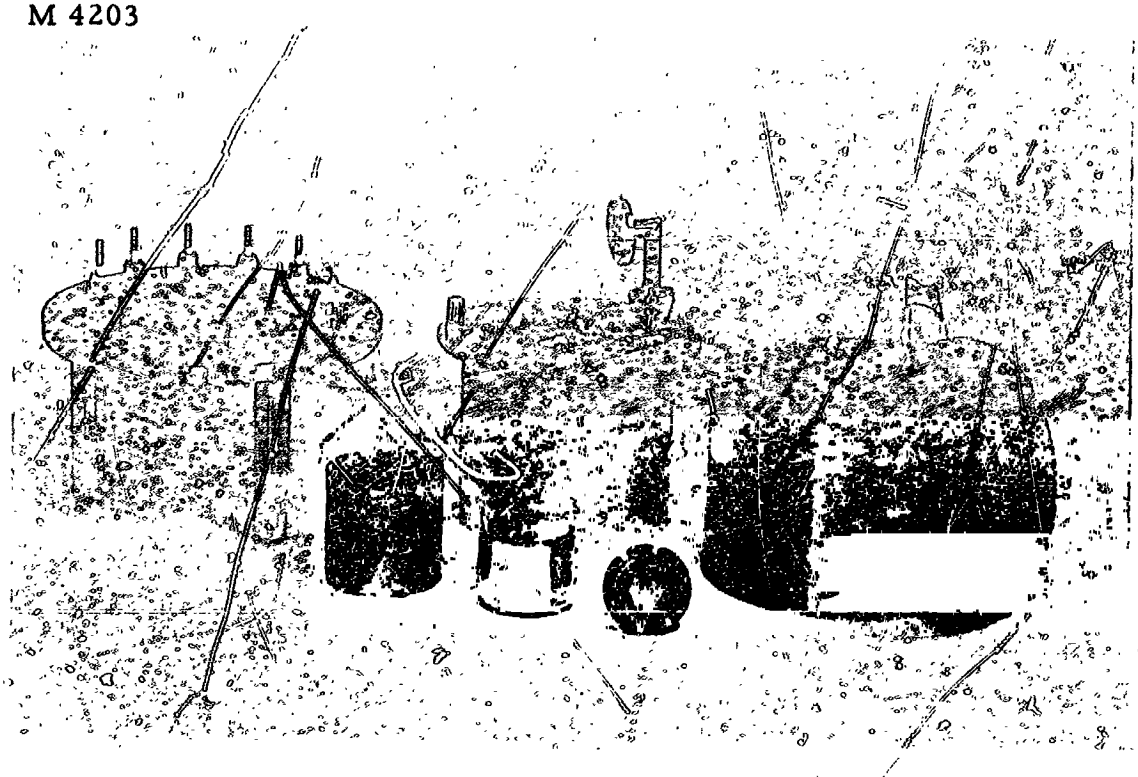

Fig. IV-1. Simulated thruster No. 1 parts, disk cathode No. 1, and thruster mounting plate.

M 4291

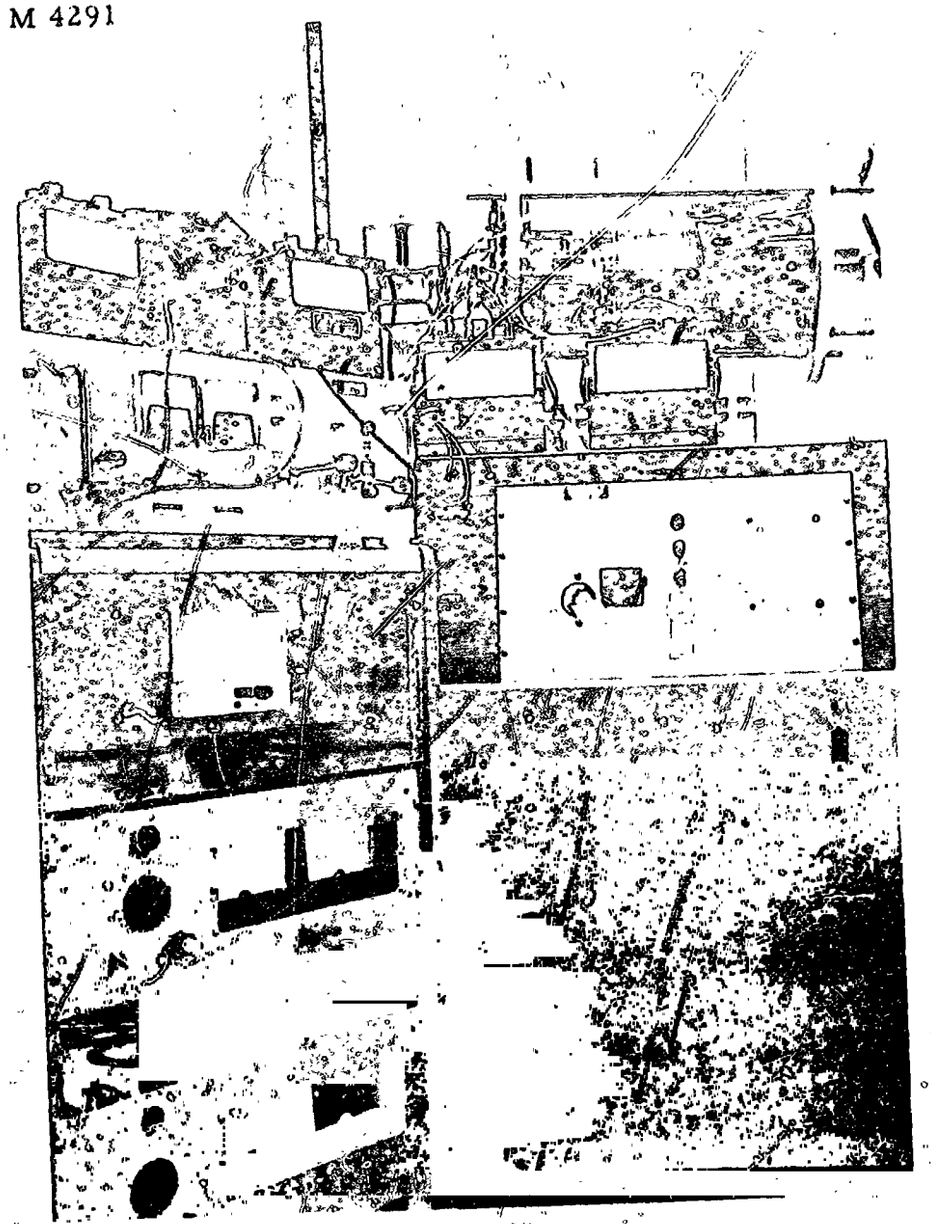

Fig. IV-2. Modified 6 in. mercury diffusion vacuum station and power conditioning console.

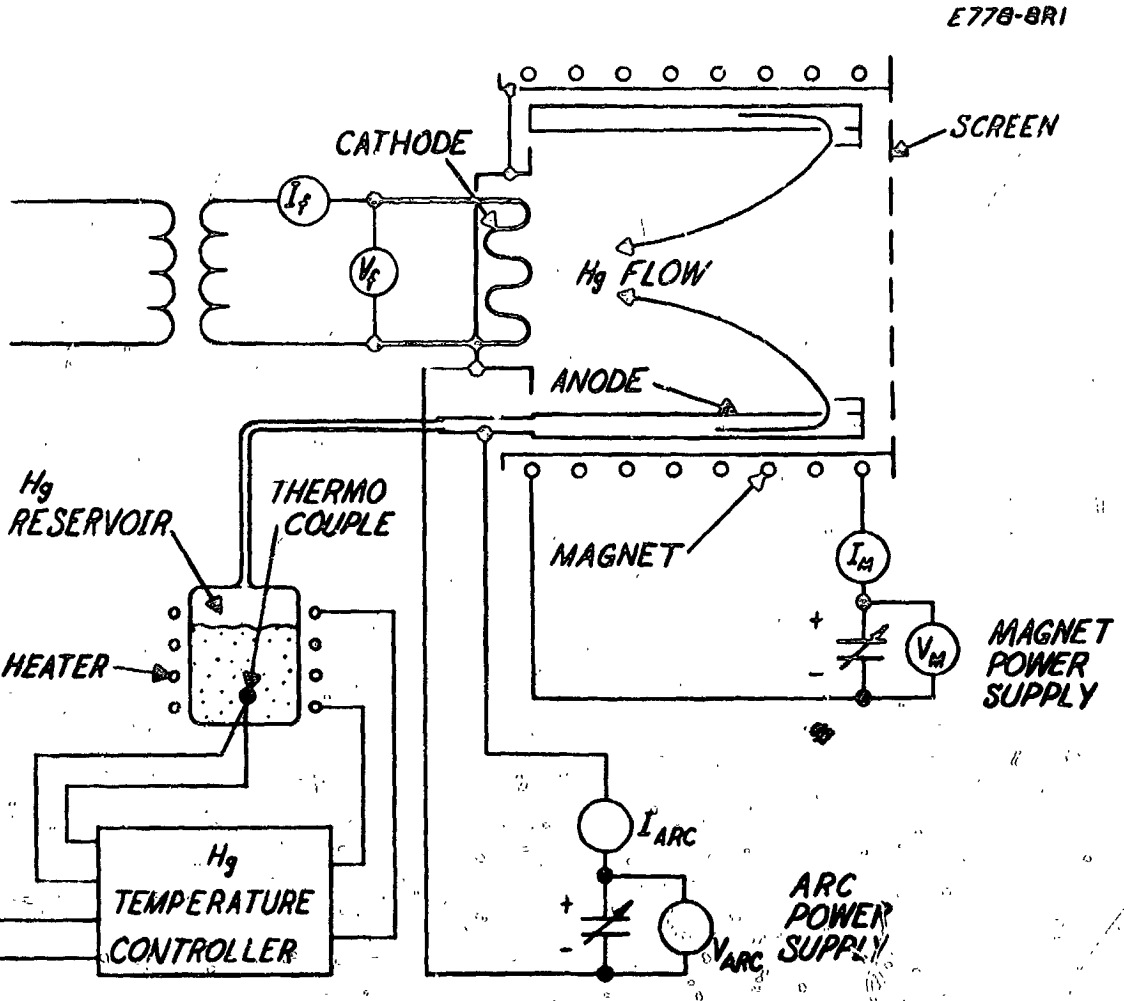

Fig. IV-3. Schematic diagram of the simulated thruster-cathode test set-up.

M 4398

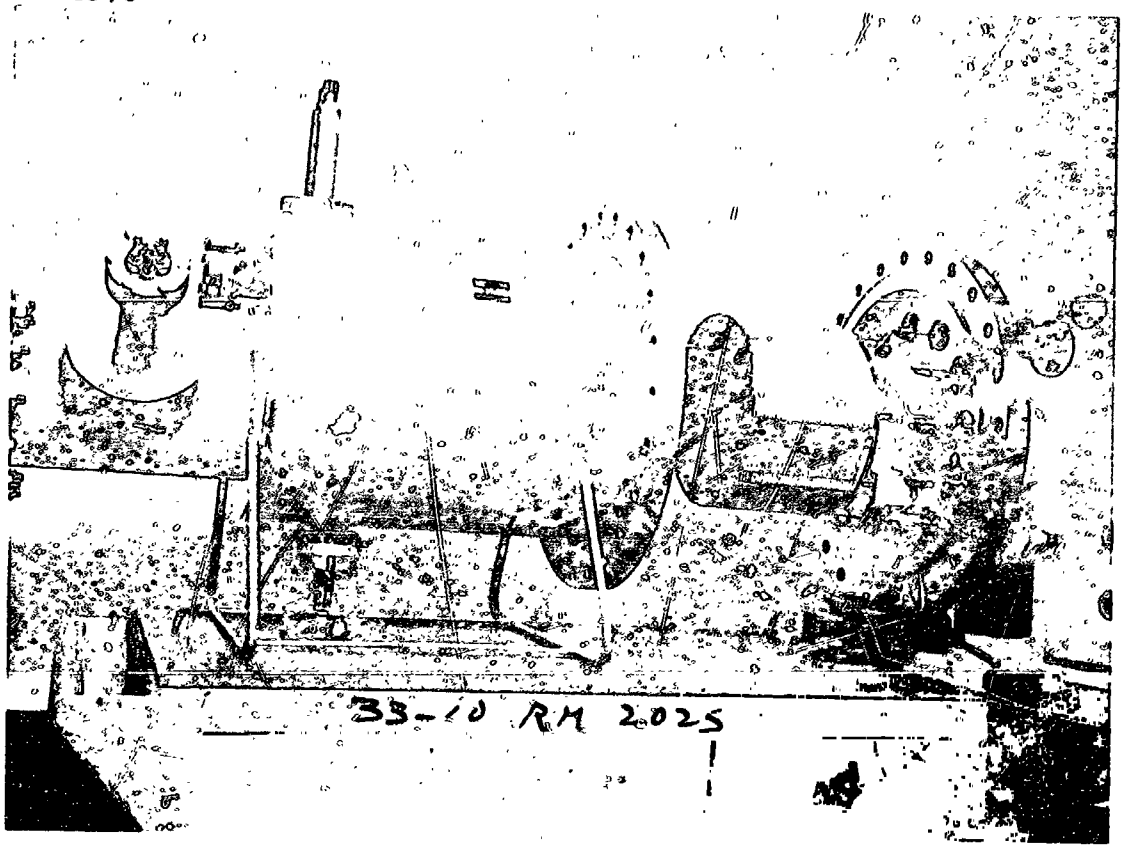

Fig. IV-4 Ion sublimation vacuum system and simulated thruster No. 1.

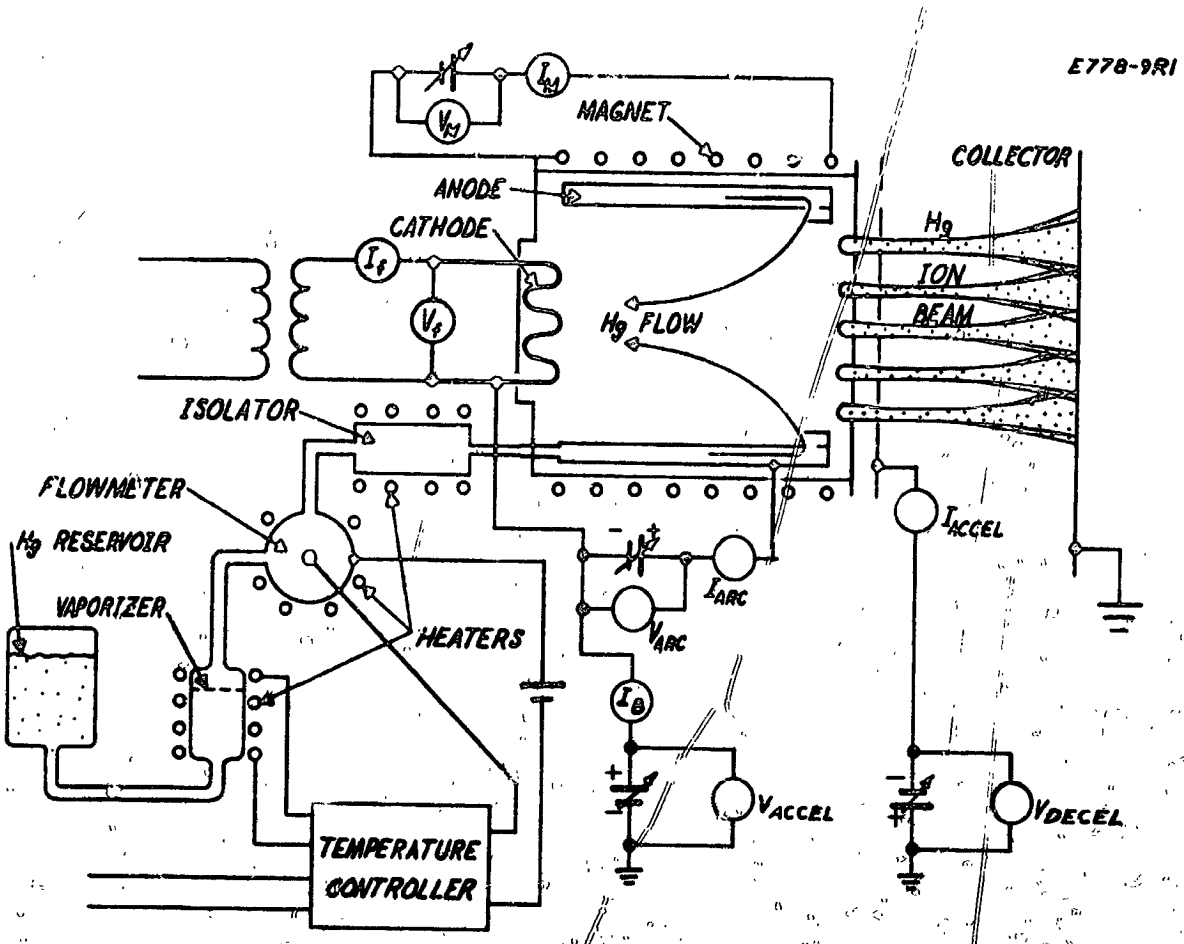

Fig. IV-5. Schematic diagram of the complete thruster and test equipment.

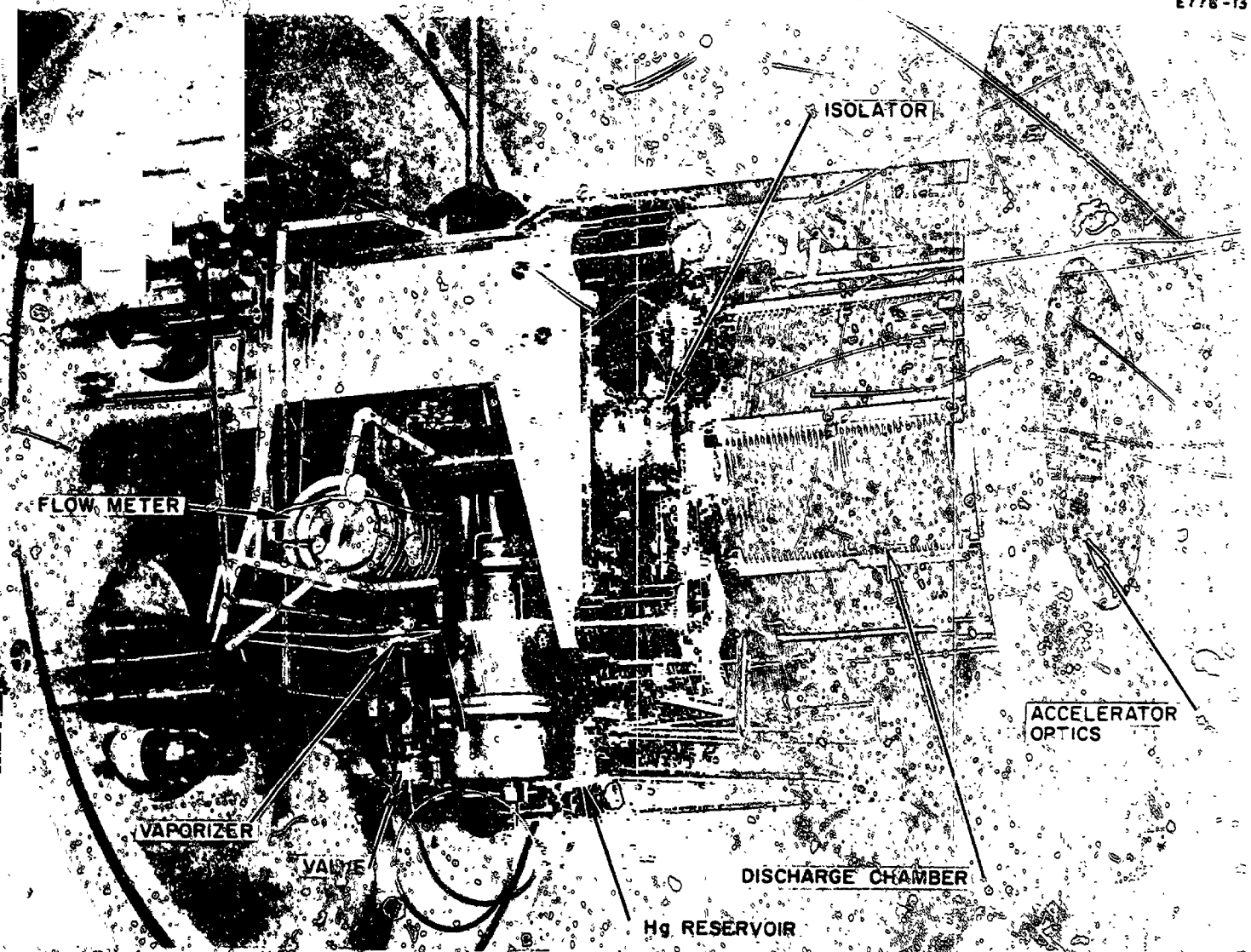

Fig. IV-6. Hg thruster used for the 1000 hour life test.

M 5156

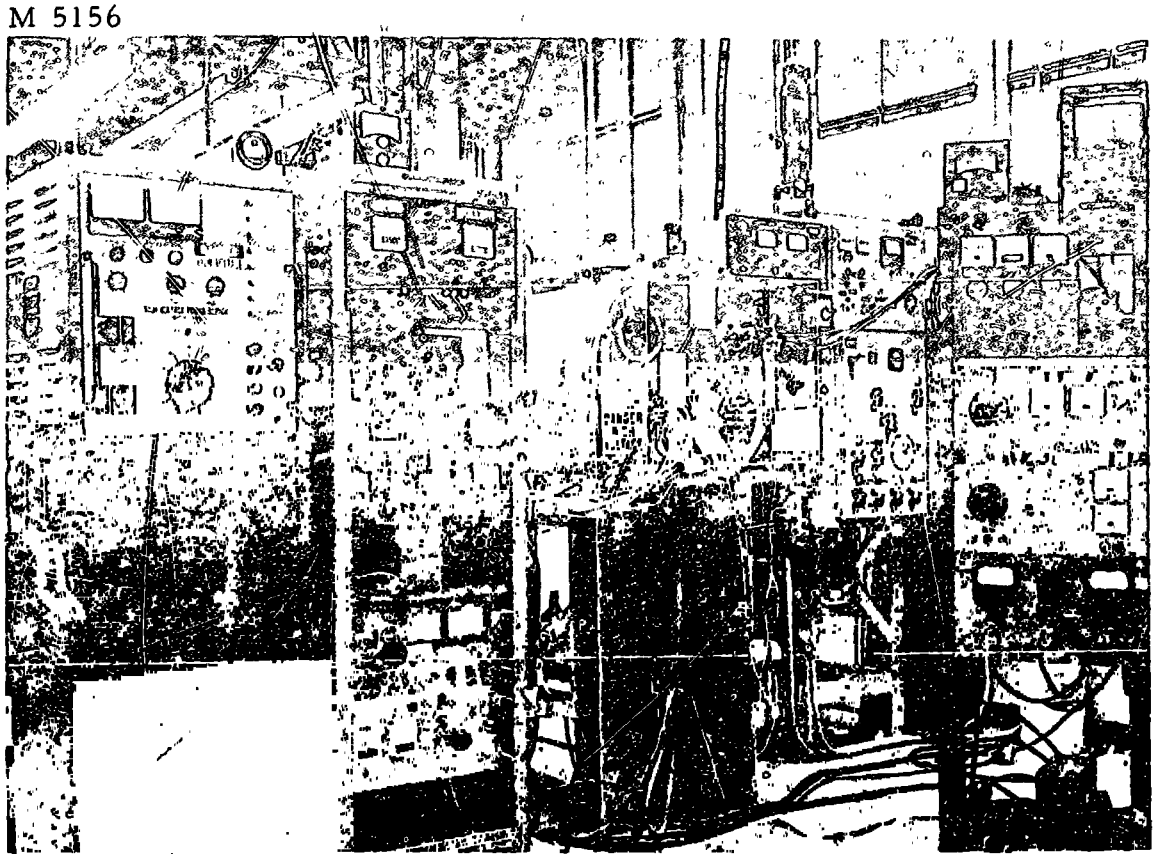

Fig. IV-7. Thruster power conditioning equipment and 2 ft vacuum chamber.

V. CONCLUSIONS AND RECOMMENDED FUTURE PROGRAM

The flower cathodes have performed satisfactorily in a number of 200, 500, and 1000 hr. life tests. These test results indicate that 10,000 hr. missions using flower cathodes are possible. Nickel encapsulated cathode powder was used for coating the flower cathodes fabricated during the latter portion of the contract period. In the body of this report, these cathodes, along with the cup cathode, were discussed under the heading of "nickel encapsulated powder cathodes." This encapsulated powder provided improved coating adhesion and reduced coating resistance. Cathode flaking (lack of coating adhesion) and cathode sparking (autocathode or high coating resistance) have limited cathode life on the early oxide cathodes fabricated under this contract, and elsewhere. This nickel encapsulated powder has provided means of increasing the oxide layer thickness, by a factor of 7.5 to 10, and minimizing the coating adhesion and resistance problems. From the measurements of oxide coating remaining after test, life projections made range from a few thousand to tens of thousands of hours. Accurate projections of the oxide coating life are not available as the coating weight is influenced by factors other than mercury ion sputtering. These factors influencing coating weight include carbon deposits, sputtered metal deposit (flower cathode No. 13), evaporative loss from overheated inactive areas, coating flaking, and water absorption.

Measurements are required of the sputtering rate of oxide cathode surfaces by mercury ions of various energies and densities. The liquid-sputtering facility developed on Contract NAS 3-6273 should be suitable for measuring the oxide coating loss due to ion sputtering only. The thickness (resistance) of the oxide layers on most of the flower cathodes was adjusted so that resistive heating (autocathoding) was not a serious problem. But more definitive type measurements of oxide layer resistance are needed. For these measurements well activated-oxide layers should be used and the resistance as a function of layer thickness for various amounts of nickel encapsulating the cathode powder particles should be measured. These results would serve to optimize the methods of storing sufficient emitting material to overcome sputtering losses for the desired lifetime.

The flower cathode failures that were a result of an open circuit in the nickel mesh can be attributed to cathode inactivation resulting from poor vacuum conditions. This cathode inactivation permits the arc to concentrate within a small region and melt the nickel mesh. A possibility that should not be overlooked for increasing flower cathode reliability is the use of a higher-melting-temperature material, e. g., tungsten.

For the various flower cathode designs, one parameter that was varied was the spacing between the folds of the nickel mesh. For the design No. 2, with close spacing of the folds, most sputtering occurred at the front edge of the mesh. For the design No. 4, with increased spacing, the back heat shields were sputtered away partially (cathode No. 22). These test results indicate that the fold spacing and mesh depth are approximately correct. Nevertheless, additional study of the cathode-plasma interaction is

needed for further cathode optimization. This study would permit determination of the plasma penetration within the cathode folds, and emission density along the depth of the mesh.

During this contract some optimization of the cathode size, location, and method of mercury feed have lowered the arc current required for a 15 cm thrustor from the range of 4-6 A to approximately 2 A. Flower cathode No. 22, used in the last 1000 hour life test, was an optimum cathode design in many respects; for example, (1) the emitting area was reduced so that the heater power was only about 50 W while the required emission of 1.5-2 A was still available, (2) spacings between the mesh folds were adjusted so that the plasma sheath penetrated the depth of the mesh, and (3) nickel encapsulated powder was used to minimize oxide flaking and resistive heating problems. This optimized cathode design, cathode No. 22, performed very satisfactorily during its 1000 hour life test, although some test difficulties were encountered, such as a mercury feed system leak. Although this cathode design is optimized in many respects, additional study of cathode size in relation to discharge chamber size could result in further increases of discharge chamber efficiency.

In one case, the disk cathode operated very effectively at a heater power to arc current ratio of approximately 13 W/A. In other cases, the disk cathode heater power increased to the range of 150-180 W for arc currents of 2 A or less. These poor results were caused by heat flow problems. The proper control of the heating efficiency and the unequal sputtering of the disks and oxide coating are problems of sufficient severity that additional tests of the disk cathode are not justified.

The cup cathodes provides a means of storing ample emitting material to supply sputtering losses without autocathoding, if the proper amounts of nickel encapsulating the cathode powder are utilized. To date, preliminary tests performed with the cup cathode, have not been fully satisfactory. It is believed that in these tests the nickel encapsulation was insufficient. Additional tests using this cathode design should therefore be performed.

The results obtained with impregnated cathodes were essentially as expected. Excessively high operating temperatures were required for barium production and transport to the cathode surface. These high temperatures resulted in high ratios of heater power to arc current, and low heater reliability. Further thrustor tests of impregnated cathodes are probably not justified without modifications of their design. These modifications would consist of using a uniform small particle substrate that could be supplied with ample barium to maintain a partial monolayer under heavy ion bombardment.

REFERENCES

1. C. M. Cade, IRE Trans. ED-8, 56 (1961).

2. H. J. Lemmens, et al., Philips Tech. Rev. 11, 341 (1950).

3. A. H. W. Beck, et al., Proc. Inst. Elec. Eng. B106, 372 (1959).

4. W. R. Kerslake, NASA TM X-1105, Lewis Research Center, June 1965.

5. G. K. Wehner, Phys. Rev. 112, 1120 (1958).

6. J P. Blewett, H. A. Liebhafsky, and E. F. Hennelly, J. Chem. Phys. 7, 478 (1939).

7. S. Yoshida, N. Shibata, Y. Igarashi, and H. Arota, J. Appl. Phys. 27, 497 (1956).

8. W. W. Tyler, Phys. Rev. 76, 1887 (1949).

9. E. S. Rittner, Philips Res. Rept. 8, 194 (1953).

10. G. Herrman, The Oxide Coated Cathode (Chapman and Hall, London, 1951), Vol. 2, p. 262.

11. Ibid., p. 290.

12. I. Langmuir, Phys. Rev. 33, 954 (1929).

13. N. D. Morgulis, Radio Eng. Electron. (USSR) 2, 1 (1957).

14. P. M. Marchuk, Radio Eng. Electron. (USSR) 2, 13 (1957).

15. G. F. Mityanskii, Radio Eng. Electron. (USSR) 2, 31 (1957).

16. I. M. Dykman, Radio Eng. Electron. (USSR) 2, 83 (1957).

17. Ya. P. Zongerman, et al, Radio Eng. Electron. (USSR) 2, 100 (1957).

18. D. Mac Nair, Proc. of 6th Nat'l. Conf. on Electron Tube Techniques, (Macmillan, New York, 1963), p. 173.

19. G. A. Haas and J. T. Jensen, Jr., Rev. Sci. Instr. 28, 1007 (1957).

20. D. W. Maurer and C. M. Pleass, IEEE - Electron Device Convention, Oct. 1965, Washington, D. C.

21. A. E. De Barr, Rev. Sci. Instr. 19, 569 (1948).